ELECTROSORPTION OF TETRAALKYLAMMONIUM IONS ON SILVER IODIDE

A. DE KEIZER

ELECTROSORPTION OF

TETRAALKYLAMMONIUM IONS

ON SILVER IODIDE

PROEFSCHRIFT

TER VERKRIJGING VAN DE GRAAD
VAN DOCTOR IN DE LANDBOUWWETENSCHAPPEN,
OP GEZAG VAN DE RECTOR MAGNIFICUS,
DR. H.C. VAN DER PLAS,
HOOGLERAAR IN DE ORGANISCHE SCHEIKUNDE,
IN HET OPENBAAR TE VERDEDIGEN
OP WOENSDAG 29 APRIL 1981
DES NAMIDDAGS TE VIER UUR IN DE AULA
VAN DE LANDBOUWHOGESCHOOL TE WAGENINGEN

STELLINGEN

I

De afhankelijkheid van de adsorptie van tetraalkylammonium ionen van de oppervlaktelading wordt vooral bepaald door concurrentie tussen de Coulombse interactie van de ionen met de wandlading en de dipolaire bijdragen van de watermoleculen aan het grensvlak. Bij toenemende negatieve wandlading kan dit zelfs leiden tot een afname van de adsorptie van de positieve ionen.

Dit proefschrift, hoofdstuk 6 en 7

II

Het is waarschijnlijk, dat de χ-potentiaal t.g.v. georienteerde watermoleculen aan het AgI-electrolyt grensvlak wordt veroorzaakt door heterogene oppervlakte hydratatie. Het verschil in de mate van hydratatie van de plaatsen met een geadsorbeerd Ag^+ en I^- ion geeft een verklaring voor de asymmetrie van de ladingspotentiaal curven.

Dit proefschrift, hoofdstuk 3

III

De kwantitatieve overeenkomst tussen de Gibbs adsorptie en de analytische adsorptie voor tetraalkylammonium ionen op AgI bewijst, dat het capaciteitsoppervlak en het adsorptieoppervlak identiek moeten zijn. Een keuze van het specifiek oppervlak heeft belangrijke fysische consequenties, hetzij voor het adsorptiemodel, hetzij voor het dubbellaagmodel.

Dit proefschrift, hoofdstuk 7

IV

Bij de interpretatie van de χ-potentiaal dient meer aandacht besteed te worden aan het effect van een mogelijke orientatie van oplosmiddel moleculen t.g.v. interactie met georienteerde adsorbaten (secundaire orientatie).

A. de Keizer en J. Lyklema, Ann. Real Soc. Chim. Españ. Fis. i. Quim. 71 894 (1975)

V

Het is didactisch gewenst bij de introductie van de Wilhelmyplaat methode meer aandacht aan de bijdrage van het gewicht van het 'meniscusvolume' te besteden dan thans in leerboeken van de grensvlakchemie geschiedt.

Ervaringen KB-praktikum grensvlakchemie

VI

De toepassing van klassieke vier-keuze vragen bij tentamens geeft vaak aanleiding tot een dwangmatige formulering van de alternatieven. Het gevolg is veelal, dat er meerkeuze vragen ontstaan, waarvan afleiders triviaal zijn en/of de afleiders een verschillende graad van onjuistheid hebben.

H. van der Deen, A. de Keizer, J.W. Keuskamp en H.K. Groen, Onderzoek van Onderwijs 10 no.1, 1981.
De meerkeuze vraag met weging van alternatieven, een bevredigend alternatief voor de dwangbuis van het meerkeuze examen?

VIIa

De betekenis van de variantie van dichotome variabelen is principieel ver-
schillend van die voor Gaussisch verdeelde variabelen. In de testleer wordt dit
onvoldoende gerealiseerd.

> A.D. de Groot en R.F. van Naersen, Studietoetsen II, 2e druk, Mouton,
> Den Haag, 1969, p.207.
> C. Nunnally, Psychometric theory, McGraw-Hill, New York, 1967.

VIIb

De betrouwbaarheidscoëfficiënt is geen valide kwaliteitscriterium voor
meerkeuze examens.

> Stelling VIIb
> A.D. de Groot en R.F. van Naerssen, Studietoetsen II, 2e druk, Mou-
> ton, Den Haag, 1969, p.229

VIIIa

Het combineren van een tentamencijfer en een praktikumcijfer leidt alleen
dan tot een valide examencijfer (d.i. een examencijfer met voorspellende waarde
voor theorie en praktijk), indien tentamen- en praktikumscores een positieve
correlatie hebben.

> A. de Keizer, nota 'Praktikum-score en caesuur', O.W.C., 1980

VIIIb

Het al dan niet meewegen van de praktikumscore in het examencijfer is
meestal van invloed op de grens voldoende-onvoldoende. Examinatoren dienen
het examencijfer zodanig te berekenen, dat de eisen die aan het theoretische
deel van het examen worden gesteld om een voldoende examencijfer te behalen
voor studenten met en zonder praktikum gelijk zijn.

IXa

Hoewel zilverjodide een dood materiaal is, is het als modelstof voor funda-
menteel grensvlakchemisch onderzoek springlevend.

IXb

Groen is mooi, geel ook.

X

Fundamenteel onderzoek is van nature divergent. Het beheersen van deze
divergentie is niet alleen van belang voor 's lands schatkist, doch ook voor de
wetenschap.

Proefschrift A. de Keizer
Electrosorption of tetraalkylammonium ions on silver iodide
Wageningen, 29 april 1981.

Aan moeder

Voor Willy, Otto en Corry

VOORWOORD

Gaarne wil ik allen danken die direct of indirect tot de af-
ronding van mijn wetenschappelijke opleiding hebben bijgedragen.

Dankbaar ben ik voor de vrijheid die mijn ouders mij bij de
keuze van mijn opleiding hebben gegeven. Dit is de basis geweest
voor het volgen van mijn academische studie.

Alle hoogleraren en medewerkers van de Rijksuniversiteit in
Utrecht die hebben bijgedragen tot mijn scheikunde opleiding zou
ik hiervoor willen danken. Met name wil ik prof.dr. J.Th.G. Overbeek
danken voor de stimulerende wijze waarop hij mij in mijn huidige
specialisatie heeft ingevoerd en prof.drs. M.P. Groenewege voor de
plezierige wijze waarop hij mij in de molecuulspectroscopie heeft
ingeleid.

Beste Hans, hooggeleerde Lyklema, ik beschouw het als een
voorrecht hier in Wageningen onder jouw bezielende leiding te mogen
werken. De vrijheid, die je mij bij het onderzoek hebt gegeven en
de intensieve en creatieve begeleiding bij de afronding van mijn
onderzoek vormen een belangrijke bijdrage tot de verdere ontplooiing
van mijn wetenschappelijke loopbaan.

De collegiale en plezierige sfeer op het laboratorium voor
Fysische en Kolloidchemie is een stimulans bij de vervulling van
mijn onderwijs- en onderzoekstaken binnen de vakgroep. Ik prijs me
dan ook gelukkig, dat ik me ook de komende jaren kan inzetten voor
de vakgroep Fysische en Kolloidchemie, en voor de Landbouwhogeschool
in het algemeen.

De voltooiing van dit proefschrift is tot stand gekomen met de
hulp van velen binnen en buiten de vakgroep.

Met name zou ik Joekje Eikelboom-Akkerman willen danken voor
de oriënterende metingen met tetraalkylammonium ionen. In het bij-
zonder wil ik Jikkie Hibma bedanken voor de energieke wijze waarop
zij zich gedurende ruim een jaar voor het onderzoek heeft ingezet.
Veel van de in dit proefschrift vermelde experimentele gegevens
zijn door haar gemeten.

De keuze van de automatiseringsapparatuur is mede tot stand
gekomen in overleg met de Commissie Automatisering Laboratorium-
apparatuur (COALA). De Technische en Fysische Dienst voor de Land-
bouw (TFDL) en het Instituut voor Toepassing van Atoomenergie in de

CONTENTS

CHAPTER 1

INTRODUCTION

1.1 ON ELECTROSORPTION

The adsorption of molecules or ions on a *charged interface* in
contact with an electrolyte solution is called *electrosorption*. In
a more restricted sense, the term electrosorption is used for ad-
sorption on electrodes only. The most important aim of basic elec-
trosorption studies is to investigate the relation between the
electrical parameters, such as charge or potential of the interface,
and the adsorption. In addition it is tried to develop a molecu-
lar picture of the interfacial region and to interpret the adsorp-
tion data in terms of a theoretical adsorption isotherm. This may
be useful to predict adsorption on other systems with respect to
the concentration and the electrical state of the surface.

Electrosorption can take place on liquid and on solid sub-
strates in contact with an electrolyte solution. It can take place
on metals, ionic conductors, oxides etc., in fact on any surface
that can obtain an electrical charge. Strictly speaking, every ad-
sorption can be considered as electrosorption, because every surface
bears at least some electrical charge. However, only in few systems
one is able to fix the electrical parameters in a well-defined way.
Only these systems will be a potential object of fundamental elec-
trosorption studies. In this context the most important example is
the classical system of a liquid *mercury-electrode* in contact with
an electrolyte solution. Since the development by Lippmann (1) of
his capillary electrometer there has been a continuous vital in-
terest in studies of the electrical double layer and adsorption
phenomena on this electrode. Over the last two decades this has
led to an advanced and detailed description of the interfacial
region on mercury. An other important system for electrosorption

1

studies is the *silver iodide-electrolyte interface*. This is a classical system for the study of colloidal stability. Typical electrosorption studies have been done only during the last three decennia.

The mercury/electrolyte interface and the silver iodide/electrolyte interface are quite differing in nature. Historically, electrosorption on silver iodide was mainly performed in a colloid-chemical environment, whereas studies of electrosorption on mercury were either related with polarographic studies or studies of liquid interfaces. As a consequence the two kinds of experiments were mainly performed in different schools. In the physical sense the differences are even more distinct. First, mercury is a liquid, whereas silver iodide is a solid. Mercury is a metal, the surface of which is ideally *polarizable* i.e. there is no current flowing through the interface when a potential (lower than a critical value) is applied. Silver iodide, on the contrary, is a solid ionic conductor with a crystal lattice. Electrochemically, the AgI-interface is an ideal *reversible* interface, i.e. when we fix the concentration of potential-determining ions, the resulting potential is determined by Nernst's law. Nevertheless, the electrochemical properties of the two systems have very much in common. This means, that it is especially the solution side of the interface which determines most characteristics of the interfacial region. Hence the solution sides of the electrical double layers on the two systems are supposed to be very similar. The comparison between the results for both systems is especially valuable for a generalization of the developed theories. Due to the seniority of the mercury system with respect to the silver iodide system, the theoretical level is more sophisticated for mercury.

From the *experimental* point of view, the mercury and silver iodide system are quite different. For the mercury system, surface charge and adsorption are calculated indirectly from measurements of the interfacial tension and/or the differential capacitance measurements. The accuracy of these measurements is on a very high level. Direct measurement of the surface charge and the amount adsorbed is very difficult and too inaccurate. For the silver iodide system, on the contrary, it is possible to measure the surface charge and the adsorption analytically by using a suspension with

2

a large surface area. This aspect was already noticed by Freundlich (2) many years ago. Moreover, it is possible to gain more information about the interfacial region by performing electrokinetic and colloidal stability measurements on silver iodide sols.

In conclusion, both from a theoretical and experimental point of view the two systems are antipoles in some respect, whereas in many respects it is possible that the different results just supplement each other. This makes the comparison of the systems very interesting from a scientific point of view.

The importance of electrosorption studies stems from many scientific and practical fields. In research areas as different as technology, biology, soil science, etc. one is concerned with surfaces on which adsorption can take place and where the interfacial region determines some of the properties of the system. It is not the intention to be exhaustive, but a few characteristic examples may suffice to illustrate the importance of electrosorption.

The use of pesticides and herbicides in agriculture leads to a potential accumulation of these compounds in soil. The adsorption behaviour of these chemicals at the *soil particles* as a function of potential, surface charge, salt concentration etc. will be of particular importance in estimating accumulation and leaching of the soil (3).

Another application field of adsorption is found in *water purification*. Adsorption of poisonous compounds on active carbon is of major importance.

In general, electrosorption of charged organic ions has a large influence on *colloidal stability*. If the sign of the charge of the adsorbent is opposite to the charge of the adsorbate, then upon (superequivalent) adsorption the stability goes first through a minimum, after which the stability rises mostly to a weak maximum again. Thus in this particular case the effect is much more pronounced than with neutral adsorption.

Also, the influence of adsorption on the *flotation* of mineral powders may be very pronounced (4). This is important for the technological enrichment of minerals. Sometimes there is a critical concentration where the flotation is very strong, whereas at zero

concentration as well as at high concentration the flotation is almost zero. It follows that insight in the principles leading to this critical concentration is of great technological importance.

The application of silver iodide as a *rain-maker* (5,6) is noteworthy. If a solution of silver iodide in aceton is burned, the resulting AgI-smoke is a powerful cloud-seeder. This phenomenon is probably related to the adsorption of water molecules on the charged sites at the surface and the crystallographic analogy between AgI and ice. Both these conditions enable the formation of an ice nucleus in the atmosphere.

1.2   ELECTROSORPTION ON MERCURY

Many workers have reviewed the immense literature of the mercury/electrolyte interface during the last three decades. There are the classical reviews of Grahame (7), Parsons (8,9), Frumkin and Damaskin (10), and Delahay (11). Some of the more recent review articles are written by Damaskin, Petrii and Batrakov (12), Payne (13,14), Sparnaay (15), Trasatti (16,17), Reeves (18), and Habib(19).

Since the introduction of the capillary electrometer by Lippmann (20) and the classical experiments by Gouy (21) the study of the interfacial region at the mercury/aqueous electrolyte inter-face has an ever growing attention among many physical chemists. The results of Gouy already showed that the adsorption of neutral compounds was a function of the potential of the electrode, because the lowering of the interfacial tension near the electrocapillary maximum was greater than in the extreme potential regions. Both the theories for adsorption of ionic and of neutral compounds were developed. The first quantitative theory for the adsorption of neutral organic compounds at electrodes was given by Frumkin (22, 23) in two classical papers. The basic Gouy-Chapman-Stern theory was elaborated and extented by Grahame (7) a.o. by the introduction of two characteristic planes in the Stern-layer, the inner Helm-holtz plane (iHp) and the outer Helmholtz plane (oHp).

After the development of these macroscopic theories the atten-tion has been changed. At present, particular emphasis is being laid on the theoretical molecular approach. Much attention has been di-rected to the *structure of the solvent* near the interface and the

4

orientation of the solvent molecules in this region. Basically, all recent models are elaborations of the model of Watts-Tobin (24). Watts-Tobin assumed a two-state orientation for the water molecules near the surface. The recent models developed by Frumkin and Damaskin (25) and Parsons (26) assume the presence of clusters of water molecules having an effective dipole moment differing from the single water dipoles. Bockris and Habib (27) proposed a three-state water model. Recently, Parsons (28,29) has shown that models derived from two-, three- and multi-state orientations must be inconsistent, because a layer of dipoles oriented parallel to a neutral surface is more stable than a layer with 'up' and 'down' orientations. However, the problem of the dipolar potential even near the mercury-electrolyte interface has not been solved satisfactoryly until now.

1.3 ELECTROSORPTION ON SILVER IODIDE

There are many studies of double layer properties and of adsorption of organic compounds at the silver iodide-electrolyte interface. Recently, the interfacial electrochemistry of silver iodide has been reviewed by Sparnaay (15) and by Bijsterbosch and Lyklema (30). In this section, a brief review is given as far as relevant to the present study.

Electrosorption studies of organic molecules on silver iodide arise from the work of Mackor (31), who took aceton as the adsorbent. Elaborate systematic investigations of electrosorption of organic molecules on silver iodide with well-defined electrical parameters have been done by Bijsterbosch (32). He has investigated the adsorption of urea, n-propylalcohol, some butylalcohols, and n-amylalcohol. The curves of the surface charge against the surface potential at different adsorbate concentrations can be considered as an "*electrosorption finger-print*" of the system studied. It appeared that these charge-potential curves have a common intersection point. By a thermodynamic analysis Bijsterbosch has shown that in this point the adsorption of the alcohol as a function of the potential is at a maximum, independent of the adsorbate concentration. It seems that the structure of the water molecules at the surface is responsible for this adsorption maximum. From appli-

5

cation of Gibbs' adsorption law it follows that the desorption of alcohols around the maximum is rather small as compared to the amount present in a complete monolayer. The potential range covered was far too limited to obtain complete desorption. From Gibbs' law only relative adsorption values are obtainable. Absolute adsorption values are obtained indirectly by assuming a Langmuir-type of adsorption. It appears that the adsorption free energy of n-butanol is less negative than in the case of mercury.

Also, de Wit (33) found a common intersection point for the adsorption of ethylene glycol. As compared with butanol, the common intersection point was shifted to the more negative side, which was ascribed to a stronger competition between the ethylene glycol and water dipoles. In this case the desorption around the adsorption maximum is again parabolic as a function of the potential, whereas the total desorption in the measuring range is no more than 5%.

Direct measurements of the double layer capacitance as a function of the potential at the silver iodide-electrolyte interface were performed by de Vooys and Pieper (34). They performed electrosorption measurements of potassium biphthalate and concluded that a virial isotherm fits the measurements. Their results suggest that the standard adsorption free energies of the phthalate ion, the biphthalate ions and phthalic acid are the sum of the electrical energies, as calculated from the potential at the adsorption site and a constant.

1.4 OBJECTS OF THIS STUDY

It was our intention to investigate the effect of the charge of a monomer on the adsorption, and the electrical double layer properties at a reversible surface. This is an extension of the electrosorption study of neutral compounds as performed earlier (32,33). The reason for this choice is twofold. First, the study of charged monomers can be considered as the starting point for future investigations on polyelectrolytes. Second, introduction of a charge on a monomer affects the adsorption equilibrium to a large extent. Introduction of a new variable not always makes the analysis more difficult, but in some cases it is a tool which may sug-

gest a potential solution to several open questions for the adsorption of neutral monomers.

In the present study solutions will be sought for a number of specific questions:

1. *How is the electrical double layer influenced by the charge on an adsorbed monomer?*

Strong specific adsorption of an oppositely charged monomer to the surface will in general lead to reversal of the diffuse charge. It is thus to be expected that the diffuse layer potential is strongly influenced by the adsorption. The effect on the Stern layer is less easy to predict. Also the effect on the charge-potential curves is not known à priori.

2. *How is interfacial thermodynamics affected by introduction of a strongly adsorbed, charged component?*

Interfacial thermodynamics does not tell us where a component will be adsorbed. Introduction of an organic ion is equivalent to the incorporation of a new electrolytic component. Depending on the quantitative experimental conditions equations can be derived which relate the adsorption of both the inorganic and the organic electrolytic components to the electrical parameters.

3. *Is the use of Gibbs' adsorption equation allowed?*

In other words: are the thermodynamic prerequisites met in the particular case studied? For example, is it correct to presume that the differential of the surface tension applies only to that part of the solid-liquid interfacial tension that changes reversibly upon alteration of the experimental condition? Can the adsorption as defined by direct measurements be identified with adsorptions defined in the thermodynamic treatment? Positive answers to these questions are a prerequisite for comparison of thermodynamic and direct adsorptions.

4. *How can we describe the orientation of water molecules at a solid-liquid interface?*

Solid-liquid interfaces are charged by adsorption of ionic species from solution. It is likely that in many cases these charges are more or less localized. In the localized case the dipoles are not orientated by a smeared-out homogeneous electrical field, but a patchwise heterogeneity makes the orientation of the surface dipoles to depend mainly on the local situation.

7

5.   *What is the origin of the common intersection point?*
It is an experimental fact that charge-potential curves at differ-
ent adsorbate concentrations often intersect in a common point.
Intersection points of two or more charge-potential curves are
related by interfacial thermodynamics to an adsorption maximum as
a function of the electrical parameter. We will try to develop a
molecular explanation and investigate whether a common intersection
point also exists with charged adsorbates.
6.   *Are the isotherms congruent in the charge or the potential?*
If congruency applies, the elaboration of the thermodynamic treat-
ment can be simplified to a large extent. Moreover, some conclu-
sions on the molecular situation in the interface may be deduced
from the occurrence of charge or potential congruency in the system.
7.   *What type of isotherm equation is applicable to a system in*
     which an organic ion is specifically adsorbed at a charged
     surface?
An adsorption isotherm equation can be introduced after the assump-
tion of some molecular model. The applicability of a particular
adsorption isotherm equation to a given system may give some infor-
mation on the mutual interactions between the adsorbed molecules
and on the interactions between the adsorbate and the surface.

1.5   OUTLINE OF THIS INVESTIGATION

     The aim of the present investigations was to study the adsorp-
tion of charged organic adsorbates at the silver iodide-electrolyte
interface.
     In order to direct our attention mainly to the adsorption of
the organic ion itself and its dependence on the surface charge,
effects due to the variation of activity coefficients are excluded
in almost all experiments by choosing an indifferent electrolyte
concentration of 0.1 M KNO_3.
     The choice of the adsorbate demands special attention. Some
preliminary measurements on long chain surface active agents (35)
showed that the interpretation is generally complicated by the
occurrence of the formation of a second layer and/or by reorienta-
tion of the asymmetric molecule. Thus a spherical molecule is pre-
ferred. It is advantageous if the substance can be determined ana-

lytically in solution by an easy and relatively fast procedure.
Finally, in order to simplify the theoretical analysis, a compound
which dissociates more or less completely in solution is preferred.
It appeared that symmetrical tetraalkylammonium salts conformed
to all these requirements satisfactorily. Tetrapropyl-, tetrabutyl-
and tetrapentyl ammonium nitrates are used mainly; some other qua-
ternary ammonium ions are also included in some experiments.

A tedious procedure in the electrical characterization of the
silver iodide surface was the potentiometric determination of
charge-potential curves. At the start of the investigations it was
judged useful to automatize this procedure by use of a minicomputer
and a data acquisition system.

This thesis can be subdivided into three substantially differ-
ent parts: the theoretical chapters 2 and 3, the automation chap-
ter 4, and the experimental chapters including the work on tetra-
alkylammonium ions 5, 6 and 7.

Chapter 2 treats the interfacial thermodynamics of the silver
iodide-electrolyte interface in the presence of charged organic
molecules specifically adsorbed at the surface. The basic equations
of interfacial thermodynamics are written out in *ionic* chemical
potentials. Some aspects of earlier treatments (30) are critized
and alternative solutions are offered.

In chapter 3* a molecular model is developed to describe the
orientation of water molecules on a patchwise heterogeneous surface
and the dependence of the χ-potential on surface charge. The conse-
quences of a difference in hydration properties of the potential
determining ions on the χ-potential is given special attention. The
effects on the charge-potential curves are also discussed.

The automation of the potentiometric determination of charge
potential curves is described in chapter 4. Both a description of
the hardware and software of a PDP 11/10-CAMAC data acquisition
system are given in some detail.

Chapter 5 combines some details of the experimental procedures
not given in chapters 6 and 7. This chapter is subdivided in sec-
tions on the analytical determination of the adsorption of tetra-

---

*   Accepted for publication in Can. J. Chem.

alkylammonium ions, on particle electrophoresis measurements, and on the potentiometric titration procedure as far as not given in chapter 3.

The adsorption measurements are treated in chapter 6*. Special attention is given to the occurrence of the adsorption maximum and the correspondence with the common intersection point as present in the charge potential curves. A theoretical model for the common intersection point as a function of the surface potential has been offered. Congruence analysis is applied to the experimental results.

Chapter 7 describes the results of the potentiometric titrations. Integration of charge potential curves gives adsorption values which can be compared with the adsorption measured directly from depletion in solution. The shift of the common intersection point with the length of the alkyl chains on the tetraalkylammonium ions will be explained semi-quantitatively.

1.6 ADSORPTION OF TETRAALKYLAMMONIUM IONS AT A MERCURY ELECTRODE

The adsorption of symmetrical quaternary ammonium halides at the mercury electrode interface has been extensively studied during the last fifteen years with an enhanced emphasis in the past five years. Especially the relation between solution properties and interfacial behaviour has obtained much attention. Apparently, the (hydrophobic) hydration of these ions forms the key factor in the adsorption behaviour. The intermediate position that these ions take in adsorption studies is of particular interest. On the one hand, there is the link with the typical specific adsorption of simple cations, on the other hand there are many relations to the adsorption of neutral molecules.

Adsorption of quaternary ammonium salts at the mercury electrode has already been studied in the beginning of this century. As long ago as 1903 Gouy (21) showed by his classical experiments with the capillary electrometer, that quaternary ammonium ions are ad-

---

sorbed at a negative mercury interface. Frumkin (36) suggested that the adsorption of the organic cation was accompanied by a penetration of the inorganic halide ions in the adsorbed layer. The conclusion that at a certain negative potential a strong desorption of the organic cations (and anions) takes place was derived from capacity measurements by Frumkin, Damaskin and Nikolaeva-Fedorovich (37). Grahame (38) suggested that the adsorption could be interpreted as a "specific" adsorption of the voluminous cations. Bockris, Devanathan and Müller (39) and Devanathan and Tilak (40) showed that the specific adsorbability of quaternary ammonium cations was proportional to their ionic radii in a logarithmic relation.

By electrocapillary experiments, Devanathan and Fernando (41) studied the adsorption behaviour of pure R_4NI-solutions, where R stands for methyl, ethyl, propyl or butyl. The components of charge were calculated by differentiating electrocapillary curves and estimating bulk activity coefficients. They concluded that at the positive side cations are adsorbed onto specifically adsorbed anions. Their results lead to the hypothesis that a second layer must be formed. However, their calculations were heavily attacked by Stokes (42) and H.S. Franks (43). According to these authors the selected activity coefficients of the R_4N^+ were unreasonably high and stemmed from wrong calculations. The criticism of Fernandez and Prue (44) bears the same conclusion, but was derived from a different picture. They concluded that the measurements of the activity coefficients were incorrect because the silver iodide and the tetraalkylammonium iodide formed a complex.

Piro, Bennes and Bou Karam (45) tried to avoid the strong specific adsorption of the iodide ion in replacing it by the bromide ion. The adsorptions calculated from electrocapillary experiments and direct charge measurements showed a typical Langmuir behaviour without any indication of the formation of a second layer. A model was proposed in which the inner layer consists of a monolayer of tetraalkylammonium ions nearest to the mercury, an incomplete layer of anions onto the first, and at the boundary of the diffuse layer there exists a thin, structured water layer.

The electrocapillary measurements by Kůta and Smoler (46) with tetrabutyl- and tetrapropylammonium cations were performed in a me-

dium of 0.1 M HClO$_4$ or 0.05 M H$_2$SO$_4$. Their curves of the charge against the potential at different adsorbate concentrations showed a common intersection point, which is shifted slightly to *less* negative potentials when going from propyl to butyl. The limiting maximum adsorption amounts 2.4 × 10^{-6} and 2.2 × 10^{-6} mol. m^{-2} for the propyl and butyl compound respectively, which agreed well with the values calculated for a close-packed layer using the geometrical model.

Ikeda et al. (47) stressed that the adsorbabilities of the tetraalkylammonium cations were governed by the hydration entropy, and not by the hydration enthalpy. In this respect the specific adsorption of the cations has much in common with the so-called hydrophobic bond.

A very profound study was made by Ménard and Kimmerle (48,49). They investigated the adsorption of 16 tetraalkylammonium halides, R$_4$NX, where R = CH$_3$, C$_2$H$_5$, n-C$_3$H$_7$, and n-C$_4$H$_9$ and X = F, Cl, Br, I. The Esin-Markov effect was critically examined. The specific adsorptions of the cations were interpreted in terms of the same ion-ion and ion-solvent interactions as proposed for homogeneous solutions.

The water structure around the hydrophobic surfaces of quaternary ammonium ions increases significantly if the alkyl chains include three or more carbon atoms. In the case of methyl- and ethyl groups the increase in water structure is absent due to the fact that the much shorter chains cannot penetrate into the intramolecular cavities of the surrounding water to form hydrophobic bonds. This is the reason why Vanel and Schuhmann (50) obtained a very different result for the trimethyl-n-propyl and the tetra-n-pentyl-ammonium ions.

Recently, Hamdi, Bennes, Schuhmann and Vanel (51) studied the influence of the nature of the anion on the adsorption of the tetrabutylammonium cation from halide solutions. Their results are explained by the formation, at the surface of the electrode, of both paired and non-paired ions, the latter neutralizing the charge on the electrode. The importance of the role of hydrophobic forces is stressed. They suggest the formation of superficial aggregrates.

Summarizing, the adsorption of tetraalkylammonium ions on mercury is a sensitive tool in studying the influence of hydrophobic forces and ion-ion interactions at an electrically charged surface. In view of the many similarities between the double layers on

mercury and silver iodide, it would be interesting to study to which extent the picture developed for mercury applies to the silver iodide system. As the metallic mercury phase and the crystalline silver iodide phase do not resemble each other, quantitative differences between the results of the two systems may be expected.

1.7 REFERENCES

1. G. Lippmann, Ann. Physik *149* 546 (1873).

2. H. Freundlich, "Kapillarchemie", Vol. I, 4th ed. p.413. Akad. Verlagsgesellschaft, Leipzig, 1930.

3. M. Frissel, Thesis, Agricultural Research Reports, 67-3 (1961) Pudoc, Wageningen.

4. A.W. Adamson, "Physical Chemistry of Surfaces", 3rd ed., p.464. Interscience, London, 1976.

5. J. Rosinski, Advan. Colloid Interface Sci. *10* 315 (1979).

6. B.N. Hale, J. Kiefer, S. Terrazas and R.C. Ward, J. Phys. Chem. *84* 1473 (1980).

7. D.C. Grahame, Chem. Rev. *41* 441 (1947).

8. R. Parsons, in "Modern Aspects of Electrochemistry" (J.O'M. Bockris, ed.), Vol. 1, p.103. Butterworth, London, 1954.

9. R. Parsons, J. Electroanal. Chem. *7* 136 (1964).

10. A.N. Frumkin and B.B. Damaskin, in "Modern Aspects of Electrochemistry" (J.O'M Bockris and B.E. Conway, eds.), Vol. 3, p.149. Butterworth, London, 1964.

11. P. Delahay, "Double Layer and Electrode Kinetics", Wiley (Interscience), New York, 1965.

12. B.B. Damaskin, A.N. Frumkin and V.V. Batrakov, "Adsorption of Organic Compounds at Electrodes", Part. I, Plenum, New York, 1971.

13. R. Payne, J. Electroanal. Chem. *41* 277 (1973).

14. R. Payne, in "Progress in Surface and Membrane Science" (J.F. Danielli, M.D. Rosenberg and D.A. Cadenhead, Eds.), Vol. 6, p.51. Academic Press, New York, 1973.

15. M.J. Sparnaay, "The Electrical Double Layer". Pergamon Press, Oxford, 1972.

16. S. Trasatti, J. Electroanal. Chem. *53* 335 (1974).

17. S. Trasatti, in "Modern Aspects of Electrochemistry" (B.E. Conway and J.O'M Bockris, eds.), Vol. 13, p.81. Plenum Press, London, 1979.

18. R.M. Reeves, in "Modern Aspects of Electrochemistry" (J.O'M. Bockris and B.E. Conway, eds.), Vol. 10, p.1. Plenum Press, New York, 1974.

19. M.A. Habib, in "Modern Aspects of Electrochemistry" (J.O'M. Bockris and B.E. Conway, eds.). Vol. 12, p.131, Plenum Press, New York, 1977.

20. G. Lippmann, Ann. Chim. Phys. 5 494 (1875).

21. G. Gouy, Ann. Chim. Phys. *29* 145 (1903).

22. A.N. Frumkin, Z. Phys. Chem. *116* 466 (1925).

23. A.N. Frumkin, Z. Phys. *35* 792 (1926).

24. R.J. Watts-Tobin, Philos. Mag. *6* 133 (1961).

25. B.B. Damaskin and A.N. Frumkin, Electrochim. Acta *19* 173 (1974).

26. R. Parsons, J. Electroanal. Chem. *59* 229 (1975).

27. J.O'M. Bockris and M.A. Habib, Electrochimica Acta *22* 41 (1977).

28. R. Parsons, Proc. V International Symposium on Solute-Solute-Solvent Interactions (Florence, 1980). Inorganica Chimica Acta, X31.

29. R. Parsons, J. Electroanal. Chem. *109* 369 (1980).

30. B.H. Bijsterbosch and J. Lyklema, Advan. Colloid Interface Sci. *9* 147 (1978).

31. E.L. Mackor, Thesis, 1951, Utrecht.

32. B.H. Bijsterbosch, Thesis, 1965, Utrecht.

33. J.N. de Wit, Thesis, 1975, Agricultural University, Wageningen.

34. D.A. de Vooys and J.H.A. Pieper, J. Electroanal. Chem. *72* 147 (1976).

35. A. de Keizer and J. Lyklema, Ann. Real Soc. Chim. Espan. Fis. i. Quim. *71* 894 (1975).

36. A.N. Frumkin, "Electrocapillary phenomena and electrode potentials", 1919, Odessa.

37. A.N. Frumkin, B.B. Damaskin and N.V. Nikoloeva-Fedorovich, Doklady Akad. Nauk. S.S.S.R. *115* 751 (1957).

38. D.C. Grahame, Z. Electrochem. *59* 773 (1955).

39. J.O'M. Bockris, M.A.V. Devanathan, K. Müller, Proc. R. Soc. Lond. *A 274* 55 (1963).

40. M.A.V. Devanathan and B.V.K.S.R.A. Tilak, Chem. Rev. *65* 635 (1965).

41. M.A.V. Devanathan and M.J. Fernando, Trans. Far. Soc. *58* 368 (1962).

42. R.H. Stokes, Trans. Faraday Soc. *59* 761 (1963).

43. H.S. Franks, J. Phys. Chem. *67* 1554 (1963).

44. R. Fernandez-Prini and J.E. Prue, J. Phys. Chem. *69* 2793 (1965).

45. J. Piro, R. Bennes and E. Bou Karam, J. Electroanal. Chem. *57* 399 (1974).

46. J. Kûta and I. Smoler, Collection Czechoslov. Chem. Commun. *40* 225 (1975).

47. O. Ikeda, Y. Matsuda, H. Yoneyama and H. Tamura, Electrochimica Acta *21* 519 (1976).

48. F.M. Kimmerle and H. Ménard, J. Electroanal. Chem. *54* 101 (1974).

49. H. Ménard and F.M. Kimmerle, Can. J. Chem. *54* 2488 (1976).

50. P. Vanel and D. Schuhmann, J. Electroanal. Chem. *87* 119 (1978).

51. A. Mazhar, R. Bennes, P. Vanel and D. Schuhmann, J. Electroanal. Chem. *100* 395 (1979).

CHAPTER 2

ON THE CHEMICAL THERMODYNAMICS OF THE
SILVER IODIDE-SOLUTION INTERFACE

2.1 INTRODUCTION

In a lyophobic colloidal system, the relations between the
physical properties of the surface and those of the liquid phase
are in principle governed by the first and the second law of ther-
modynamics. Thermodynamics refers to *macroscopic* properties. There-
fore it is not possible to obtain molecular properties by purely
thermodynamic arguments. For instance, in a system which contains
an interface, thermodynamics does not inform us *where* in the sur-
face phase adsorption of a component takes place, but only that
adsorption *does* occur.

Below, the interfacial thermodynamics will be evaluated for
strong specific adsorption of positively *charged organic ions* to
the solid crystalline surface of silver iodide from an aqueous
electrolyte solution. The Gibbs adsorption law will be used as a
starting point for application to the specific system. Several re-
lations between the macroscopic parameters of the system, such as
temperature, salt concentration, adsorbate concentration, adsorp-
tion of the components from the solution, surface charge, and sur-
face potential, will result. The application of thermodynamics
necessitates that a thermodynamic quantity is identified with a
corresponding experimental one.

In the present study the electrical behaviour of the surface
is of major importance. It will be shown that from a thermodynamic
point of view all equations can be equally well formulated with
the surface charge or the surface potential as the independent elec-
trical parameter. However, a choice is usually made if adsorption
isotherms are analysed, so that an isotherm is described at a con-

stant value of one of them. The importance and the consequences of this choice will be discussed.

Very recently, Bijsterbosch and Lyklema (1) have reviewed the interfacial thermodynamics of AgI. Here we will treat the subject for the case of strong specific adsorption of organic ions instead of neutral molecules. Our treatment differs with respect to some details.

The present treatment has been limited to the case of small concentrations where the ionic strength is completely determined by a swamping, indifferent electrolyte. Removing this restriction would imply that rather complex relations between the chemical potentials have to be taken into account, e.g. according to the theory of Kirkwood and Buff (2,3). Moreover, this would also require tremendous extension of the necessary experimental data without leading to substantially new insight. Therefore, we have not pursued this path.

2.2 BASIC EQUATIONS

The system consists of a crystalline solid phase α (silver iodide) and an aqueous electrolyte solution phase β. Viewed on a molecular scale the physical properties of one bulk phase change over a finite distance into the properties of the other bulk phase. The physical space in which this transformation takes place is called the *interfacial layer*. The ideal situation would be that we know in detail how the different properties, especially the concentrations of all components, change within this inhomogeneous layer. This cannot be obtained by thermodynamics.

Interfacial properties can be derived from macroscopic properties by using the *Gibbs convention* (4,5). A Gibbs dividing surface, located somewhere in the interfacial layer, formally defines the two bulk volumes. Excess thermodynamic quantities referred to this Gibbs surface can now be defined as the excess of matter, entropy etc. in the real system over the hypothetical system which consists of two homogeneous phases up to the Gibbs surface. The choice of the location of the Gibbs surface is, in principle, free. However, for the system used in the present study it will appear that the interpretation of some parameters is easiest if we identify the Gibbs surface with the physical crystal surface.

18

The *Gibbs adsorption equation* (2.1) can be considered as the basic equation of interfacial thermodynamics.

$$d\gamma = - s^{\sigma}dT - \sum_i \Gamma_i^{\sigma} d\mu_i \tag{2.1}$$

Here, γ is the interfacial tension, T is the temperature, and the μ_i's are the chemical potentials of the components i. The surface excess concentration Γ_i^{σ} and the surface excess entropy s^{σ} are de-fined according to the Gibbs convention as

$$\Gamma_i^{\sigma} \equiv (n_i - n_i^{\alpha} - n_i^{\beta})/A_s \tag{2.2}$$

$$s^{\sigma} \equiv (S - S^{\alpha} - S^{\beta})/A_s \tag{2.3}$$

where n_i, n_i^{α} and n_i^{β} are the numbers of moles of component i in the total system and in the phases α and β respectively, S is the entropy, and A_s the area of the interface.

In applying (2.1) to experimental data, the adsorption process must be *reversible* and the system must attain *equilibrium.* The phys-ical significance of the interfacial tension γ for a solid-liquid interface is a subject for discussion, because the solid surface can-not easily be enlarged reversibly and consequently the equilibrium condition is not positively met. A non-thermodynamic argument can be used to solve the problem. As discussed by Bijsterbosch and Lyklema (1) the solid structure is not changed during the time of the experiment. The consequence is, that although γ is not well defined, dγ is, since the differential dγ refers to only that part of γ attributable to adsorption-desorption processes on the solution side. Nevertheless, it will always be useful to test the Gibbs equation by direct experiment, which can be considered as a check of the occurrence of reversibility and attainment of equilib-rium in the system.

The Gibbs equation can now be applied to the specific system studied. This system consists of a dispersion of silver iodide par-ticles in an aqueous electrolyte solution of silver nitrate or po-tassium iodide, potassium nitrate, and a nitrate salt with an organ-ic cation A^+ (e.g. tetraalkylammonium). The silver and iodide ions

19

determine the potential drop across the interface and are called *potential-determining (p.d.) ions*. Potassium nitrate is present in a much higher concentration than $AgNO_3$, KI and ANO_3. The KNO_3 determines mainly the ionic strength of the solution and is called the *indifferent electrolyte*. The organic cation A^+ is strongly specifically adsorbing. Obviously, the equation derived can be easily generalized for other electrolytes present in solution. It is assumed that all electrolytes present in the solution are fully dissociated (*strong electrolytes*) and that dissociation of the water may be neglected.

One can introduce either neutral or ionic components in the summation of (2.1). However, in order to apply the Gibbs equation, it must contain only variables which can be identified with the experimental ones. This can be obtained by combination of some ionic components or separating some electroneutral combinations into ionic parameters. Since the ions are the real physical entities in the solution, it seems more straightforward to start with ionic components. One must realize, that although chemical potentials of separate ions are not absolutely measurable, differentials are in principle. For instance, $d\mu_{Ag+}$ can be measured with a reversible AgI- and NO_3^--electrode, if a swamping, "indifferent" electrolyte (KNO_3) is present. A serious drawback of the use of only neutral components is, that it is often suggested that the chemical potential of one of the components say $AgNO_3$ is mainly determined by its concentration (apart from activity effects) whereas the presence of KNO_3 in solution may be of the same importance ($\mu_{AgNO_3} = \mu_{Ag+} + \mu_{NO_3-}$).

The components of our system are introduced in (2.1).

$$dy = - s^\sigma dT - \Gamma^\sigma_{AgI} d\mu_{AgI} - \Gamma^\sigma_{H_2O} d\mu_{H_2O} - \Gamma^\sigma_{Ag+} d\mu_{Ag+} - \Gamma^\sigma_{I-} d\mu_{I-} - \Gamma^\sigma_{K+} d\mu_{K+} -$$

$$- \Gamma^\sigma_{NO_3-} d\mu_{NO_3-} - \Gamma^\sigma_{A+} d\mu_{A+} \tag{2.4}$$

The chemical potentials are not mutually independent and are not independent of the temperature either. It will be shown that there are two relations between the temperature and the chemical potentials, two relations between the chemical potentials, and three re-

20

lations between the excess interfacial concentrations. By means of these seven auxilary conditions, an equation can be derived with the correct number of variables. The resulting parameters will have a more intimate relation with the corresponding experimental variables.

Auxiliary conditions

1. A characteristic feature of a solid-solution system is that the solid phase consists usually of one component not occurring in measurable amounts in the solution phase. Thus, the silver iodide term can be neglected in the *Gibbs-Duhem equation* for the *solution phase*. This equation is applied to eliminate the chemical potential of one of the solution components. Water is the best choice, because it is the major component in the solution. Hence, the variation of the chemical potential of water will be small as compared to the variations of the chemical potentials of the other components.

$$d\mu_{H_2O} = -s^\beta dT - \frac{x_{Ag+}}{x_{H_2O}}d\mu_{Ag+} - \frac{x_{I-}}{x_{H_2O}}d\mu_{I-} - \frac{x_{K+}}{x_{H_2O}}d\mu_{K+} - \frac{x_{NO_3-}}{x_{H_2O}}d\mu_{NO_3-} - \frac{x_{A+}}{x_{H_2O}}d\mu_{A+} \quad (2.5)$$

The quantities s^β and x_i are defined according to (2.6) and (2.7). In ideal dilute solutions s^β and x_i can be identified with the molar entropy of the solution and the mole fraction of solution component i respectively.

$$s^\beta \equiv S^\beta/n^\beta_{H_2O} \quad (2.6)$$

$$x_i \equiv n^\beta_i/\sum_i n^\beta_i \quad (2.7)$$

2. The *Gibbs-Duhem equation* can also be applied to the *solid phase* to eliminate μ_{AgI}. The quantity s^α is defined according to (2.9).

$$d\mu_{AgI} = -s^\alpha dT \quad (2.8)$$

$$s^\alpha \equiv S^\alpha/n^\alpha_{AgI} \quad (2.9)$$

The Gibbs-Duhem equations for the solution (2.5) and the solid (2.8) can be introduced into the Gibbs equation (2.1).

$$d\gamma = - (s^\sigma - s^\alpha \Gamma_{AgI}^\sigma - s^\beta \Gamma_{H_2O}^\sigma)dT - (\Gamma_{Ag+}^\sigma - \frac{x_{Ag+}}{x_{H_2O}}\Gamma_{H_2O}^\sigma)d\mu_{Ag+} - (\Gamma_{I-}^\sigma - \frac{x_{I-}}{x_{H_2O}}\Gamma_{H_2O}^\sigma)d\mu_{I-}$$

$$- (\Gamma_{K+}^\sigma - \frac{x_{K+}}{x_{H_2O}}\Gamma_{H_2O}^\sigma)d\mu_{K+} - (\Gamma_{NO_3-}^\sigma - \frac{x_{NO_3-}}{x_{H_2O}}\Gamma_{H_2O}^\sigma)d\mu_{NO_3-} - (\Gamma_{A+}^\sigma - \frac{x_{A+}}{x_{H_2O}}\Gamma_{H_2O}^\sigma)d\mu_{A+}$$

$$(2.10)$$

The following relative surface excess quantities can be defined

$$s^{(s)} \equiv s^\sigma - s^\alpha \Gamma_{AgI}^\sigma - s^\beta \Gamma_{H_2O}^\sigma \qquad (2.11)$$

$$\Gamma_i^{(s)} \equiv \Gamma_i^\sigma - \frac{x_i}{x_{H_2O}} \Gamma_{H_2O}^\sigma \qquad (2.12)$$

The Gibbs equation can now be written as

$$d\gamma = - s^{(s)}dT - \Gamma_{Ag+}^{(s)}d\mu_{Ag+} - \Gamma_{I-}^{(s)}d\mu_{I-} - \Gamma_{K+}^{(s)}d\mu_{K+} - \Gamma_{NO_3-}^{(s)}d\mu_{NO_3-} - \Gamma_{A+}^{(s)}d\mu_{A+} \qquad (2.13)$$

The relative surface excess entropy $s^{(s)}$ and the relative surface excess concentration $\Gamma_i^{(s)}$ are independent of the choice of the Gibbs surface. This can be proved by introducing two Gibbs surfaces x and y located at a distance λ apart. The surface excess entropies at x and y are called s^x and s^y, and for the surface excess concentrations the symbols Γ_i^x and Γ_i^y respectively are used. From the definition of excess quantities the relation between these quantities at x and y follows directly

$$s^y = s^x - (s^\alpha \cdot c_{AgI}^\alpha - s^\beta \cdot c_{H_2O}^\beta)\lambda \qquad (2.14)$$

$$\Gamma_i^y = \Gamma_i^x - (c_i^\alpha - c_i^\beta)\lambda \qquad (2.15)$$

The identity of $s^{(s)}$ at x and y follows from (2.11), (2.14) and (2.15).

$$s^{(y)} \equiv s^y - s^\alpha \Gamma^y_{AgI} - s^\beta \Gamma^y_{H_2O} =$$

$$= s^x - (s^\alpha c^\alpha_{AgI} - s^\beta c^\beta_{H_2O})\lambda - s^\alpha(\Gamma^x_{AgI} - c^\alpha_{AgI}\lambda) - s^\beta(\Gamma^x_{H_2O} + c^\beta_{H_2O}\lambda) =$$

$$= s^x - s^\alpha \Gamma^x_{AgI} - s^\beta \Gamma^x_{H_2O} \equiv s^{(x)} \tag{2.16}$$

The identity of $\Gamma^{(s)}_i$ for i is not equal to AgI at x and y follows analogously from (2.12) and (2.13)

$$\Gamma^{(y)}_i \equiv \Gamma^y_i - \frac{x_i}{x_{H_2O}} \Gamma^y_{H_2O} = \Gamma^x_i + c^\beta_i \lambda - \frac{x_i}{x_{H_2O}} \Gamma^x_{H_2O} - \frac{x_i}{x_{H_2O}} c^\beta_{H_2O} \lambda$$

$$= \Gamma^x_i - \frac{x_i}{x_{H_2O}} \Gamma^x_{H_2O} \equiv \Gamma^{(x)}_i \tag{2.17}$$

It is concluded that $s^{(s)}$ and $\Gamma^{(s)}_i$ do not depend on the location of the Gibbs surface. It must be realized that $\Gamma^{(s)}_{AgI}$ cannot be defined according to (2.12). However, the relative surface excess concentration of AgI is not contained in the basic equation either, so that a definition is not needed.

3.   The concentrations of silver and iodide ions in solution are related by the *solubility product* of silver iodide. In fact, one can equalize the chemical potential of the solid silver iodide to the sum of the chemical potentials of the silver and iodide ions:

$$\mu_{Ag+} + \mu_{I-} = \mu_{AgI}. \tag{2.18}$$

According to (2.8), the chemical potential of silver iodide is only a function of the temperature, so that

$$d\mu_{Ag+} + d\mu_{I-} = d\mu_{AgI} = - s^\alpha dT \tag{2.19}$$

4.   The *ionic strength* of the solution is changed by variation of the KNO_3 concentration. If it is assumed that the activity coefficients of K^+ and NO_3^- in solution are equal at the same ionic concentration, the differentials of the chemical potentials of K^+ and NO_3^- must be equal too. However, it must be kept in mind that ionic activity coefficients and ionic chemical potentials are not measurable and that the splitting up into ionic contributions of the molecular quantities is not based on thermodynamics but on model considerations. In our experiments, c_{KNO_3} was always much higher than the concentrations of $AgNO_3$, KI and ANO_3. Equation (2.20) follows directly from the definition of ionic chemical potentials, whereas (2.21) is based on the assumption just mentioned (c_{KNO_3} >> all other electrolyte concentrations)

$$\mu_{KNO_3} = \mu_{K+} + \mu_{NO_3-} \tag{2.20}$$

$$d\mu_{KNO_3} = d\mu_{K+} + d\mu_{NO_3-} \cong 2d\mu_{K+} \cong 2d\mu_{NO_3-} \tag{2.21}$$

5.   The surface excess concentrations of the ionic components are related by an equation of *electroneutrality*. This applies both to Γ_i^σ and $\Gamma_i^{(s)}$. Hence:

$$\Gamma_{Ag+}^\sigma - \Gamma_{I-}^\sigma + \Gamma_{K+}^\sigma - \Gamma_{NO_3-}^\sigma + \Gamma_{A+}^\sigma = 0 \tag{2.22}$$

and

$$\Gamma_{Ag+}^{(s)} - \Gamma_{I-}^{(s)} + \Gamma_{K+}^{(s)} - \Gamma_{NO_3-}^{(s)} + \Gamma_{A+}^{(s)} = 0 \tag{2.23}$$

6.   The silver and iodide ions are potential determining ions which, upon adsorption, are incorporated in the silver iodide lattice. From a thermodynamic point of view they are indistinguishable from the ions composing the crystal lattice. The difference in adsorption of these ions is called the *surface charge* and it is usually defined according to (2.24).

$$\sigma \equiv F \ (\Gamma_{Ag+}^{(s)} - \Gamma_{I-}^{(s)}) \tag{2.24}$$

Experimentally, the adsorptions of the silver and iodide ions cannot be determined separately. This is due to the fact that by potentiometric determination the concentrations of both silver and

iodide ions follow from a single potential difference. Thus a desorption of silver ions is indistinguishable from an adsorption of iodide ions. Only the difference in adsorption, i.e. σ/F, can be estimated and this difference is thus thermodynamically defined.

As long as only differences in the adsorptions of Ag^+ and I^- occur in the equation, we do not have to worry about the significance of the single Γ values of p.d. ions. However, in the treatment of the temperature dependence single surface excess concentrations will arise. The crucial question is: can a positive adsorption of both silver and iodide ions exist simultaneously? From a molecular point of view the answer is definitely positive. On a molecular level surface charges may be discrete and overall excesses of positive charges as well as negative charges may exist. However, surface excess quantities are defined through only macroscopic quantities. Thus, thermodynamically $\Gamma^\sigma_{Ag^+}$, $\Gamma^\sigma_{I^-}$ and Γ^σ_{AgI} are related, because of a chemical reaction between Ag^+ and I^- at the surface. Thermodynamically (i.e. from macroscopic properties) the simultaneous adsorption of one Ag^+-ion and one I^--ion is indistinguishable from the adsorption of a neutral AgI entity. It is now assumed that adsorbed pairs of Ag^+ and I^- ions may be identified as one adsorbed AgI molecule. The surface charge can then be redefined according to this assumption. For convenience, we distinguish two definitions for positive and negative charges respectively.

$$\sigma \geqq 0 \qquad \sigma \equiv F\Gamma^{(s)}_{Ag^+} \qquad \Gamma^{(s)}_{I^-} \equiv 0 \tag{2.25a}$$

$$\sigma \leqq 0 \qquad \sigma \equiv -F\Gamma^{(s)}_{I^-} \qquad \Gamma^{(s)}_{Ag^+} \equiv 0 \tag{2.25b}$$

Introducing the following notations for the ionic *components of charge*,

$$\sigma_+ \equiv F\ \Gamma^{(s)}_{K^+} \tag{2.26}$$

$$\sigma_- \equiv -F\ \Gamma^{(s)}_{NO_3^-} \tag{2.27}$$

$$\sigma_{A^+} \equiv F\ \Gamma^{(s)}_{A^+} \tag{2.28}$$

it is possible to rewrite (2.13) by introducing (2.19), (2.21), (2.23), (2.25a,b), (2.26), (2.27), and (2.28).

$$\sigma \geq 0 \qquad d\gamma = -s^{(s)}dT - \frac{\sigma}{F}d\mu_{Ag+} - (\frac{\sigma}{2} + \sigma_+ + \frac{\sigma_{A+}}{2})\frac{d\mu_{KNO_3}}{F} - \Gamma_{A+}^{(s)}d\mu_{A+} \qquad (2.29a)$$

$$\sigma \leq 0 \qquad d\gamma = -s^{(s)}dT + \frac{\sigma}{F}d\mu_{I-} - (\frac{\sigma}{2} + \sigma_- + \frac{\sigma_{A+}}{2})\frac{d\mu_{KNO_3}}{F} - \Gamma_{A+}^{(s)}d\mu_{A+} \qquad (2.29b)$$

These important equations are the starting-point for further deri-
vations by use of the property of the total differential. It must
be realized that the parameters T, μ_{Ag+}, μ_{KNO_3}, and μ_{A+} are still
not independent, albeit that their mutual dependences are much
weaker than in the starting equation (2.4) (or in the corresponding
equation with only neutral components). For example, μ_{Ag+} is depen-
dent on temperature and ionic strength of the solution. Convenient
variables in the experiments are T, c_{Ag+} (or c_{I-}), c_{KNO_3}, and c_{A+},
which are now more intimately related with the variables in
(2.29a,b) than with the variables in the starting equation (2.4).

The electrical variables of the system, the surface charge and
the surface potential, can be identified with non-electrical thermo-
dynamical variables. The *surface charge* σ was already defined from
relative excess surface concentrations of potential-determining
ions according to (2.24) or alternatively (2.25a) and (2.25b). The
surface potential $\Delta\phi$ is the difference of potential between the
bulk of the solid (ϕ^S) and the solution phase (ϕ^L). The potential
difference $\Delta\phi$ is in fact a Galvani-potential difference. It is re-
lated to the concentration of p.d. ions by *Nernst's law*. This law
follows from the equality of the electrochemical potentials of both
potential-determining ions in the solid phase S and the solution
phase L (see also chapter 3).

$$\tilde{\mu}_{Ag+}^{S0}(T) + F\phi^S = \tilde{\mu}_{Ag+}^L = \tilde{\mu}_{Ag+}^{L0} + RT \ln a_{Ag+} + F\phi^L \qquad (2.30)$$

$$\tilde{\mu}_{I-}^{S0}(T) - F\phi^S = \tilde{\mu}_{I-}^L = \tilde{\mu}_{I-}^{L0} + RT \ln a_{I-} - F\phi^L \qquad (2.31)$$

The introduction of electrical potentials instead of chemical po-
tentials of p.d. ions enables a comparison of the equation derived
for the AgI-electrolyte interface with those for the mercury elec-
trolyte interface.

The chemical potentials of p.d. ions as given in (2.29a,b) are independent variables, whereas the surface charge is a dependent variable. Equations (2.29a,b) can be transformed by the introduction of two new total differentials in order to make the surface charge the independent variable. From a thermodynamic point of view, both descriptions have the same rigour. In analysing the experiments one description may be preferable to the other. New variables are defined according to

$$\xi^+ \equiv \gamma + \frac{\sigma}{F} \mu_{Ag+} \tag{2.32a}$$

$$\xi^- \equiv \gamma - \frac{\sigma}{F} \mu_{I-} \tag{2.32b}$$

Differentiation of (2.32a,b) and elimination of $d\gamma$ from (2.29a,b) offers the desired equation.

$$\sigma \geqq 0 \qquad d\xi^+ = - s^{(s)}dT + \mu_{Ag+} \frac{d\sigma}{F} - (\frac{\sigma}{2} + \sigma_+ + \frac{\sigma_{A+}}{2}) \frac{d\mu_{KNO_3}}{F} - \Gamma_{A+}^{(s)}d\mu_{A+} \tag{2.33a}$$

$$\sigma \leqq 0 \qquad d\xi^- = - s^{(s)}dT - \mu_{I-} \frac{d\sigma}{F} - (\frac{\sigma}{2} + \sigma_- + \frac{\sigma_{A+}}{2}) \frac{d\mu_{KNO_3}}{F} - \Gamma_{A+}^{(s)}d\mu_{A+} \tag{2.33b}$$

Also from (2.33a,b) several new relations can be derived by cross-differentiation.

2.3 ELABORATIONS OF THE GIBBS ADSORPTION EQUATION

The property of the total differential can be used in the cross-differentiation of all the RHS terms of (2.29a,b) and (2.33a,b) respectively. It is not our goal to evaluate all the possible cross-differentiations, but some practical examples will be selected.

2.3.1 *Adsorption and charge-potential relation*

The adsorption of the organic cation A^+ can be derived from the relation between the surface charge and the concentration of p.d. ions (or the potential). Cross-differentiation of the $\frac{\sigma}{F} d\mu_{Ag+}$ and $\Gamma_{A+}^{(s)}d\mu_{A+}$ terms in (2.29a) gives

$$\left(\frac{\partial \Gamma_{A+}^{(s)}}{\partial \mu_{Ag+}} \right)_{T,\mu_{KNO_3},\mu_{A+}} = \left(\frac{\partial \sigma/F}{\partial \mu_{A+}} \right)_{T,\mu_{Ag+},\mu_{KNO_3}} \tag{2.34}$$

Because according to (2.19) at constant temperature $d\mu_{Ag+} = - d\mu_{I-}$, (2.34) can also be derived from (2.29b). The chemical potentials of the Ag^+ and A^+ ions are related to the activities of these ions, a_{Ag+} and a_{A+}, in solution.

$$\mu_{A+} = \mu_{A+}^0 + RT \ln a_{A+} = \mu_{A+}^0 + RT \ln f_{A+} + RT \ln c_{A+} \tag{2.35}$$

$$\mu_{Ag+} = \mu_{Ag+}^0 + RT \ln a_{Ag+} = \mu_{Ag+}^0 + RT \ln f_{Ag+} + RT \ln c_{Ag+} \tag{2.36}$$

If the concentration of K^+ is much higher than c_{A+} and c_{Ag+}, the activity coefficients f_{A+} and f_{Ag+} can be assumed constant by approximation. Then the following approximate equations hold

$$d\mu_{A+} \cong 2.303 \, RT \, d\log c_{A+} \equiv - 2.303 \, RT \, d \, pA \tag{2.37}$$

$$d\mu_{Ag+} \cong 2.303 \, RT \, d\log c_{Ag+} \equiv - 2.303 \, RT \, d \, pAg \tag{2.38}$$

Integration of (2.34) leads to the interfacial adsorption $\Gamma_{A+}^{(s)}$ at a given pAg relative to that at a reference pAg*

$$\Gamma_{A+}^{(s)} - \Gamma_{A+}^{(s)*} = \frac{1}{F} \int_{pAg*}^{pAg} \left(\frac{\partial \sigma}{\partial pA} \right)_{T,pAg,\mu_{KNO_3}} dpAg \tag{2.39}$$

To obtain absolute values $\Gamma_{A+}^{(s)}$ as a function of the pAg, the adsorption in some reference point, $\Gamma_{A+}^{(s)*}$, has to be estimated.

From (2.33a) or (2.33b) a corresponding integral can be obtained with the surface charge as the independent variable

$$\Gamma_{A+}^{(s)} - \Gamma_{A+}^{(s)*} = \frac{1}{F} \int_{\sigma*}^{\sigma} \left(\frac{\partial pAg}{\partial pA} \right)_{T,\sigma,\mu_{KNO_3}} d\sigma \tag{2.40}$$

The results derived from (2.39) and (2.40) must be equal. One must realize, however, that experimental inaccuracies may have a different weight in the two equations. If differences are not a result of experimental errors, they must be ascribed to the inadequacy of the thermodynamic premises or the approximations made. This fact may be a potential but not necessarily exclusive test of the applicability of interfacial thermodynamics to a specific system.

From (2.39) or (2.40) relative surface excess concentrations are determined. These $\Gamma_{A+}^{(s)}$ values are numerically equal to the surface excess concentrations Γ_{A+}^{σ} with the Gibbs surface located in such a way that $\Gamma_{H_2O}^{\sigma}$ is zero. According to Everett (5), the relative adsorption $\Gamma_{A+}^{(s)}$ can also be obtained from experiment as the excess, per unit area of solid/liquid interface, of the amount of component i in the actual system, over the amount of i in a reference system containing the same amount of H_2O as the real system and in which a constant composition, equal to that of the bulk liquid in the real system, is maintained throughout the liquid phase:

$$\Gamma_i^{(s)} = A_s^{-1} (n_i - n_{H_2O} x_i^1 / x_{H_2O}^1) \tag{2.41}$$

where n_i and n_{H_2O} are the number of moles of component i and H_2O in the system, and x_i^1 is defined according to (2.7), whereas 1 denotes the situation after adsorption. Thus the relative surface excess concentration is experimentally well accessible. One must be warned that to obtain the *relative* adsorption the calculation must be based on the number of H_2O molecules in the system, n_{H_2O}, and not on the *total* number of molecules in the system nor on the volume of the aqueous phase. In the limiting case of very low concentrations of the adsorbate, calculations of Γ^{σ} do not depend on the location of the Gibbs surface anymore, and $\Gamma_i^{(s)} \cong \Gamma_i^{\sigma}$. This will be the case for all our measurements.

2.3.2 *Temperature dependence of the electrical parameters*

In this and the next section we will limit ourselves to the case of $\sigma \geqq 0$. For $\sigma \leqq 0$ the derivations are completely analogous. The dependencies of σ and μ_{Ag+} on temperature follow from (2.29a)

and (2.33a)

$$F \left(\frac{\partial s^{(s)}}{\partial \mu_{Ag+}} \right)_{T,\mu_{KNO_3},\mu_{A+}} = \left(\frac{\partial \sigma}{\partial T} \right)_{\mu_{Ag+},\mu_{KNO_3},\mu_{A+}} \tag{2.43}$$

$$F \left(\frac{\partial s^{(s)}}{\partial \sigma} \right)_{T,\mu_{KNO_3},\mu_{A+}} = \left(\frac{\partial \mu_{Ag+}}{\partial T} \right)_{\sigma,\mu_{KNO_3},\mu_{A+}} \tag{2.44}$$

The temperature dependence of σ and μ_{Ag+} given in the equations above does not follow directly from the experiments, because the measurements are not performed at constant μ_{KNO_3} and μ_{A+} but (as a first approximation) at constant c_{KNO_3} and c_{A+}. Variations of T at constant c_{KNO_3} changes μ_{KNO_3}. Thus the partial differential quotients in the RHS of (2.43) and (2.44) have to be transformed. This can be done by the extended chain rule according to appendix 1. In previous work (1,4) only (2.43) has been used and three- and four-product terms have been neglected.

In applying (A2.3) and (A2.2) to (2.43) and (2.44) the following relations and approximations are used:

$$\left(\frac{\partial \mu_{Ag+}}{\partial T} \right)_{pAg,c_{KNO_3},c_{A+}} = - s_{Ag+}^0 + R \ln a_{Ag+} = - s_{Ag+}^\phi - 2.3 \, R \, pAg \tag{2.45}$$

$$\left(\frac{\partial \mu_{A+}}{\partial T} \right)_{pAg,c_{KNO_3},c_{A+}} = - s_{A+}^0 + R \ln a_{A+} = - s_{A+}^\phi - 2.3 \, R \, pA \tag{2.46}$$

$$\left(\frac{\partial \mu_{KNO_3}}{\partial T} \right)_{pAg,c_{KNO_3},c_{A+}} = - s_{KNO_3}^0 + R \ln a_{KNO_3} \tag{2.47}$$

$$\left(\frac{\partial \sigma}{\partial \mu_{Ag+}} \right)_{T,c_{KNO_3},c_{A+}} = \frac{0.058}{2.3RT} \, C \tag{2.48}$$

$$\left(\frac{\partial \mu_{Ag+}}{\partial \mu_{A+}} \right)_{\sigma,T,\mu_{KNO_3}} \cong 0 \tag{2.49}$$

where $s_i^\phi = s_i^0 + R \ln f_i$ with f_i the activity coefficient of i and C is the differential capacitance $(d\sigma/d\Delta\phi)$. We have used the fact that c_{K+} is much higher than c_{Ag+} and c_{A+}. Finally, we considered that at fixed T a constant c_{KNO_3} implies a constant μ_{KNO_3} and, moreover, at fixed T and fixed c_{KNO_3} a constant c_{Ag+} and c_{A+} implies a constant μ_{Ag+} and μ_{A+}.

The transformation of (2.43) gives

$$- F \left(\frac{\partial s^{(s)}}{\partial pAg}\right)_{T,c_{KNO_3},c_{A+}} =$$

$$\left(\frac{\partial\sigma}{\partial T}\right)_{pAg,c_{A+},c_{KNO_3}} - \frac{0.058}{2.3RT} C \left[-s_{Ag+}^\phi -2.3RpAg\right] - \left(\frac{\partial\sigma}{\partial\mu_{A+}}\right)_{T,pAg,c_{KNO_3}}\left[-s_{A+}^\phi -2.3RpA\right]$$

$$\left[-\left(\frac{\partial\sigma}{\partial\mu_{KNO_3}}\right)_{T,pAg,c_{A+}} +\frac{0.058}{2.3RT}C\left(\frac{\partial\mu_{Ag+}}{\partial\mu_{KNO_3}}\right)_{pAg,c_{A+},T} +\left(\frac{\partial\sigma}{\partial\mu_{A+}}\right)_{pAg,T,c_{KNO_3}}\left(\frac{\partial\mu_{A+}}{\partial\mu_{KNO_3}}\right)_{pAg,c_{A+},T}\right].$$

$$\left(-s_{KNO_3}^0 + R \ln a_{KNO_3}\right) \tag{2.50}$$

Evidently, in the absence of an organic adsorbate some of the RHS term will vanish. It can easily be shown that exchange of z_2 and z_3 in (A2.3) gives exactly the same equation. Equation (2.50) differs in some respects from the corresponding equation given earlier (ref. 1). Apart from some details, the dependencies of μ_{Ag+} and μ_{A+} on μ_{KNO_3} are neglected in ref. 1, due to the application of a reduced chain rule. Terms, containing single Ag^+ or I^- adsorption are absent in (2.50) as follows from an alternative definition of σ.

Application of (A2.2) on (2.44) and introduction of (2.45-2.49) gives the dependence of the excess interfacial entropy on surface charge

$$F \left(\frac{\partial s^{(s)}}{\partial\sigma}\right)_{T,c_{KNO_3},c_{A+}} =$$

$$- s_{Ag+}^\phi -2.3 R pAg - \frac{2.3 RT}{0.058C}\left(\frac{\partial\sigma}{\partial T}\right)_{pAg,c_{KNO_3},c_{A+}} -\left(\frac{\partial\mu_{Ag+}}{\partial\mu_{KNO_3}}\right)_{\sigma,T,c_{A+}}\left[-s_{KNO_3}^0 + R\ln a_{KNO_3}\right]$$

$$\tag{2.51}$$

The differentials in (2.51) follow from experiment, whereas $(\partial\mu_{Ag+}/\partial\mu_{KNO_3})\sigma,T,c_{A+}$ can also be evaluated from Gouy-Chapman theory in first approximation. The application of (2.51) seems much easier than (2.50), although both equations must ultimately lead to the same results.

2.3.3 *Temperature dependence of the adsorption*

An experimentally well-accessible property is the temperature dependence of the adsorption of the organic ion at constant σ, c_{KNO_3} and c_{A+}. Application of (A2.2) to (2.33a) gives

$$\left(\frac{\partial s^{(s)}}{\partial\mu_{A+}}\right)_{T,\sigma,\mu_{KNO_3}} = -\frac{1}{2.3RT}\left(\frac{\partial s^{(s)}}{\partial pA+}\right)_{T,\sigma,c_{KNO_3}} = \left(\frac{\partial\Gamma^{(s)}_{A+}}{\partial T}\right)_{\sigma,\mu_{KNO_3},\mu_{A+}}$$

or

$$-\frac{1}{2.3RT}\left(\frac{\partial s^{(s)}}{\partial pA}\right)_{T,\sigma,c_{A+}} = \left(\frac{\partial\Gamma^{(s)}_{A+}}{\partial T}\right)_{\sigma,c_{A+},c_{KNO_3}} - \left(\frac{\partial\Gamma^{(s)}_{A+}}{\partial\mu_{A+}}\right)_{\sigma,c_{KNO_3},T}\left[-s^{\phi}_{A+}-2.3RpA\right]$$

$$-\left[\left(\frac{\partial\Gamma^{(s)}_{A}}{\partial\mu_{KNO_3}}\right)_{T,\sigma,c_A+} - \left(\frac{\partial\Gamma^{(s)}_{A+}}{\partial\mu_{A+}}\right)_{T,\sigma,c_{KNO_3}}\left(\frac{\partial\mu_{A+}}{\partial\mu_{KNO_3}}\right)_{\sigma,T,c_{A+}}\right]\cdot\left[-s^{0}_{KNO_3} + Rlna_{KNO_3}\right]$$

$$(2.52)$$

The excess entropy $s^{(s)}$, as obtained from (2.51) or (2.52), is a very useful parameter in the molecular interpretation of adsorption phenomena, because it contains information on the entropy of the adsorbate and on the structuring of the interfacial solvent with and without adsorbate.

2.3.4 *Ionic components of charge and the Esin-Markov coefficient*

The surface charge on the solid is compensated by the charge due to the ionic species K^+, NO_3^- and A^+ in the electrolyte solution (if the concentrations of Ag^+ and I^- can be neglected). These ionic contributions σ_+, σ_- and σ_{A+} are defined in (2.26-2.28) and called ionic components of charge. The dependence of the surface charge on the concentration of A^+ has been derived in section 2.3.1. Here we will derive expressions for σ_+ and σ_- in order to show the effect of the presence of an organic adsorbate on these expressions.

32

The dependence of the surface charge on the KNO_3 concentration follows from either (2.29a) or (2.29b):

$$\left(\frac{\partial \sigma}{\partial \mu_{KNO_3}}\right)_{T,\mu_{Ag+},\mu_{A+}} = \left(\frac{\partial(\frac{\sigma}{2} + \sigma_+ + \frac{\sigma_{A+}}{2})}{\partial \mu_{Ag+}}\right)_{T,\mu_{KNO_3},\mu_{A+}} \quad (2.53a)$$

$$- \left(\frac{\partial \sigma}{\partial \mu_{KNO_3}}\right)_{T,\mu_{I-},\mu_{A+}} = \left(\frac{\partial(\frac{\sigma}{2} + \sigma_- + \frac{\sigma_{A+}}{2})}{\partial \mu_{I-}}\right)_{T,\mu_{KNO_3},\mu_{A+}} \quad (2.53b)$$

It must be realized that in the RHS terms of these equations μ_{Ag+}, μ_{I-}, and μ_{A+} are not independent of μ_{KNO_3} and consequently, in order to evaluate these terms from experiment, one has to apply the extended chain rule according to appendix 1.

Explicit expressions for σ_+ and σ_- are obtained by integration of (2.53a) and (2.53b):

$$\sigma_+ = F \int_{pAg(pzc)}^{pAg} \left(\frac{\partial \sigma}{\partial \mu_{KNO_3}}\right)_{T,\mu_{Ag+},\mu_{A+}} dpAg - \tfrac{1}{2}\sigma - \tfrac{1}{2}\sigma_{A+} + \left(\sigma_+ + \frac{\sigma_{A+}}{2}\right)_{pzc} \quad (2.54a)$$

$$\sigma_- = F \int_{pAg(pzc)}^{pAg} \left(\frac{\partial \sigma}{\partial \mu_{KNO_3}}\right)_{T,\mu_{I-},\mu_{A+}} dpI - \tfrac{1}{2}\sigma - \tfrac{1}{2}\sigma_{A+} + \left(\sigma_- + \frac{\sigma_{A+}}{2}\right)_{pzc} \quad (2.54b)$$

In the absence of a charged organic adsorbate the σ_{A+}-terms and the constant μ_{A+} vanish.

The Esin-Markov coefficient β has been defined for the silver iodide-electrolyte system in the absence of an organic adsorbate (1). In the presence of an organic adsorbate, and particularly a charged organic adsorbate, an analogous definition can be given, except that one has to take a parameter concerning the organic adsorbate constant. More specifically, one could either choose the concentration c_{A+}, the chemical potential μ_{A+}, or the adsorption Γ_{A+}. I have chosen the concentration, because it is kept easiest constant in the experiment.

$$\beta \equiv \left(\frac{\partial pAg}{\partial \ln a_{KNO_3}}\right)_{T,\sigma,c_{A+}} = \left(\frac{\partial pAg}{\partial \ln a_{KNO_3}}\right)_{T,\sigma,\mu_{A+}} + \left(\frac{\partial pAg}{\partial \mu_{A+}}\right)_{T,\sigma,a_{KNO_3}} \cdot \left(\frac{\partial \mu_{A+}}{\partial \ln a_{KNO_3}}\right)_{T,\sigma,c_{A+}}$$

(2.55)

Using $d\mu_{KNO_3} = 2\ RTd\ln a_{KNO_3}$ for swamping electrolyte, expressions for β are easily derived from (2.33a) and (2.33b):

$$\beta = \left(2\frac{\partial \sigma_+}{\partial \sigma} + \frac{\partial \sigma_{A+}}{\partial \sigma} + 1\right)_{T,\mu_{KNO_3},\mu_{A+}} + \left(\frac{\partial pAg}{\partial \mu_{A+}}\right)_{T,\sigma,a_{KNO_3}} \left(\frac{\partial \mu_{A+}}{\partial \ln a_{KNO_3}}\right)_{T,\sigma,c_{A+}}$$

(2.56a)

$$\beta = -\left(2\frac{\partial \sigma_-}{\partial \sigma} + \frac{\partial \sigma_{A+}}{\partial \sigma} + 1\right)_{T,\mu_{KNO_3},\mu_{A+}} + \left(\frac{\partial pAg}{\partial \mu_{A+}}\right)_{T,\sigma,a_{KNO_3}} \left(\frac{\partial \mu_{A+}}{\partial \ln a_{KNO_3}}\right)_{T,\sigma,c_{A+}}$$

(2.56b)

It must be concluded that in the presence of an adsorbate the Esin-Markov coefficient as defined above is a function of the de-pendence of the adsorption of the organic substance on the surface charge. Alternatively, one could introduce a definition of β, where Γ_{A+} is constant. In that case one has to introduce a new total dif-ferential instead of γ or ξ.

2.4   SOME CONSIDERATIONS OF THE ADSORPTION FROM BINARY SOLUTIONS

Adsorption from a multicomponent solution is always an *exchange process*, in which molecules of component i in the interface are ex-changed against molecules of component j in the bulk solution:

$$(i)_I + v(j)_L \rightleftharpoons (i)_L + v(j)_I$$

(2.57)

For adsorption from an n-component solution there exist (n-1) exchange equations. In order to explain some basic aspects of the thermo-dynamics of the exchange process, we will simplify our treatment to the adsorption at an uncharged surface from binary solutions.

In the binary systems the two components are denoted by (1) and (2), called respectively the solvent (say water) and the solute. For the present purpose we assume that the dimensions of the mole-cules of (1) and (2) are equal and consequently v is equal to 1. Equation (2.57) can then be written as

$$(1)_I + (2)_L \rightleftarrows (1)_L + (2)_I \tag{2.58}$$

If equilibrium is attained, we can evaluate the equilibrium condition $*\mu = 0$, or

$$\mu_1^I + \mu_2^L = \mu_1^L + \mu_2^I \tag{2.59}$$

Assuming that both solution and interface are a perfect system, the following equations for the μ's are valid:

$$\mu_1^L = \mu_1^{L0} + RT \ln x_1 = \mu_1^{L0} + RT \ln (1-x_2) \tag{2.60}$$

$$\mu_2^L = \mu_2^{L0} + RT \ln x_2 \tag{2.61}$$

$$\mu_1^I = \mu_1^{I0} + RT \ln (1-\theta) \tag{2.62}$$

$$\mu_2^I = \mu_2^{I0} + RT \ln \theta \tag{2.63}$$

where x_1 and x_2 are the mole fractions of component 1 and 2 respectively and θ is the degree of occupation ($= \Gamma_2^{(s)}/\Gamma_{2,max}^{(s)}$). From (2.59-2.63) it follows

$$\frac{\theta}{1-\theta} = K_a \cdot \frac{x_2}{1-x_2} \tag{2.64}$$

where

$$K_a = \exp ((\mu_1^{I0} - \mu_2^{I0} - \mu_1^{L0} + \mu_2^{L0})/RT) \tag{2.65}$$

If $x_2 \ll 1$ equation (2.64) reduces to the *Langmuir equation* for adsorption from solution.

The chemical potentials of the components in the interface can also be evaluated from molecular thermodynamics by assuming a model. If we assume localized adsorption, a homogeneous surface and no lateral interaction, we obtain the following equations for the chemical potentials:

$$\bar{\mu}_1^I = \bar{\mu}_1^{I0} + RT \ln \frac{1-\theta}{\theta} \tag{2.66}$$

$$\bar{\mu}_2^I = \bar{\mu}_2^{I0} + RT \ln \frac{\theta}{1-\theta} \tag{2.67}$$

Virtually, a contradiction with regard to equation (2.64) arises if we introduce (2.66) and (2.67) instead of (2.62) and (2.63) in

(2.59). In order to solve this problem we have to look closer at the definition of the chemical potentials in the surface layer.

Let us first give a derivation for the condition of (adsorption) equilibrium (2.59). Generally, the equation for the total free energy F of a two-phase system can be written as

$$dF = - SdT - pdV + \gamma dA_s + \sum_i \mu_i^I d n_i^I + \sum_i \mu_i^L d n_i^L \tag{2.68}$$

with entropy S, temperature T, pressure p, volume V, interfacial tension γ, surface area A_s, chemical potentials μ_i^I and μ_i^L, and number of moles of component i, n_i^I and n_i^L. The quantities n_i^L and n_i^1 are not independent because of the exchange reaction given in (2.59). We assume $dn_1^I = v_1 d\xi$, $dn_2^I = v_2 d\xi \dots$ and $dn_1^L = - v_1 d\xi$, $dn_2^L = -v_2 d\xi \dots$, whereas v_i are coefficients (including sign) in the exchange reaction. Accordingly, (2.68) can be written as

$$dF = - SdT - pdV + \gamma dA_s + {}^*\mu d\xi \tag{2.69}$$

with

$$^*\mu = \sum_i v_i \mu_i^I - \sum_i v_i \mu_i^L \tag{2.70}$$

The system has established equilibrium if

$$\left(\frac{\partial F}{\partial \xi}\right)_{T,V,A_s} = - {}^*\mu = 0 \tag{2.71}$$

The discrepancy between (2.62-2.63) and (2.66-2.67) arises from the difference in definition of μ_i^I. According to (2.68):

$$\mu_i^I = \left(\frac{\partial F}{\partial n_i^I}\right)_{T,V,A_s,n_i^{I'},n_i^L} \tag{2.72}$$

In principle it is not possible to add a molecule i to the surface while keeping the surface area and the number of molecules, except i, constant. The constant A_s can be replaced by γ using the extented chain rule.

$$\mu_i^I = \left(\frac{\partial F}{\partial n_i^I}\right)_{T,V,\gamma,n_i^{I'},n_i^L} - \gamma a_i \tag{2.73}$$

36

with

$$a_i = \left(\frac{\partial A_s}{\partial n_i^I}\right)_{T,V,\gamma,n_i^{I'},n_i^L} \tag{2.74}$$

The interfacial chemical potential derived from molecular thermo-
dynamics is defined at a constant number of adsorption sites and
accordingly at constant $n_0 = \sum\limits_i n_i^I$

$$\bar{\mu}_i^I = \left(\frac{\partial F}{\partial n_i^I}\right)_{T,n_0,n_i^L} \tag{2.75}$$

This is equivalent to adding a molecule i to the surface at con-
stant V and γ leading to an amount of work γa_i to increase the sur-
face and subsequently taking away a molecule j at constant V and γ
giving an amount of work $-\gamma a_j$. In other words:

$$\bar{\mu}_2^I = \mu_2^I - \mu_1^I \tag{2.76}$$

It may be concluded that combination of (2.62) and (2.63) according
to (2.76) leads to the expression for the chemical potential de-
rived from molecular thermodynamics. Moreover, $\bar{\mu}_2^I$ is the only
independent variable.

In principle, an explicit form for $\bar{\mu}_2^I$, or alternatively, of
μ_2^I and μ_1^I is obtained only after introduction of a molecular model
and subsequent application of molecular thermodynamics. In this way,
non-thermodynamic arguments are introduced in the treatment.

In binary solutions, one molecule of the adsorbate is usually
exchanged against v solvent molecules. Equation (2.76) can then be
modified to

$$\bar{\mu}_2^I = \mu_2^I - v\mu_1^I \tag{2.77}$$

It will be clear that the statistics both at the surface as well
as in the solution becomes more complicated. As a consequence μ_i^L
and μ_i^I also become more complicated functions of x_i and θ_i respec-
tively. As the concentrations in solution are assumed to be low,
the limiting expression (2.61) can also be used in this case, but
the expressions for the interface have to be modified.

37

There may be many other reasons (e.g. asymmetry, lateral interaction etc.) which render (2.66) more complicated. In general, we can write

$$\bar{\mu}_2^l = \mu_2^l - \nu\mu_1^l = f(\theta) \qquad\qquad (2.78)$$

From experimental evidence as well as from statistical calculations we obtain the composite chemical potentials $\bar{\mu}_2^l$. As will be shown in the next section, the exchange character of the process, leading to the unseparability of the pairs of chemical potentials, will become particularly interesting if the exchanging particles have different electrical properties. In literature it is not always obvious if the interfacial potentials are single or composite variables. However, if the limiting form of (2.78) is equal to (2.67), we are always concerned with composite variables.

A more detailed treatment of the definitions of interfacial chemical potentials has been given by Defay, Prigogine and Bellemans (7). Especially their introduction of additional cross-chemical potentials differs from our treatment. However, these authors have shown that in the equilibrium situation these terms vanish and then their theory reduces essentially to the one given here.

2.5 THE ELECTRICAL COMPONENT OF THE ADSORPTION GIBBS ENERGY

In this section we want to discuss how we can acquire from adsorption measurements the electrical parts of the Gibbs energy of adsorption. In section 2.4 it was shown that model assumptions were necessary in order to evaluate K_a or, alternatively, the combination of standard chemical potentials of the components in the interface (and the solution). In addition, model assumptions have to be made also to separate the electrical and the chemical part of the adsorption Gibbs energy.

Let us first extend our treatment of neutral adsorption to the adsorption of charged adsorbates and adsorbents. If potential differences between the interfacial region and the solution occur, the chemical potentials as given in (2.60-2.63) are not only a function of the mole fractions and the degree of occupation respectively, but also of the electrical state at the locus of the par-

38

ticle. Thus an electrical term must be added to the chemical potentials to obtain electrochemical potentials.

In the case of a silver iodide-electrolyte interface we are not concerned with a binary, but with a multicomponent system. For the present purpose we assume that our system can be treated as a quasi-binary system in which an organic ion A^+ is exchanged against v water molecules. This will not be a bad approximation as long as the ions A^+ adsorb in a monolayer at the surface and the other ions are indifferent in the sense of not competing with A^+ for sites on the surface.

The electrochemical potentials of A^+ and H_2O in the interface and the solution can generally be written as

$$\tilde{\mu}_{A+}^{I} = \mu_{A+}^{I} + g_1(\phi^A, \phi^{A'}, \phi^{A''} \ldots \ldots) \tag{2.79}$$

$$\tilde{\mu}_{H_2O}^{I} = \mu_{H_2O}^{I} + g_2(\phi^A, \phi^{A'}, \phi^{A''} \ldots \ldots) \tag{2.80}$$

$$\tilde{\mu}_{A+}^{L} = \mu_{A+}^{L} + F\,\phi_L \tag{2.81}$$

$$\tilde{\mu}_{H_2O}^{L} = \mu_{H_2O}^{L} \tag{2.82}$$

where ϕ^A is the Galvani potential at the adsorption site A and $\phi^{A'}$, $\phi^{A''} \ldots \ldots$ are the first, second $\ldots \ldots$ derivative of the Galvani potential with respect to the normal of the surface (for flat surfaces). As the electrical work to transport ionic charges between two positions depends only on the potential difference, the leading term in (2.79) will be $F\phi^A$. The dipolar energy is dependent on the electrical field strength or $\phi^{A'}$, whereas quadrupole moments are dependent on $\phi^{A''}$.

The composite electrochemical potentials can now be written as

$$\tilde{\mu}_{A+}^{I} - v\,\tilde{\mu}_{H_2O}^{I} = \mu_{A+}^{I0} - v\,\mu_{H_2O}^{I0} + RT \ln f(\theta) + F\phi_A + g(\phi^{A'}, \phi^{A''} \ldots \ldots) \tag{2.83}$$

$$\tilde{\mu}_{A+}^{L} - v\,\tilde{\mu}_{H_2O}^{L} = \mu_{A+}^{L0} - v\,\mu_{H_2O}^{L0} + RT \ln a_{A+} + F\phi_L \tag{2.84}$$

We have assumed, that the activity a_{A+} in the bulk phase is very low. The Coulombic term has been separated from the general electrical function g.

If thermodynamic equilibrium is established

$$\tilde{\mu}_{A+}^I + \nu \; \tilde{\mu}_{H_2O}^L = \tilde{\mu}_{A+}^L + \nu \; \tilde{\mu}_{H_2O}^I \qquad (2.85)$$

and the adsorption isotherm reads

$$f(\Theta) = K_a \; a_{A+} \qquad (2.86)$$

where

$$K_a = \exp \; [(\mu_{A+}^{IO} - \nu\mu_{H_2O}^{IO} - \mu_{A+}^{LO} + \nu\mu_{H_2O}^{LO} + F \; \phi_A - F \; \phi_L + g(\phi^{A'},\phi^{A''}......))/RT]$$

$$= \exp \; [- \Delta G_{ads}^0/RT]$$

$$= \exp \; [- (\Delta G_{chem}^0 + \Delta G_{el}^0)/RT]$$

$$= K_a^{chem} \; K_a^{el} \qquad (2.87)$$

The electrical component of the adsorption Gibbs energy (ΔG_{el}^0) is dependent on both Coulombic, dipolar, and quadrupolar contributions of all the components at the interface. In special cases where ΔG_{el}^0 is a function of σ or pAg *only*, the adsorption is called *congruent* in the surface charge or in the surface potential respectively. In the case congruency applies, the thermodynamic treatment can be extended in the following useful way.

The principle of congruency will be treated from a phenomenological point of view in chapter 6. The geometrical meaning of the terms "charge congruency" and "potential congruency" is based on (2.86). If K_a is only a function of σ or only of pAg, curves relating the degree of occupancy of component A^+ to $\ln c_{A+}$ at different σ- or pAg-values respectively coincide after shifting along the $\ln c_{A+}$-axis. This shift is related to $\Delta K_a(\sigma)$ or $\Delta K_a(pAg)$. The parameters $K_a(\sigma)$ and $K_a(pAg)$ are renamed $G(\sigma)$ and $F(pAg)$ respectively, corresponding with the definitions in chapter 6.

If the adsorption isotherm is congruent in either the charge or the potential (or pAg), the following relation will generally hold:

$$\frac{d\theta}{d\ln K_a} = \frac{d\theta}{d\ln a_{A+}} \tag{2.88}$$

This can be proved from (2.86) realizing that K_a is only a function of pAg or σ and *not* of c_{A+}, so that

$$\frac{df(\theta)}{dK_a} = a_{A+} \qquad \text{and} \qquad \frac{df(\theta)}{da_{A+}} = K_a$$

Thus

$$K_a \frac{df(\theta)}{dK_a} = a_{A+} \frac{df(\theta)}{da_{A+}} \tag{2.89}$$

or

$$K_a \frac{df(\theta)}{d\theta} \frac{d\theta}{dK_a} = a_{A+} \frac{df(\theta)}{d\theta} \frac{d\theta}{da_{A+}} \tag{2.90}$$

which leads to (2.88)

The property of congruency as given in (2.88) can be used to rewrite (2.34), leading to a basic relation between the surface charge and the degree of occupancy or to a basic relation between pAg and θ.

$$\left(\frac{\partial\sigma}{\partial pA}\right)_{T,pAg,\mu_{KNO_3}} = F\left(\frac{\partial\Gamma_{A+}^{(s)}}{\partial pAg}\right)_{T,pA,\mu_{KNO_3}} = F\left(\frac{\partial\Gamma_{A+}^{(s)}}{\partial\ln F(pAg)}\right)_{T,pA,\mu_{KNO_3}} \frac{d\ln F(pAg)}{dpAg} \tag{2.91}$$

Integration of this equation gives

$$\sigma - \sigma_b = F \frac{d\ln F(pAg)}{dpAg} \int_{\infty}^{pA} \left(\frac{\partial\Gamma_{A+}^{(s)}}{\partial\ln F(pAg)}\right)_{T,pA,\mu_{KNO_3}} dpA \tag{2.92}$$

where σ_b is the surface charge in the absence of adsorbate A^+, but at the same T, pAg and μ_{KNO_3}. If it is allowed to replace θ by $\Gamma_{A+}^{(s)}$ in (2.88), we can apply (2.88) to (2.92). After carrying out the integration this leads to

$$\sigma - \sigma_b = -\frac{F}{2.3}\left(\frac{d\ln F(pAg)}{dpAg}\right)\Gamma_{A+}^{(s)} \tag{2.93}$$

or, as the differential quotient is independent of $\Gamma_{A+}^{(s)}$ or θ

$$\sigma = \sigma_b \ (1-\theta) + \sigma_c \ \theta \qquad (2.94)$$

where σ_b and σ_c can be considered as the surface charge at the completely uncovered and covered part respectively. This important equation is the basic relation of the *parallel capacitors model* as introduced by Frumkin (8). In this model the fraction $(1-\theta)$ of the surface covered by adsorbate having a surface charge σ_c is treated as if it were independent of the covered fraction of the surface (θ) with a surface charge σ_b. The two parts act as capacitors in parallel.

The counterpart of the parallel capacitors model is the *series capacitors model* corresponding to a system where congruency in the surface charge occurs (9). The equations corresponding to (2.93) and (2.94) are

$$pAg - pAg_b = \frac{F}{2.3} \ \left(\frac{d\ln G(\sigma)}{d\sigma}\right) \ \Gamma_{A+} \qquad (2.95)$$

and

$$pAg = pAg_b \ (1-\theta) + pAg_c \ \theta \qquad (2.96)$$

respectively. Here pAg_b is the pAg value in the absence of adsorbate A^+ but at the same T, σ and μ_{KNO_3}. The latter equation can also be written in terms of Galvani potentials according to Nernst's equation (2.30).

$$\Delta\phi = \Delta\phi_b \ (1-\theta) + \Delta\phi_c \theta \qquad (2.97)$$

where $\Delta\phi_b$ and $\Delta\phi_c$ can be considered as the surface potential at the completely uncovered and covered part respectively.

The change in adsorption Gibbs energy upon variation of the electrical parameter can be obtained from $\Gamma_{A+}^{(s)} - \ln c_{A+}$ curves if congruency is assumed. In the case of congruency the variation of ΔG_{ads}^0 with the pAg or σ can be obtained from (2.93) and (2.95) respectively.

$$\ln F(pAg) - \ln F(pAg^*) = -\frac{2.3}{F} \int_{pAg^*}^{pAg} \frac{\sigma - \sigma_b}{\Gamma_{A+}^{(s)}} \, dpAg \tag{2.98}$$

$$\ln G(\sigma) - \ln G(\sigma^*) = \frac{2.3}{F} \int_{\sigma^*}^{\sigma} \frac{pAg - pAg_b}{\Gamma_{A+}^{(s)}} \, d\sigma \tag{2.99}$$

These equations can be applied if charge-potential curves ánd ad-
sorption isotherms are available.

It may be concluded that the assumption of either charge or
potential congruency is an essential step in the acquisition of the
electrical part of the adsorption Gibbs energy.

2.6 SUMMARY

Gibbs' adsorption law has been elaborated for a silver iodide-
electrolyte interface in the presence of an adsorbing organic ion
A^+ in swamping, indifferent electrolyte. Ionic chemical potentials
have been introduced, whereas the Gibbs convention has been chosen
to define interfacial quantities. It has been shown that single
adsorption values of Ag^+ and I^- ions are not measurable, because
these ions can combine to neutral AgI at the surface. In a strict
thermodynamic analysis these single adsorption values do not occur.

Two integral equations are derived in order to calculate the
adsorption of the organic ion from charge-potential curves. The
temperature dependence of the electrical parameters in the presence
of organic adsorbate is discussed. It has been shown that the de-
pendence of the interfacial excess entropy on the surface charge
gives a less complicated equation than the dependence on the pAg.
Explicit equations are also derived for the charge attributed by K^+
and NO_3^- ions. For the Esin-Markov coefficient in the presence of
an organic adsorbate a definition has been given and an expression
was derived.

Finally, the principle of congruency of adsorption isotherms
has been discussed. Basic equations relating the degree of occupan-
cy to the surface charge and the potential have been derived. Some
methods for evaluating the adsorption Gibbs energy using the con-
gruency principle are given.

2.7 REFERENCES

1. B.H. Bijsterbosch and J. Lyklema, Advan. Colloid Interface Sci. 9 147 (1978)

2. J.G. Kirkwood and F.P. Buff, J. Chem. Phys. 19 774 (1951)

3. D.G. Hall, Trans Faraday Soc. II 74 405 (1978)

4. J.W. Gibbs, The Collected Works of J.W. Gibbs, Longmans, Green, New York, 1928

5. D.H. Everett, Pure and Applied Chem. 31 581 (1972)

6. B.H. Bijsterbosch and J. Lyklema, J. Colloid Interface Sci. 28 506 (1968)

7. R. Defay, I. Prigogine, A. Bellemans and D.H. Everett, Surface Tension and Adsorption, Wiley, New York, 1960

8. A.N. Frumkin, Z. Phys. Chem. 116 466 (1925)

9. R. Parsons, Trans. Faraday Soc. 51 1512 (1955)

APPENDIX: The extended chain rule.

a. *Partial differential quotient with one constant parameter*

$$\left(\frac{\partial f}{\partial x}\right)_z = \left(\frac{\partial f}{\partial x}\right)_y - \left(\frac{\partial f}{\partial z}\right)_x \cdot \left(\frac{\partial z}{\partial x}\right)_y \tag{A2.1}$$

b. *Partial differential quotient with two constant parameters*

$$\left(\frac{\partial f}{\partial x}\right)_{z_1,z_2} = \left(\frac{\partial f}{\partial x}\right)_{y_1,z_2} - \left(\frac{\partial f}{\partial z_1}\right)_{x,z_2}\left(\frac{\partial z_1}{\partial x}\right)_{y_1,z_2}$$

$$= \left(\frac{\partial f}{\partial x}\right)_{y_1,y_2} - \left(\frac{\partial f}{\partial z_2}\right)_{y_1,x} \cdot \left(\frac{\partial z_2}{\partial x}\right)_{y_1,y_2}$$

$$- \left(\frac{\partial f}{\partial z_1}\right)_{x,z_2} \cdot \left(\frac{\partial z_1}{\partial x}\right)_{y_1,y_2} + \left(\frac{\partial f}{\partial z_1}\right)_{x,z_2} \cdot \left(\frac{\partial z_1}{\partial z_2}\right)_{x,y_1} \cdot \left(\frac{\partial z_2}{\partial x}\right)_{y_1,y_2}$$

$$\tag{A2.2}$$

c. *Partial differential quotient with three constant parameters*

$$\left(\frac{\partial f}{\partial x}\right)_{z_1,z_2,z_3} = \left(\frac{\partial f}{\partial x}\right)_{y_1,y_2,z_3} - \left(\frac{\partial f}{\partial z_2}\right)_{y_1,x,z_3} \cdot \left(\frac{\partial z_2}{\partial x}\right)_{y_1,y_2,z_3}$$

$$- \left(\frac{\partial f}{\partial z_1}\right)_{x,z_2,z_3} \cdot \left(\frac{\partial z_1}{\partial x}\right)_{y_1,y_2,z_3} + \left(\frac{\partial f}{\partial z_1}\right)_{x,z_2,z_3} \cdot \left(\frac{\partial z_1}{\partial z_2}\right)_{z,y_1,z_3} \cdot \left(\frac{\partial z_2}{\partial x}\right)_{y_1,y_2,z_3}$$

$$= \left(\frac{\partial f}{\partial x}\right)_{y_1,y_2,y_3} - \left(\frac{\partial f}{\partial z_3}\right)_{x,y_1,y_2} \cdot \left(\frac{\partial z_3}{\partial x}\right)_{y_1,y_2,y_3}$$

$$- \left(\frac{\partial f}{\partial z_2}\right)_{y_1,x,z_3} \cdot \left[\left(\frac{\partial z_2}{\partial x}\right)_{y_1,y_2,y_3} - \left(\frac{\partial z_2}{\partial z_3}\right)_{y_1,y_2,x} \cdot \left(\frac{\partial z_3}{\partial x}\right)_{y_1,y_2,y_3}\right]$$

$$- \left(\frac{\partial f}{\partial z_1}\right)_{x,z_2,z_3} \cdot \left[\left(\frac{\partial z_1}{\partial x}\right)_{y_1,y_2,y_3} - \left(\frac{\partial z_1}{\partial z_3}\right)_{y_1,y_2,x} \cdot \left(\frac{\partial z_3}{\partial x}\right)_{y_1,y_2,y_3}\right]$$

$$+ \left(\frac{\partial f}{\partial z_1}\right)_{x,z_2,z_3} \cdot \left(\frac{\partial z_1}{\partial z_2}\right)_{x,y_1,z_3} \cdot \left[\left(\frac{\partial z_2}{\partial x}\right)_{y_1,y_2,y_3} - \left(\frac{\partial z_2}{\partial z}\right)_{y_1,y_2,x} \cdot \left(\frac{\partial z_3}{\partial x}\right)_{y_1,y_2,y_3}\right]$$

45

This results leads to

$$\left(\frac{\partial f}{\partial x}\right)_{z_1,z_2,z_3} = \left(\frac{\partial f}{\partial x}\right)_{y_1,y_2,y_3} - \left(\frac{\partial f}{\partial z_1}\right)_{x,z_2,z_3} \cdot \left(\frac{\partial z_1}{\partial x}\right)_{y_1,y_2,y_3}$$

$$- \left(\frac{\partial f}{\partial z_2}\right)_{y_1,x,z_3} \cdot \left(\frac{\partial z_2}{\partial x}\right)_{y_1,y_2,y_3}$$

$$- \left(\frac{\partial f}{\partial z_3}\right)_{y_1,y_2,x} \cdot \left(\frac{\partial z_3}{\partial x}\right)_{y_1,y_2,y_3}$$

$$+ \left(\frac{\partial f}{\partial z_1}\right)_{x,z_2,z_3} \cdot \left(\frac{\partial z_1}{\partial z_3}\right)_{y_1,y_2,x} \cdot \left(\frac{\partial z_3}{\partial x}\right)_{y_1,y_2,y_3}$$

$$+ \left(\frac{\partial f}{\partial z_1}\right)_{x,z_2,z_3} \cdot \left(\frac{\partial z_1}{\partial z_2}\right)_{x,y_1,z_3} \cdot \left(\frac{\partial z_2}{\partial x}\right)_{y_1,y_2,y_3}$$

$$+ \left(\frac{\partial f}{\partial z_2}\right)_{y_1,x,z_3} \cdot \left(\frac{\partial z_2}{\partial z_3}\right)_{y_1,y_2,x} \cdot \left(\frac{\partial z_3}{\partial x}\right)_{y_1,y_2,y_3}$$

$$- \left(\frac{\partial f}{\partial z_1}\right)_{x,z_2,z_3} \cdot \left(\frac{\partial z_1}{\partial z_2}\right)_{x,y_1,z_3} \cdot \left(\frac{\partial z_2}{\partial z_3}\right)_{y_1,y_2,x} \cdot \left(\frac{\partial z_3}{\partial x}\right)_{y_1,y_2,y_3} \tag{A2.3}$$

CHAPTER 3

*PATCHWISE INTERFACIAL DIPOLE LAYERS ON SOLIDS. APPLICATION TO THE
SILVER IODIDE - AQUEOUS SOLUTION INTERFACE*[*]

3.1 INTRODUCTION

The description of the orientation of water (and other) di-
poles near a phase boundary remains one of the most difficult prob-
lems of interfacial electrochemistry. The majority of models refer
to the metal-water interface. The state of art in this field has
been covered in an excellent review by Trasatti (1). However, it is
questionable whether the results obtained for metal-water inter-
faces are of immediate applicability to non-metal solid-water inter-
faces as occurring in many disperse systems. More often than not
the charge on the surface is localized, while moreover solid sur-
faces are often heterogeneous. It follows that the state of hydra-
tion or, for that matter, the interfacial polarization varies
along the surface. For instance, with negatively charged AgI-sols
one would expect a mode of orientation of the water dipoles near
an adsorbed I^- ion differing from that near an uncharged part of the
surface: the adsorbed I^- ion would create a small hydrophilic patch
in an otherwise hydrophobic surface. Similar reasoning would apply
to, say, negatively charged polystyrene latex particles.

Below we shall refer to models based on interfacial water
molecules treated as if their orientation is due to a homogeneous
electrical field as *"homogeneous interfacial hydration models"*, in
contradistinction to *"patchwise interfacial hydration models"* in
which the existence on the surface of loci or patches of differing
hydration properties is explicitly accounted for. The first category
encompasses the main body of what has hitherto been studied, but
here we intend to emphasize the second. "Interfacial hydration" is

---

interpreted here in the general sense as including *all* variations
of the properties of water due to an adjacent phase, including '
those near water-rejecting surfaces, giving rise to hydrophobic
hydration.

In this paper we will emphasize the orientational properties
of the solvent molecules. The model to be developed will be applied
to the silver iodide-aqueous solution interface (2) and incorpo-
rated in a theory of the AgI-electrolyte interface, which is based
on the individual adsorptions of the potential determining (p.d.)
ions. It will be shown that the proposed picture is entirely com-
patible with experimental charge-potential curves.

3.2 PATCHWISE INTERFACIAL HYDRATION. SOME BASIC ASPECTS

The discrimination between systems where a homogeneous hydra-
tion model applies and those in which a patchwise treatment is in-
dicated is not always obvious. Clearly, air in contact with water
is homogeneous; so are other fluids, including mercury. If the mer-
cury bears a charge due to, say, an excess of electrons, these
electrons move very rapidly along the surface, so that the surface
charge density σ is really smeared-out and the electrical field
near the surface is homogeneous. A patchwise model is obvious for
most heterogeneous surfaces. Heterogeneity can arise if the surface
consists of a collection of different but homogeneous patches or
if it carries a number of fixed charges (of one or more types) on
an otherwise uncharged area. For instance, polystyrene latex spheres,
negatively charged by immobile, covalently bound, completely dis-
sociated sulphate groups, clearly belong to the patchwise category
because the charged groups cannot move at all. An intermediate sit-
uation exists for homogeneous surfaces on which the surface charges
have a limited tangential mobility. The discriminating question is
then whether or not the relaxation rate of the lateral motion of
these ions exceeds that of the adjustment of water dipoles. Silver
iodide is intermediate because the adsorbed p.d. ions (Ag^+ and I^-)
have a certain tangential mobility, either inside the solid or by
desorption and readsorption at a different site.

Some indication of the applicability of the patchwise model
can be obtained from different kinetic interfacial parameters. For

the AgI-aqueous solution interface, the rotational relaxation time of water, as obtained from NMR-measurements, is of order 10^{-9}s or faster. The relaxation time for the adjustment of surface charges can be inferred from recent work by Peverelli and van Leeuwen (3), who found a relaxation time order of 10^{-3}s. Although the latter is related to the transfer of charges across the interface and is probably controlled by the dehydration process of p.d. ions, it is so much slower than the relaxation time for the adjustment of an interfacial water molecule that for the purpose of description of the properties of the interfacial water layer the distribution of adsorbed Ag^+ and I^--ions is virtually fixed. In other words, in this case a patchwise approach is indicated.

In a patchwise hydration model, the electrical interfacial properties due to free and induced charges will be locally dependent on the surface properties of the patch. We intend to evaluate the total Galvani potential difference $\phi^S - \phi^L$ between the interior of the (homogeneous) solid and that of the liquid in terms of its components. To be rigorous, one should take into account both the discreteness of the surface charge (and counter charge), as well as the patchwise behaviour of interfacial hydration. However, for the present purpose we will use the following first-order approximation: (i) The Galvani potential is considered a statistical mean of the local properties. (ii) The charges will also be taken as smeared out except for their effect on interfacial hydration. (iii) Local solvent properties are calculated with a patchwise model, but in a later stage these properties will be averaged over the surface.

It is not always meaningful to average or to smear out the local hydration properties in the patchwise interfacial hydration model. This can be illustrated by considering the orientation of solvent dipoles and the dipolar potential. For reversible interfaces like that between AgI and an electrolyte solution, the dipolar potential is part of the Galvani potential difference $\phi^S - \phi^L$. It is likely that adsorption of p.d. ions will be related to the dipolar (macro) potential. However, for systems consisting of a non-conducting solid and fixed surface groups chargeable by a dissociation equilibrium only the effect of hydration on the micropotential is meaningful. This local hydration can be incorporated in the equilibrium constant or the adsorption free energy.

49

3.3 INTERFACIAL DIPOLE POTENTIALS, IN FIRST ORDER APPROXIMATION

Assume a surface to be composed of a collection of patches of differing properties denoted by i, j, k ... . Patches i are characterized by a surface charge density σ_i, a relative dielectric constant in the fluid ε_i, and an effective number of normally oriented water molecules $n_i^\perp$. The sign of $n_i^\perp$ denotes the direction of the oriented dipoles. We will simplify our treatment by assuming σ_i, ε_i and $n_i^\perp$ to be independent of the total surface charge density σ. This limits our treatment either to heterogeneous surfaces with a fixed surface charge or to homogeneous surfaces with localized charges determining surface hydration. It is our aim to evaluate the dipolar potential difference of the entire interface $\Delta\phi$ (dip) from local properties.

The electrical potential difference across a homogeneous layer of surface dipoles is given by the Helmholtz equation (3.1).

$$\Delta\phi \ (dip) = \frac{n^\perp \mu}{\varepsilon_0 \varepsilon^H} \qquad (3.1)$$

Rational units are used throughout, thus ε_0 is the dielectric permittivity of vacuum (8.854×10^{-12} C V^{-1} m^{-1}). As discussed by Trasatti (1) difficult points in the application of (3.1) are assigning values to the effective dipole moment of water μ and to the relative dielectric constant ε^H. For μ we take the value for isolated water molecules, i.e. 1.84 D (= 6.13×10^{-30} Cm). This choice automatically implies a choice on the value of ε^H, a point to which we return below. Before discussing ε^H it is useful to analyse the overall behaviour of the dielectric constant near the surface.

It is assumed that the region between the homogeneous surface and the outer Helmholtz plane (oHp), the inner or Stern layer, has a uniform dielectric constant ε^S. In the absence of specific adsorption the Stern layer can be considered as a molecular condenser for which the potential difference is written as

$$\Delta\phi \ (Stern) = \frac{\sigma \ d}{\varepsilon_0 \varepsilon^S} \qquad (3.2)$$

where d is the thickness of the Stern layer. This potential differ-
ence is a function of the charge of the surface and the orientation
of permanent dipoles at the surface, and can thus formally be sepa-
rated into two components, a dipolar contribution $\Delta\phi$ (dip) and an-
other one $\Delta\phi$ (mol), to be discussed later:

$$\Delta\phi \text{ (Stern)} = \Delta\phi \text{ (mol)} + \Delta\phi \text{ (dip)} \tag{3.3}$$

Formally, also this separation can be extended to the right hand
side of (3.2). Assuming σ and d to be equal for the two components,
we can write

$$\Delta\phi \text{ (Stern)} = \frac{\sigma \, d}{\varepsilon_0 \varepsilon^M} - \frac{\sigma \, d}{\varepsilon_0 \varepsilon^O} \tag{3.4}$$

which is equivalent with a separation of the reciprocal Stern per-
mittivity ε^S according to

$$\frac{1}{\varepsilon^S} = \frac{1}{\varepsilon^M} - \frac{1}{\varepsilon^O} \tag{3.5}$$

Here, ε^M is the apparent dielectric constant due to molecular po-
larization only, and ε^O is the same due to the orientational effect
of the water dipoles only. The minus sign follows from the fact
that the orientation of permanent dipoles is opposite to the field
vector. The parameter ε^M is the dielectric constant at fixed orien-
tation of permanent dipoles and will be close to the high-frequency
value ε_∞. It is assumed that ε^M is isotropic and thus independent
of $\Delta\phi$ (dip). It follows also, that for different patches i ε_i^M is
independent of the patch properties ($\varepsilon_i^M = \varepsilon^M$). The quintessence of
the separation of ε^S is that all variations of ε^S with surface
charge are ascribed to ε^O and hence to $\Delta\phi$ (dip). The dependence of
the dipolar potential on the surface charge follows from model
considerations.

Let us now return to the choice of the value for dielectric
permittivity of the Helmholtz layer, ε^H. First, it is noted that
in (3.2) ε^S applies over the entire region between the centres of
the surface charges and the oHp, whereas in (3.1) ε^H applies only to
a monolayer of water molecules. Strictly speaking ε^H could well be
unity, but we have to account for the approximation made above that

for μ the value of isolated water dipoles has been substituted. This is an overestimation because of the lateral interaction of the dipoles (4,5) and a correction factor is needed in the denominator of (3.1), which in our formalism is included in ε^H. The precise resulting value of ε^H is difficult to assess; the actual choice has no influence on our line of reasoning although it affects the values of the parameters to be substituted.

Let the fraction of the surface covered with patches i be denoted by θ_i. The total surface charge density and the total effective number of normally oriented water molecules per unit area can be written as

$$\sigma = \sum_{i=1}^{N_p} \sigma_i \, \theta_i \tag{3.6}$$

$$n^\perp = \sum_{i=1}^{N_p} n_i^\perp \, \theta_i \tag{3.7}$$

where N_p is the number of patches. From the previous discussion it follows that ε^M, μ, and d are independent of the specific patch properties. In our first order approximation the density of the patchwise oriented dipoles and the surface charge density on the different patches can be taken as smeared out. The additivity of the components of the dipolar potentials and those of the molecular polarizability part of the Stern layer potential (3.8), (3.9) can be derived from (3.1), (3.4), (3.6) and (3.7).

$$\Delta\phi \; (mol) = \frac{\left[\sum_{i=1}^{N_p} \sigma_i \, \theta_i\right] d}{\varepsilon_0 \varepsilon^M} = \sum_{i=1}^{N_p} \Delta\phi_i \; (mol) \tag{3.8}$$

$$\Delta\phi \; (dip) = \frac{\left[\sum_{i=1}^{N_p} n_i^\perp \, \theta_i\right] \mu}{\varepsilon_0 \varepsilon^H} = \sum_{i=1}^{N_p} \Delta\phi_i \; (dip) \tag{3.9}$$

The potential differences $\Delta\phi_i(mol)$ and $\Delta\phi_i(dip)$ are considered components of a total potential difference and analyzed regarding the charge density and the density of oriented dipoles at the patches i respectively as smeared out over the whole surface.

If the origin of a patch on a surface is the adsorption of localized surface charges on a homogeneous neutral surface, the degree of occupation θ_i is mostly not well defined. However, we can eliminate θ_1, the surface fraction of neutral patches, from (3.9), because the condition (3.10) is valid.

$$\sum_{i=1}^{N_p} \theta_i = 1 \tag{3.10}$$

Moreover, the surface fractions of the charged patches are proportional to the surface excesses of the corresponding ions, expressed in eq/unit area, according to (3.11).

$$\theta_i = k_i' \, F \, \Gamma_i \tag{3.11}$$

Here F is the Faraday constant and k_i' is a measure for the effective patch area per adsorbed ion. If we introduce (3.10) and (3.11) in (3.9), the surface fractions θ_i are eliminated.

$$\Delta\phi \ (dip) = \frac{n_1^{\perp} \mu}{\varepsilon_0 \varepsilon^H} + \sum_{i=2}^{N_p} \frac{(n_i^{\perp} - n_1^{\perp}) \mu}{\varepsilon_0 \varepsilon^H} \, k_i' F \Gamma_i$$

$$= \Delta\phi_N(dip) + \sum_{i=2}^{N_p} k_i F \Gamma_i$$

$$= \Delta\phi_N(dip) + \sum_{i=2}^{N_p} \Delta\phi_i^R(dip) \tag{3.12}$$

Application of the same procedure to (3.8) is not meaningful because σ_1 is zero. The value of $\Delta\phi_N(dip)$ is a constant (independent of the surface charge) and applies to the neutral surface. On the other hand, the dipolar potential components $\Delta\phi_i^R$ are proportional to the surface excesses of the ions.

3.4 THE LOCAL INTERFACIAL HYDRATION MODEL APPLIED TO AgI

On silver iodide the surface charge σ is related to the surface excesses of silver and iodide ions according to (3.13).

$$\sigma = F(\Gamma_{Ag+} - \Gamma_{I-}) \tag{3.13}$$

Physically, the charge may be a real surface excess of the p.d. ions (relative to AgI) or a surface vacancy or a space charge in the solid. In our model, all charges are attributed to local positive excesses on the surface.

As explained before, it is likely that the relaxation of water molecules near adsorbed p.d. ions is much faster than the lateral movement of these ions. Moreover, the absolute value of the charge density σ never exceeds $5\mu C/cm^2$ in experimental situations. This surface charge corresponds with mutual distances between the charges of minimally 1.8 nm. Hence, the charges are sufficiently well separated and localized on the time-scale of the reorientation of water and, therefore, for the purpose of our analysis they may be treated as individual sites.

We distinguish three kinds of randomly distributed patches, Ag^+ patches, I^- patches and the remaining uncharged AgI patch. The resulting expression for the dipolar potential according to (3.12) reads for this case

$$\Delta\phi \ (dip) = \Delta\phi_{Ag+}^R(dip) + \Delta\phi_{I-}^R(dip) + \Delta\phi_{AgI}(dip)$$

$$= k_{Ag+}F\Gamma_{Ag+} + k_{I-}F\Gamma_{I-} + \Delta\phi_{AgI}(dip) \tag{3.14}$$

The coefficients k_{Ag+} and k_{I-} are parameters related to the net degree of orientation of water molecules at an Ag^+ and an I^- patch respectively.

On the neutral part of an AgI surface the silver and iodide atoms are only partly charged, because the silver iodide lattice is essentially covalent. Here, the orientation is determined by a competitive effect of the solid *and* the solution phase. As silver iodide behaves as a hydrophobic solid, it is not unlikely that on

54

the neutral part of the surface the orientation of H_2O dipoles (and hence the potential difference $\Delta\phi_{AgI}(dip)$) is mainly determined by the solution side. Consequently, it is not very different from that at the air-solution interface. At the air-solution interface water molecules are oriented with the O-atom outwards. The surface- or χ-potential amounts to ca. 0.13 V (1).

It may be a good first approximation that the hydration of the water molecules on the Ag^+ and I^- patches is similar (or at least related) to that of the corresponding ions in solution. The hydration free energies $G_{Ag+}^{h,L}$ and $G_{I-}^{h,L}$ of the silver and iodide ions in solution are very different and amount to -479.4 kJ/mol and -257.1 kJ/mol respectively (6). It appears that $G_{Ag+}^{h,L}$ is very high as compared to the same quantity for an alkali ion of the same radius. This fact points to a specific interaction between the Ag^+ ion and the surrounding water molecules. We assume that the high hydration free energy of Ag^+ corresponds to a relatively high degree of radial orientation of water molecules around the ion. If this behaviour is similar at the surface, the effective orientation of water molecules on Ag^+ patches will be stronger than that on I^- patches. As a con-sequence k_{Ag+} will exceed k_{I-} and this fact is probably the main reason for the asymmetry of the charge-potential curve of AgI in 0.1 M KNO_3 as will be shown later.

The effective number of oriented water molecules of a given kind of patch can be estimated from the Helmholtz equation (3.1) or (3.12). To that end we will use some parameters obtained by anticipating the fitting of an experimental charge-potential curve to an electrical double layer model including patchwise interfacial hydration. The origin of the data will be given below. The data used are the values obtained at the p.z.c.. For $\Delta\phi_{Ag+}^{R}(dip)$, $\Delta\phi_{I-}^{R}(dip)$ and $\Delta\phi_{AgI}(dip)$ we have introduced -94 mV, +34 mV and -140 mV re-spectively. $F\Gamma_{Ag+}$ and $F\Gamma_{I-}$ are both 1 $\mu C/cm^2$, whereas the relative dielectric constant ε^H was given a value of 6. Substituting these parameters into the Helmholtz equation (3.1) the averaged number of oriented water dipoles per nm^{-2} (inclusive sign indicating polarity) $\bar{n}_{Ag+}^{\perp}$, $\bar{n}_{I-}^{\perp}$ and $\bar{n}_{AgI}^{\perp}$ can be calculated as -0.81, +0.29 and -1.21 re-spectively. For Ag^+ and I^- patches this corresponds to a number of 11 and 5 effectively oriented water molecules per adsorbed p.d.

ion respectively. These values seem rather high for half the hydration of a single ion. Although effectively the number of oriented water molecules is not only in contact with an adsorbed ion, but also with neighbouring (partly charged) atoms of the same kind, it is likely that a number of 11 water molecules on an Ag^+ patch is too high. Other values for $\Delta\phi^R_{Ag^+}(dip)$ and $\Delta\phi^R_{I-}(dip)$ as resulting from a different parameter choice give a worse correspondence of calculated and experimental charge-potential curves. However, it must always be realized that assignment of reliable hydration numbers is thwarted by the uncertainty inherent in the choice of ε^H, as discussed above.

3.5 ADSORPTION OF P.D. IONS AND THE NERNST EQUATION

Unlike the surface charge given in (3.13), the individual surface excesses Γ_{Ag^+} and Γ_{I-} are experimentally inaccessible. However, in order to obtain $\Delta\phi$ (dip) these individual values are needed. They can be obtained by assuming some adsorption model and by making a proper choice of the isotherm parameters.

The adsorption of p.d. ions is an equilibrium process. This means that the electrochemical potentials ($\tilde{\mu}$) of these ions in the bulk of the solid (S), the interface (I), and the bulk of the solution (L) must be equal.

$$\tilde{\mu}^S_{Ag^+} = \tilde{\mu}^I_{Ag^+} = \tilde{\mu}^L_{Ag^+} \tag{3.15}$$

$$\tilde{\mu}^S_{I-} = \tilde{\mu}^I_{I-} = \tilde{\mu}^L_{I-} \tag{3.16}$$

To split the electrochemical potentials of the interface into an electrical and a chemical contribution, the position of the interface has to be fixed. The electrochemical potentials of p.d. ions in the two bulk phases are readily given by (3.17) to (3.20).

$$\tilde{\mu}^S_{Ag^+} = \tilde{\mu}^{S0}_{Ag^+}(T) + F\phi^S \tag{3.17}$$

$$\tilde{\mu}^S_{I-} = \tilde{\mu}^{S0}_{I-}(T) - F\phi^S \tag{3.18}$$

56

$$\tilde{\mu}^L_{Ag+} = \tilde{\mu}^{L0}_{Ag+}(T) + RT \ln c_{Ag+} + F\phi^L \tag{3.19}$$

$$\tilde{\mu}^L_{I-} = \tilde{\mu}^{L0}_{I-}(T) - RT \ln c_{I-} - F\phi^L \tag{3.20}$$

The potentials ϕ^S and ϕ^L are unmeasurable in principle, but variations of $\Delta\phi = \phi^S - \phi^L$ are accessible because they are related to changes of cell potentials. If the indifferent electrolyte concentration is much higher than c_{Ag+} and c_{I-}, the ionic strength is approximately constant during variations of c_{Ag+} and c_{I-}. The (constant) activity coefficients are then included in $\tilde{\mu}^{L0}_{Ag+}$ and $\tilde{\mu}^{L0}_{I-}$.

Equating (3.17) and (3.19) or (3.18) and (3.20) leads to the *Nernst equation.*

$$\Delta\phi = \tilde{\mu}^{L0}_{Ag+}(T) - \tilde{\mu}^{S0}_{Ag+}(T) + \frac{RT}{F} \ln c_{Ag+} \tag{3.21}$$

$$\Delta\phi = \tilde{\mu}^{L0}_{I-}(T) - \tilde{\mu}^{S0}_{I-}(T) - \frac{RT}{F} \ln c_{I-} \tag{3.22}$$

The Nernst equation is a relation between bulk properties of the system. Interfacial quantities, particularly interfacial potentials, are only obtainable by introducing model assumptions for the adsorption of p.d. ions. In our picture, it is assumed that the adsorption of p.d. ions occurs on a lattice consisting of a finite number of adsorption sites. Let ϕ^A be the electrical potential in the adsorption plane. The potential ϕ^A will be equal for the adsorption of Ag^+ and I^- ions. This is so because for ϕ^A we substitute the average electrostatic macropotential, which is the same for each site by definition. Local deviations due to the discreteness of the charges are in first instance independent of Γ_{Ag+} and Γ_{I-} and are incorporated in $\tilde{\mu}^{I0}_{Ag+}$ and $\tilde{\mu}^{I0}_{I-}$. For a p.d. ion to become adsorbed from the solution it must pass through the diffuse layer, the Stern layer, and the hydration layer successively. Hence, $\Delta\phi$ (ads) can be written as:

$$\Delta\phi \text{ (ads)} \equiv \phi^A - \phi^L = \Delta\phi \text{ (diff)} + \Delta\phi \text{ (mol)} + \Delta\phi \text{ (dip)}. \tag{3.23}$$

Potential differences due to volume charges in or polarization of the solid phase are not included in (3.23), because we assumed positive excess adsorption values of p.d. ions being present *on* the solid surface.

We assume that the adsorption of p.d. ions statisfies a *Langmuir equation*. The interfacial electrochemical potentials can then be written as

$$\tilde{\mu}_{Ag+}^{I} = \tilde{\mu}_{Ag+}^{I0} + RT \ln \frac{\Gamma_{Ag+}}{\Gamma_{Ag+}^{max} - \Gamma_{Ag+}} + F\phi^{A} \tag{3.24}$$

$$\tilde{\mu}_{I-}^{I} = \tilde{\mu}_{I-}^{I0} + RT \ln \frac{\Gamma_{I-}}{\Gamma_{I-}^{max} - \Gamma_{I-}} - F\phi^{A} \tag{3.25}$$

Our ultimate aim is to establish a relation between σ and $\Delta\phi$ (or between σ and c_{Ag+} or c_{I-}). To that end we have to express Γ_{Ag+} and Γ_{I-} as a function of σ. The values of Γ_{Ag+} and Γ_{I-} can be related with (3.15), (3.16), (3.17), (3.18), (3.24) and (3.25).

$$RT \ln \frac{\Gamma_{Ag+}}{\Gamma_{Ag+}^{max} - \Gamma_{Ag+}} \cdot \frac{\Gamma_{I-}}{\Gamma_{I-}^{max} - \Gamma_{I-}} = \tilde{\mu}_{Ag+}^{S0} + \tilde{\mu}_{I-}^{S0} - \tilde{\mu}_{Ag+}^{I0} - \tilde{\mu}_{I-}^{I0} = K \tag{3.26}$$

Hence, $\Gamma_{Ag+}(\sigma)$ and $\Gamma_{I-}(\sigma)$ can be solved from (3.13) and (3.26). The value of K is related to the adsorption values of Ag^{+} and I^{-} in the p.z.c. ($\sigma = 0$ and $\Gamma_{Ag+} = \Gamma_{I-}$) and hence to the molecular partial free energies of adsorbed ions. It is interesting to note that (3.26) resembles an expression for the "solubility product in the interface", analogous to the solubility product in solution which follows from (3.19) and (3.20).

Finally, the equations presented in this section enable the calculation of the potential difference between the bulk of the solid and the adsorption plane. The value of $\Delta\phi$ (solid) follows from equating (3.17) and (3.24) (or alternatively from (3.18) and (3.25).

$$\Delta\phi \text{ (solid)} \equiv \phi^{S} - \phi^{A} = \frac{\mu_{Ag+}^{I0} + \mu_{Ag+}^{S0}}{F} + \frac{RT}{F} \ln \frac{\Gamma_{Ag+}}{\Gamma_{Ag+}^{max} - \Gamma_{Ag+}} \tag{3.27}$$

The necessity of a non-zero potential difference in the solid is thus a consequence of thermodynamic equilibrium within the theoretical framework presented. However, the molecular interpretation of $\Delta\phi$ (solid) is not so clear. It may be due either or both to free space charges (Frenkel defects) and molecular polarization of the solid. We recall that in our picture we neglect the presence of a space charge in the solid phase attributing the surface charge entirely to p.d. ions adsorbed at the interface proper.

It may be repeated that for the purpose of our analysis only those components of the potential differences have to be accounted for that are dependent on the surface charge or on the adsorption of ions or molecules. Other contributions, such as a constant dipolar potential inside the solid, may be included in the standard electrochemical potentials (e.g. $\tilde{\mu}_{Ag+}^{\sim IO}$).

3.6 THE POINT OF ZERO CHARGE

In the absence of specific adsorption the p.z.c. of AgI (pAg = 5.67) does not coincide with its stoichiometric equivalence point (pAg = 8.1). It is possible to interpret this fact within the theoretical framework of the previous section. In addition, a more quantitative explanation can be offered by application of the principles of the patchwise-hydrated interface model.

We assume that the covalent part of the free energies of bonding for Ag^+ and I^- ions to the AgI surface is equal, on the argument that bonding of each of these ions involves the forming of an AgI bond. Let this contribution be G_{AgI}^{cov}. Then the difference in affinity of the adsorption from solution is only a function of the difference of the hydration free energy in the surface ($G_{Ag+}^{h,I}$, $G_{I-}^{h,I}$) and in the solution ($G_{Ag+}^{h,L}$, $G_{I-}^{h,L}$). As silver ions are more difficult to dehydrate than iodide ions, they have a lower adsorption in the stoichiometric equivalence point. From this it follows immediately that the p.z.c. is to the positive side of the stoichiometric equivalence point, that is: at lower pAg.

The standard affinities of the p.d. ions for the AgI surface may be defined as

$$\Delta G^0_{Ag+} = G^{cov}_{AgI} + G^{h,I}_{Ag+} - G^{h,L}_{Ag+} \quad (= \tilde{\mu}^{I0}_{Ag+} - \tilde{\mu}^{L0}_{Ag+}) \tag{3.28}$$

$$\Delta G^0_{I-} = G^{cov}_{AgI} + G^{h,I}_{I-} - G^{h,L}_{I-} \quad (= \tilde{\mu}^{I0}_{I-} - \tilde{\mu}^{L0}_{I-}) \tag{3.29}$$

Considering that

$$\Gamma_{Ag+}(p.z.c.) \ll \Gamma^{max}_{Ag+} \text{ and } \Gamma_{I-}(p.z.c.) \ll \Gamma^{max}_{I-},$$

the difference in standard affinities can be directly related to
the position of the p.z.c. by application of (3.19), (3.20), (3.24),
(3.25), (3.28) and (3.29).

$$\Delta G^0_{Ag+} - \Delta G^0_{I-} = 2.30RT[pL-2(pAg)_{pzc}] - 2F\Delta\phi (dip)_{pzc} - RTln \frac{\Gamma^{max}_{Ag+}}{\Gamma^{max}_{I-}} \tag{3.30}$$

We have assumed the absence of any specifically adsorbing electro-
lyte in the p.z.c. Furthermore, we used $\Delta\phi (ads)_{pzc} = \Delta\phi (dip)_{pzc}$
and the following expression for the solubility product of AgI in
solution.

$$pL = -log(c_{Ag+} c_{I-}) = pAg + pI \tag{3.31}$$

The last term in (3.30) is comparatively small and we shall neglect
it in the following.

Equation (3.30) can be applied after making proper choices of
the parameters. The value of $\Delta\phi (dip)_{pzc}$ can be estimated from the
maximum shift of the p.z.c. upon adsorption of non-polar or weakly
polar organic molecules (7, 8). A value of -200 mV appears to be a
good estimation. Using for the p.z.c. and pL the familiar values of
5.67 and 16.11 respectively, we find

$$\Delta G^0_{Ag+} - \Delta G^0_{I-} = 26.9 \ RT = 65.6 \ kJ/mol \tag{3.32}$$

If the AgI were structureless and the adsorbed Ag^+ and I^- ions would
be half-way immersed in the solid, then upon adsorption the Ag^+ and
I^- ions would be half-way dehydrated. In this case the difference
in adsorption free energy would be half the difference of the bulk

Gibbs energies of hydration, i.e. (479.4 - 257.1)/2 = 111 kJ/mol.
The actual difference is lower, indicating that the effective dehy-
dration is less than half. This is in accordance with the picture
that each adsorbed Ag^+ and I^- ion is surrounded by a number of
ions of the same kind, giving a reinforcement of the hydration ef-
fect at the interface.

It must be realized that the shift of the p.z.c. upon adsorp-
tion of organic molecules is due to the variation of both the elec-
trical and the chemical part of the difference in adsorption free
energy of the two p.d. ions. If upon adsorption of the p.d. ions
from a (dilute) aqueous solution of organic molecules the ions are
more strongly dehydrated than they do from pure aqueous electrolyte,
ΔG^0_{Ag+} - ΔG^0_{I-} will be larger and, consequently, a larger shift of
the p.z.c. to more positive potentials is expected. Hence, the in-
terpretation of the shift of the p.z.c. in terms of a dipolar poten-
tial on a neutral surface is thwarted by the lack of information
on the separation of the electrical and chemical part. Consequently,
one must be aware of the fact that conclusions on the net orienta-
tion of water molecules at the silver iodide surface based on the
shift of the p.z.c. must be taken with due care.

3.7 THE CHARGE-POTENTIAL RELATION

The model developed enables us to evaluate the relation be-
tween the surface charge σ and the Galvani potential difference
$\Delta\phi = \phi^S - \phi^L$ or the pAg. To that end the components of ϕ are cal-
culated as a function of σ.

$$\Delta\phi = \Delta\phi \text{ (solid)} + \Delta\phi \text{ (dip)} + \Delta\phi \text{ (mol)} + \Delta\phi \text{ (diff)} \tag{3.33}$$

Expressions for the first three terms have already been given. The
potential in the diffuse layer follows from the Poisson-Boltzmann
equation for a flat surface.

$$\Delta\phi \text{ (diff)} = \frac{2RT}{F} \sinh^{-1} \left(\frac{\sigma F}{2\varepsilon_0 \varepsilon^L RT\kappa}\right) \tag{3.34}$$

$$\kappa^2 = 2cF^2/\varepsilon_0 \varepsilon^L RT \tag{3.35}$$

61

Here ε^L is the relative dielectric constant of the solution containing a (1-1) electrolyte of concentration c. The parameter κ is usually called the reciprocal thickness of the diffuse double layer. In our picture, for σ the surface charge is substituted, as specific adsorption is neglected.

We are now in a position to calculate the charge-potential curves theoretically by assigning proper values to the different parameters. The parameters are chosen so as to obtain an optimal fit to the experimental charge-potential curve.

The relative dielectric constant ε^M and the thickness of the Stern layer d are chosen as 6 and 0.5 nm respectively. These values are close to those obtained in earlier work (9). The apparent relative dielectric constant for the Stern layer at mercury is frequently (1) also taken as 6, whereas the thickness of the Stern layer at AgI is expected to exceed the corresponding value at mercury (ca. 0.3 – 0.4 nm) due to the radii of the silver- and iodide ions of the crystal lattice.

We have estimated the value of $\Delta\phi \, (dip)_{pzc}$ as -200 mV. This is almost identical to the value of -192 mV derived from the butanol work (2). This value is split up into -140 mV for $\Delta\phi_{AgI}(dip)$ and -60 mV for $\Delta\phi^R_{Ag+}(dip) + \Delta\phi^R_{I-}(dip)$. This choice followed from optimization considering the fact that the number of water molecules to be oriented by Ag^+ and I^- ions is limited.

$F\Gamma^{max}_{Ag+}$ and $F\Gamma^{max}_{I-}$ were rather arbitrarily chosen as 15 $\mu C/cm^2$, which was considered realistic. However, this choice is not critical at all, as long as the value exceeds 1.5 times the surface charge.

Finally, two adjustable parameters are left, i.e. the surface excesses of the two p.d. ions at the p.z.c. and the ratio k_{Ag+}/k_{I-}.

The values of Γ_{Ag+} and Γ_{I-} are solved from (3.13) and (3.26) as explained above. The potentials $\Delta\phi$ (Stern), $\Delta\phi$ (dip), $\Delta\phi$ (solid) and $\Delta\phi$ (diff) follow from (3.2), (3.14), (3.27) and (3.34), realizing that $\Delta\phi$ (solid) at the p.z.c. is set equal to zero. Furthermore, $\Delta\phi$ follows from (3.33), and the pAg is then calculated according to Nernst's equation. Following the procedure given, an optimal correspondence between the calculated and experimental charge potential curves was obtained if the surface excesses of the two p.d. ions at the p.z.c. would correspond to +1.0 and -1.0 $\mu C/cm^2$ respectively

and if the ratio k_{Ag^+}/k_{I^-} amounts to 2.75. The agreement between the two curves is illustrated in fig. 3.1. The correspondence between
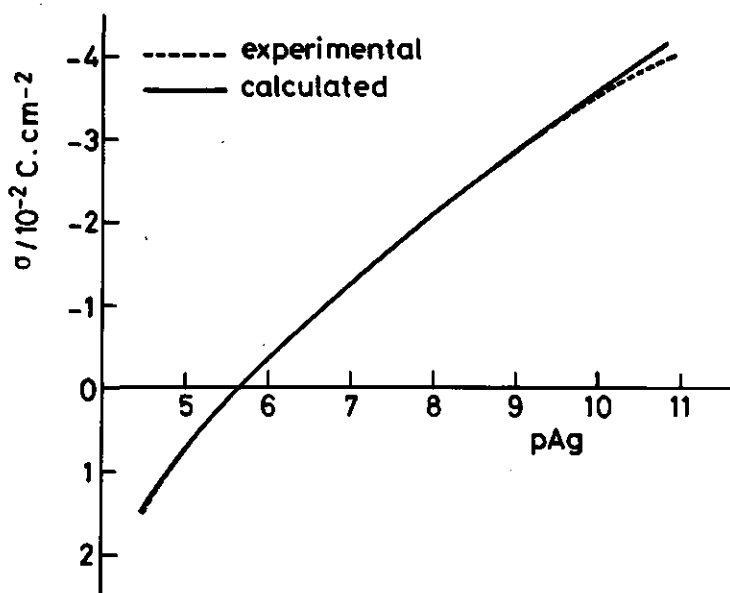
Fig. 3.1 Comparison of the calculated and experimental relation between charge and potential for the double layer on AgI. Electrolyte 0.1 M KNO_3, T = 25°C.

the calculated and experimental curve is excellent, except at the extreme negative side where the calculated curve somewhat exceeds the experimental one. A likely reason for this discrepancy is that at extreme negative surfaces specific adsorption of counterions may not be neglected. Some numerical results obtained with these data are summarized in table 3-1.

The effect of the various input parameters on the final outcome is quite different. It appears that ε^M, d and k_{Ag^+}/k_{I^-} do not affect the curvature of the charge-potential curve. Neither do the parameters $\Delta\phi_{AgI}(dip)$, $\Gamma_{I^-}^{max}$, and $\Gamma_{Ag^+}^{max}$ affect the results significantly. However, the curvature is sensitive to the choices of $\Delta\phi_{Ag^+}^R(dip)$, $\Delta\phi_{I^-}^R(dip)$ and the surface excesses of the p.d. ions at the p.z.c. Other assignments of values to these parameters may

Table 3-1 Calculated composition of the double layer on AgI[1]

σ	FΓ_{Ag+}	FΓ_{I-}	Δφ (solid)[2]	Δφ (dip)	Δφ (mol)	Δφ (diff)	Δφ	pAg	pAg-exp[3]
-4.0	0.19	4.19	-43	- 15	-376	-48	-482	10.50	10.95
-3.5	0.23	3.73	-39	- 34	-329	-44	-445	9.87	10.02
-3.0	0.27	3.27	-34	- 53	-282	-38	-408	9.23	9.25
-2.5	0.32	2.82	-30	- 74	-235	-33	-371	8.60	8.57
-2.0	0.39	2.39	-25	- 95	-188	-27	-335	7.97	7.90
-1.5	0.49	1.99	-19	-118	-141	-21	-299	7.34	7.28
-1.0	0.61	1.61	-13	-142	- 94	-14	-263	6.74	6.70
-0.5	0.78	1.28	- 7	-170	- 47	- 7	-230	6.17	6.12
0.0	1.00	1.00	- 0	-200	0	0	-200	5.65	5.65
0.5	1.28	0.78	7	-234	47	7	-173	5.19	5.25
1.0	1.61	0.61	13	-271	94	14	-150	4.79	4.83
1.5	1.99	0.49	19	-311	141	21	-130	4.44	4.50

1)   The following units are used

σ ($\mu C.cm^{-2}$), FΓ ($\mu C.cm^{-2}$), $\Delta\phi$ (mV)

2) $\Delta\phi$ (solid) is given relative to its value at the p.z.c.

3)   Experimental data from reference 2. The reproducibility of the experimental
     curve is ca. 0.05 $\mu C/cm^2$ but deteriorates at the ends of the curve. The
     absolute accuracy depends mainly on the uncertainty of the specific surface
     area, which is much higher but of no consequence for the present analysis,
     because it would affect the entire curve by a constant factor.

mathematically appear equally successful but in the authors' opin-
ion they are physically less realistic.

The calculations are performed for a concentration of indif-
ferent electrolyte of 0.1 N. As is shown by Lijklema (9) the dif-
ferences between curves at different salt concentrations are com-
pletely accounted for by the different contribution of the dif-
fuse part of the double layer. Hence, our model is also compatible
with the behaviour of charge-potential curves at other salt concen-
trations.

3.8   COMPARISON WITH PREVIOUS WORK

Mackor (10) has already qualitatively interpreted charge-poten-
tial curves on AgI by assuming a constant Stern layer capacitance
and a variable dipolar potential. The behaviour of the dipolar po-
tential on mercury and AgI were assumed to be equivalent. In later
studies with the AgI-system little attention has been paid to the
dependence of the dipolar potential on the surface charge.

The steep rise in capacitance at the positive side of the p.z.c. is typical for the AgI system. In previous work this has been explained by assuming that silver ions are adsorbed as $AgNO_3$ (9, 11). However, to this explanation some objections can be raised. The capacitance rise is also quite pronounced for the fluoride ion, although with this ion the p.z.c. is not shifted at all, indicating absence of specific adsorption, at least at the p.z.c.

3.9 COMPARISON WITH OTHER MODELS

Apart from the solute and solvent orientation, the given model is equivalent with the ionizable surface group model as described by Healy and White (12). Introduction of surface equilibria is equivalent to using the Langmuir model for the adsorption of p.d. ions. However, in the Healy and White model the charge-"potential" relation is almost linear over the same experimental range of charges as encountered in the AgI case, i.e. this picture implies a constant capacitance.

Trasatti (1) has reviewed the various models for the mercury-electrolyte interface in some detail. All these models predict an almost linear relationship of the potential with surface charge for charge densities between +4 and -4 $\mu C/cm^{-2}$, contrary to our model. It can be inferred from table 3-1 that in our model the variation of dipolar potential with surface charge is in the order of 50-100 $mV/\mu C.cm^{-2}$. For mercury Bockris and Habib (13) calculate 8 $mV/\mu C.cm^{-2}$, whereas on the other extreme Levine et al. (14) find 360 $mV/\mu C.cm^{-2}$. The other models discussed by Trasatti predict potential drops in the order of 30-50 $mV/\mu C.cm^{-2}$. This is also the case for Parsons' model (15), in which a four-state water orientation was assumed with single water molecules and clusters. It is interesting that in Parsons' model also an asymmetry of the charge-potential curves can arise around the p.z.c. dependent on a difference in free energy of the water clusters in the two orientations.

3.10 CONCLUSIONS

In this article we offered a patchwise hydration model for the interface between silver iodide particles and aqueous electrolyte

solutions. Although several simplifying assumptions were made, it was shown that with the present picture some typical properties of the AgI system, such as the asymmetry of the capacitance curve and that of the p.z.c., could be accounted for. Therefore, the model holds promises for further quantitative analysis of other hydration-sensitive properties, such as the adsorption maximum of organic substances. In addition, it can be helpful for a better understanding of the quantitative differences between the double layers on mercury, silver iodide and other systems.

3.11 SUMMARY

The hydration of solid particles in aqueous solution is treated as a patchwise phenomenon, in which the orientation of water dipoles varies in a patchwise fashion along the surface. The idea is applied to the AgI system where besides the neutral surface Ag^+ patches and I^- patches are distinguished. A first-order elaboration is offered, including an analysis of the relation between overall macroscopic quantities and local properties. The model offers an interpretation of two characteristics of double layers on silver iodide: the asymmetry of its p.z.c. and the conspicuous capacitance rise on the positive side, and may serve as a starting point for a better description of the typical differences between the double layers on AgI and Hg.

3.12 REFERENCES

1. S. Trasatti, in Modern Aspects of Electrochemistry, Vol. 13, B.E. Conway and J.O'M. Bockris, eds. Plenum Press, London, 1979, p. 81

2. B.H. Bijsterbosch and J. Lyklema, Advan. Colloid Interface Sci. 9 147 (1978)

3. K.J. Peverelli and H.P. van Leeuwen, J. Electroanal. Chem. 110 137 (1980)

4. S. Levine. G.M. Bell, A.L. Smith, J. Phys. Chem. 73 3534 (1969)

5. S. Levine and A.L. Smith, Discussions Faraday Soc. 52 290 (1971)

6. H.L. Friedman and C.V. Krishnan, in Water, a comprehensive treatise, Vol. 3, F. Franks, ed. Plenum Press, London, 1973, Ch. 1

7. B.H. Bijsterbosch and J. Lyklema, J. Colloid Sci. *20* 665 (1965)

8. A. de Keizer and J. Lyklema, J. Colloid Interface Sci. *75* 171 (1980)

9. J. Lijklema, Thesis, 1957, Utrecht

10. E.L. Mackor, Rec. Trav. Chim. *70* 763 (1951)

11. B. Vincent, J. Lyklema, Special Discussions Faraday Soc. *1* 148 (1970)

12. T.W. Healy and L.R. White, Advan. Colloid Interface Sci. *9* 303 (1978)

13. M.A. Habib, in Modern Aspects of Electrochemistry, Vol. 12, J.O'M. Bockris and B.E. Conway, eds. Plenum Press, London, 1979, p. 131

14. S. Levine, K. Robinson, A.L. Smith and A.C. Brett, Discussions Faraday Soc. *59* 133 (1976)

15. R. Parsons, J. Electroanal. Chem. *59* 229 (1975)

67

CHAPTER 4

COMPUTER-CONTROLLED POTENTIOMETRIC TITRATION SYSTEM BASED ON CAMAC

4.1 INTRODUCTION

Studies of the electrical double layer and electrosorption at solid-aqueous electrolyte interfaces necessitates as a rule the determination of the surface charge against the surface potential at varying experimental conditions, such as temperature, indifferent electrolyte concentration, and concentration of an adsorbable compound. The theoretical basis of the analyses has to some extent been described in the previous chapters.

The description of the determination of surface charge and surface potential will be given for the silver iodide-electrolyte interface, where the surface charge is determined by adsorption of Ag^+ and I^- ions. The principle of the charge-potential determination is a potentiometric titration with silver and iodide ions, shortly called a *"silver iodide titration"*.

Many solid-liquid interfaces are charged by adsorption or desorption of protons. The procedures described in the present chapter are mutatis mutandis also applicable to these surfaces.

The silver iodide titration procedure has been used for many years. The technique has been described by de Bruyn (1), Mackor (2), van Laar (3), Lijklema (4), Agar (5), Bijsterbosch (6), de Wit (7) and Koopal (8). The method is very simple in principle. A certain volume of $AgNO_3$ or KI solution is added to a vessel containing a suspension of silver iodide in an electrolyte solution. Silver or iodide ions are subsequently adsorbed. According to Nernst's law, the equilibrium concentration follows from measurement of the e.m.f. of a cell containing a reference and a silver-silver iodide electrode.
This cell potential is at the same time a measure for the surface

potential, except for some constant bias. The change in surface charge follows from the depletion in solution due to adsorption of potential-determining (p.d.) ions, Ag^+ and I^-. The relative surface charge can be transformed into an absolute value if the surface charge at same reference pAg, e.g. the point of zero charge, is known.

A drawback of the procedure is the rather tedious character of the experiments. Dependent on the equilibrium period, the equilibrium conditions, and the number of experimental points, the manual measurements of a set of five titration curves for a silver iodide batch takes usually 5 to 8 weeks, including some readings during the evenings and the week-ends (7,8). This is caused by the fact that, while the potential reaches the equilibrium value rather slowly, a very high accuracy of the equilibrium potential is required. Moreover, more often than not a large number of experimental data are needed in order to perform the desired analyses. It is obvious that automation of the potentiometric titration procedure eliminates many of its disadvantages. The procedure is *speeded up* very much by working in a continuous fashion. This increases the overall *accuracy* of the measurements. The reproducibility is improved because all experimental condi- tions are better kept constant. The procedure is essentially quasi-dynamic; the values taken have a (constant) small difference with the real equilibrium value. On the other hand, continual oper- ation implies that discontinuities due to largely different equi- librium times (e.g. during the nights) are avoided. Last but not least, automation eliminates a lot of *manual work* like calcula- tions, readings, transfer of data to another central computer, waiting times, titrant additions etc.

In the investigations presented here, a PDP 11/10 computer with a CAMAC-interface system has been used for the data acquisi- tion and real-time control of the potentiometric titration pro- cedure. The system chosen is rather flexible and can in principle be used for many other laboratory experiments without important modifications. For instance, in our laboratory measurements of ion transport through liquid-liquid interfaces by Scholtens (9)

70

have been automatized with the same PDP11-CAMAC system, only by addition of a separate subroutine in the main computer programme. The choice of the system was also determined by the necessity of standardization of computer- and interfacing equipment within the Agricultural University.

The computer used in our equipment was the PDP11/10 computer (Digital Equipment Corp.) with 16K core memory. The computer was used in its basic version, without a disk and operating system, and equipped with a teletype only. The heart of the software system was chosen to be the papertape-BASIC-PTS interpreter, which is relatively fast and capable of incorporating assembler functions for specific I/O or time-critical functions.

The data-acquisition interface system was based on CAMAC (Computer Aided Measurements And Control). CAMAC is a standardized set of hardware and software elements, which provides for the exchange of data and control information between a computer and its peripherals (10). CAMAC originates from nuclear research centres, which traditionally have many data acquisition and control applications with high speed and moderate accuracy demands. The CAMAC standard gradually won acceptance also in other fields, e.g. chemical laboratory automation (11). The modular CAMAC interface system can be coupled with any PDP11 computer in a straightforward and simple way. The BASIC interpreter can easily be adapted for use with the CAMAC interface by the introduction of a few CAMAC specific assembler routines. In this way our PTS-BASIC was extended with six CAMAC functions, which are sufficiently general to handle all specific functions of the different modules in the CAMAC crate. Only six functions are needed for many different interface functions because of the bus nature of the CAMAC system.

In this chapter we will describe in some detail the software and hardware of the PDP11-CAMAC potentiometric titration system. In section 4.2 a short description will be given of the CAMAC assembler routines introduced in the BASIC-PTS interpreter will be given. Thereupon the electrochemical cell will be illustrated, but only electrical and automation aspects are discussed. Preparation of electrodes, materials and the description of the system used etc. are postponed till chapter 5. In the forthcoming sections the structure of the CAMAC and related hardware will be given

schematically and the operation of the BASIC-PTS titration real-time programme will be illustrated by a flow-chart. Finally, some conclusions on the functioning of the system will be drawn.

4.2 SOFTWARE MODIFICATIONS FOR THE CAMAC-PDP11 SYSTEM

The PDP11/10 computer can in principle be programmed on different levels: in assembler language, in BASIC, in FORTRAN etc. BASIC was chosen for programming of the underlying system, because this language is simple for the implementation of programmes and their modifications whenever the required data rate is limited. There were three versions of the BASIC interpreter supplied by DEC: Single User BASIC, 8-User BASIC and BASIC-PTS. Initially the first version was used. Assembler CAMAC functions were available already for this version as an overlay (12). However, this BASIC version appeared too slow for our purpose. This was the main reason for the use of a more advanced BASIC interpreter, viz. BASIC-PTS which is much faster and, in addition, has more real-time programming features (13). The available core memory had to be extended to 16K in order to provide enough room for the user programme and the data to be stored. A negative consequence was, however, that at the time of our original implementation (1974) no suitable CAMAC assembler routines were available to modify BASIC-PTS for use with a CAMAC interface.

BASIC-PTS (Paper Tape Software BASIC) has the facility which allows the user to incorporate assembly language routines in BASIC. The assembly language routines can be called in a BASIC programme by the special function CALL "name" (arguments). The CALL function is treated as a normal function within the BASIC interpreter. The assembly language routines can be written in PAL11S assembler, whereas the separate programme modules are linked with LINK-11S (14). Seven assembly language subroutines have been incorporated in our special programme module. The corresponding CALL statements are described in Table 4-1. The four functions without arguments are used to' determine the state of the CAMAC controller. The most important functions are CF, CW and CR which control in a generalized way all the necessary aspects of the different functional CAMAC modules. This means that these three routines can control

72

Table 4-1   Call statements for the PTS-BASIC interpreter to control a
              general purpose CAMAC-interface system.

CALL	Arguments	Function	Corresponding CAMAC-function codes
"CC"	none	clear CAMAC interface buffer	C
"CZ"	none	initialize id.	Z
"CIS"	none	set inhibit id.	I
"CIR"	none	reset inhibit and initialize id.	I + Z
"CF"	F,N,A,Q	dataless function with Q given	F8-F15 and F24-F31
"CW"	F,N,A,D	write D	F16-F23
"CR"	F,N,A,D	read D	F0-F7

F = CAMAC FUNCTION   D = data
N = module adress   Q = response
A = subadress

an analog-digital convertor as well as e.g. a relay multiplexer,
simply by using different arguments. The different CAMAC functions
and function codes are defined according to the ESONE standard (15)
and are described a.o. in the literature issued by the manufac-
turer of the CAMAC equipment (16).

The CAMAC assembly language subroutine module is available
on request from the author.

4.3   THE ELECTROCHEMICAL CELL

The central part of the automatic titration system is the
electrochemical cell. Here the potentials of a number of silver-
silver iodide electrodes are measured against a calomel reference
electrode. The titration vessel is schematically represented in
fig. 4.1. The set-up given is accomodated in a metal box (fig. 4.1)
which acts as a Faraday cage. The metal titration box is grounded.
The box makes it also possible to keep the silver iodide suspension
in the dark.

The silver-silver iodide electrodes are prepared electro-
analytically as described in the next chapter. All electrodes
with mutual potential differences within 1 mV were retained.
In general, the electrodes were stable over 4 weeks within a few
tenths of a millivolt. In normal operation 6 electrodes are used
concurrently. In this way unstable electrodes can be eliminated

73

during the procedure, leaving enough electrodes to finish the complete measurement. Conditions for skipping one of more electrodes can be introduced in the programme.

The measuring vessel is connected to the reference vessel through a van Laar salt-bridge (3). The van Laar salt-bridge consists of two capillaries having a resistance of ca. 0.5 MΩ each. The bridge is filled with a solution of 1.75 M KNO_3 and 0.25 M $NaNO_3$ in order to minimize liquid junction potentials. The bridge has a small overpressure to obtain constant (but very small) streaming in the capillaries. More details will be discussed in the next chapter.

The resistance of the individual capillaries can be measured with a platinum connection in the bridge (c). In the automatic procedure the total resistance is measured between the calomel electrode and a seventh silver iodide electrode used exclusively for this purpose.

The tapper construction enables us to release also the very last drop.

Purified nitrogen is led over the solution to keep the oxygen level of the solution low.

4.4 HARDWARE CONFIGURATION

A simplified block diagram of the PDP11/CAMAC titration system is given in fig. 4.2. The system consists of a PDP-11/10 computer (Digital Equipment Corporation) with 16K core memory operating in a single-programme mode (no separate operating system is needed then). Necessary print-out is performed through a Teletype terminal (ASR33). Data transfer to the central DEC-10 computer is performed by paper tape punched by the Teletype (quantity of data is low). The measuring system is based on a CAMAC data acquisition interface to the PDP11. For that purpose a PDP11-CAMAC crate controller/interface (Borer, type 1533A) is used to link the CAMAC crate directly to the PDP11-Unibus. The CAMAC crate is the basic hardware that houses the different CAMAC interface modules.

Potential differences between the Ag-AgI electrodes and the calomel electrode were measured with a CAMAC compatible inte-

74
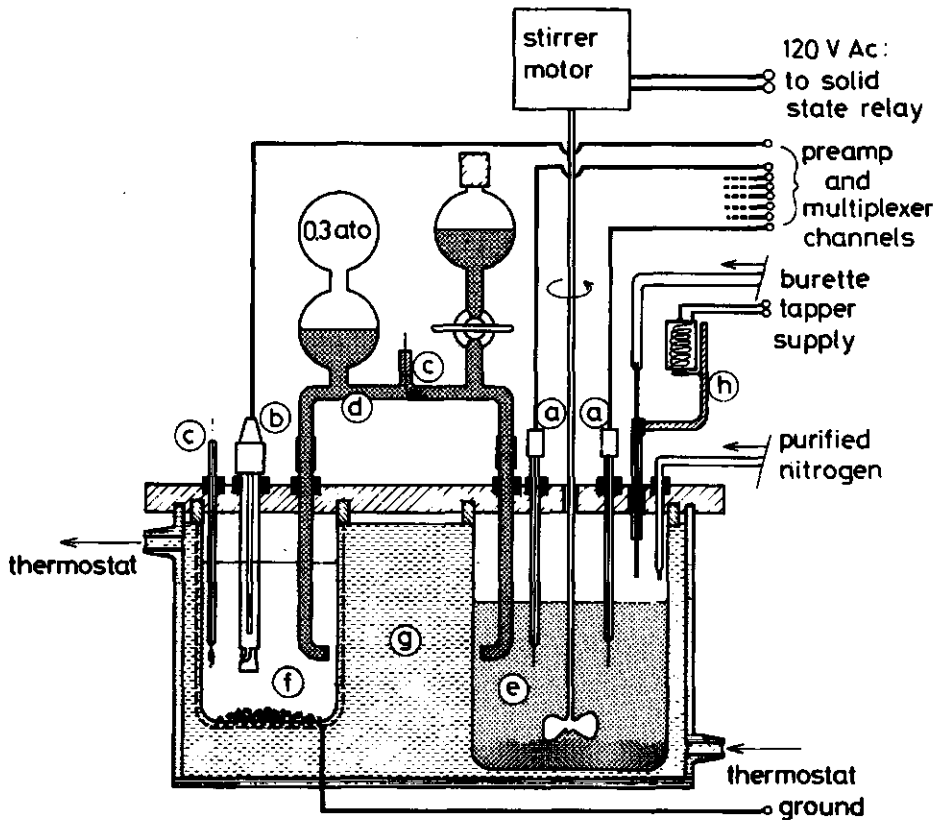
Fig. 4-1 Titration vessel with mechanical and electrical junctions

a. Silver/silver iodide electrodes (7x). One of these electrodes is used exclusively for measurements of the resistance of the salt bridge.
b. Saturated KCl-calomel electrode.
c. Auxiliary electrodes used for individual measurements of the capillary resistance.
d. Salt bridge with van Laar-mixture (1.75 M KNO_3 + 0.25 M $NaNO_3$) and two van Laar-capillaries.
e. Vessel with silver iodide suspension and measuring solution.
f. Vessel with saturated KCl.
g. Thermostatted bath with perspex cover, temperature 20.00 ± 0.05°C.
h. Tapper construction (mechanical 5V relay).

grating analog digital convertor (Borer ADC, type 1241). This ADC has a 11-bit plus sign resolution (accuracy 0.05%) and is used fixed in the 1V range. An optimal accuracy with respect to noise etc. was obtained by sampling each electrode 15 times and averaging out. The time needed for one A - D conversion amounted to 20 ms.

Multiplexing of the different electrodes was obtained by a 15 channel relay multiplexer (Borer, type 1701). Because of the high impedance of the salt-bridge (ca. 1 MΩ) the silver-silver iodide electrodes were treated as the 'low' electrodes, while the calomel electrode was treated as 'high'. The distance between the electrodes and the CAMAC crate is a few meters, hence it was necessary to use a preamplifier inside the Faraday cage. A 41J (Analog Devices) preamplifier ($R_{in} = 10^{13}$ Ω) was used for this purpose. The schematic circuit of the multiplexer and the preamplifier is given in fig. 4.3. An amplification factor of 3 was used throughout. Each multiplexer channel has three poles, two of which are used to connect the output of each preamplifier with the ADC input, whereas the third one was used to connect a silver-silver iodide electrode with the input of the preamp (IN-). In order to prevent any current leakage through the silver-silver iodide electrodes separate reed relays were used to disconnect the electrodes, after measurement. In each measuring cycle the resistance of the van Laar salt bridge was also measured. This was accomplished by measuring the potential decay over a 10 KΩ resistance due to a current induced by a battery potential. The sign of the applied potential can be reversed to avoid strong polarization of the electrodes. On the side of the measuring solution a separate silver-silver iodide electrode was used for the resistance measurement.

The dosage of the titrant was done by a METROHM motor burette (type E415 and E535) through a contact closure using the relay multiplexer. Each dosage step corresponds to a volume of 10 and 50 µl for the two types of burettes respectively. The burette volume used was 5 ml. Separate changing units of 5 ml were used for the solutions of $AgNO_3$ and KI.

The stirrer was controlled by a relay-output register (Borer, type 1082) using a solid-state relay. The output register was also used to activate a mechanical relay in order to detach the final drop from the tip of the (narrow) teflon delivery tube. Thus, diffusion of titrant in the solution during the measurements was avoided. The accuracy obtained for the delivery volume was in the order of a few micro-liters.

The process was controlled with respect to real time by a clock/timer (Borer, type 1411). The dataway-display module (Borer,
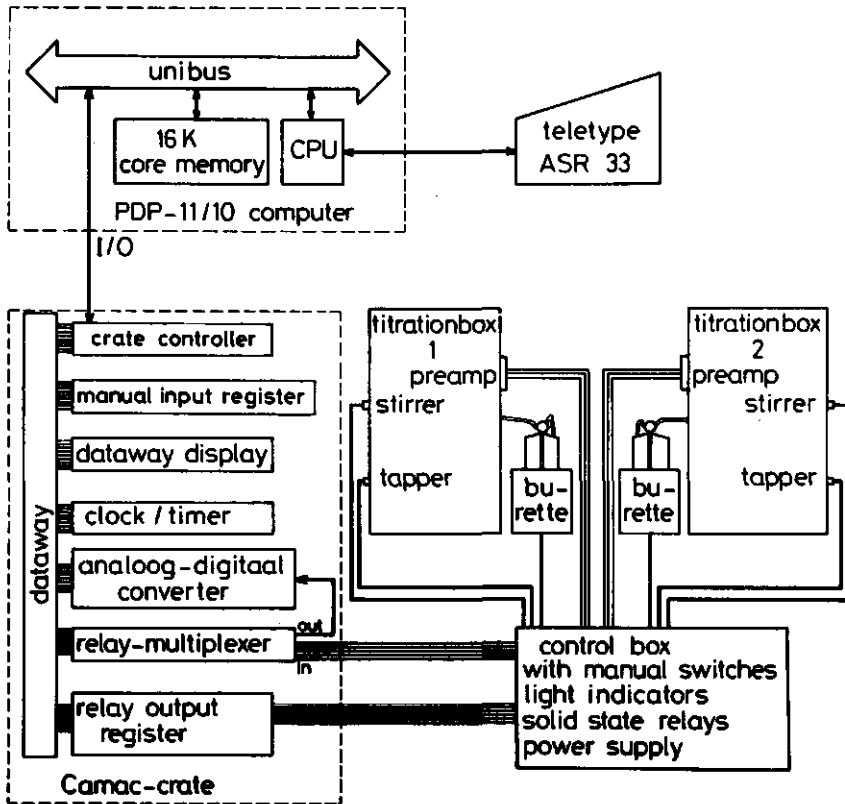
Fig. 4.2 Simplified block diagram of the PDP11/CAMAC titration system
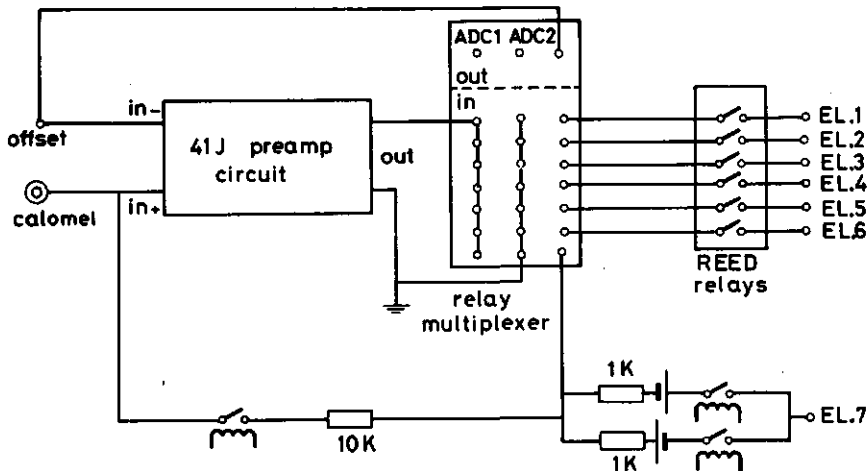
Fig. 4.3 Multiplexing of input signals

type 1801) was used to check the dataway in order to be able to detect hardware and/or software faults in the system. During normal operation of the titration system these dataway diodes display some characteristics of the titration process in addition to the diodes on the control box, which are controlled by the output register. The manual input register (Borer, type 1041) enables a data word to be constructed manually with front panel switches. The word can be read whenever required by the programme. This device was used for checking the hardware or for the debugging of the programmes. During normal operation of the titration programme the manual input register enables special interrupts to start specific functions or routines, such as printing of preliminary output, calibrations etc.

The titration system was situated in a thermostatted room (22.0 ± 0.3°C). In this way the total volume of the burette cylinder was constant to within a few microliters, and the electric signals were as stable as possible. The measuring cell was thermostatted by flowing water of 20.00 ± 0.05°C through the perspex box.

4.5 TITRATION COMPUTER PROGRAMME

The flow-chart of the main programme is represented in fig. 4.4. The illustrated programme also contains routines to accomplish real time measurements of ionic conductivity for calculating the rate of transport of ions through liquid-liquid interfaces (9). These routines marked with an asterisk (*) are not explained here.

Apart from the conductivity measurements, the programme performs the following functions:
1. Calibration of the burettes
2. Calibration of the potential measurement (preamplifier + ADC)
3. Calibration of the resistance measurement
4. Determination of the standard potential by titration
    a. with Ag^+ (E^O_{Ag+})
    b. with I^- (E^O_{I-})
5. Determination of the surface charge by titration
    a. with Ag^+
    b. with I^-

The calibration functions (1-3) are executed in the test subroutines.

The programme can be subdivided into five blocks representing its main tasks. These blocks are indicated in the right margin. After starting the programme and giving the initiating commands to the CAMAC crate, the programme is able to accept new input. Three input modes are present as far as the titration concerns.

(i) One introduces parameters needed to start a new titration,

(ii) one can change parameters after the procedure has been interrupted for some reason (e.g. addition of adsorbate), continuing the titration with the same titrant (i.e. the same direction) and, finally,

(iii) one can change input parameters and continue the titration in the opposite direction, which as a matter of course is done after changing the burette unit.

The system is interrupted by a clock-timer LAM (Look-At-Me bus status) every minute to read the content of the manual input register. If the manual input register requires no action, the 10-minute LAM of the clock-timer is checked. The timing of the titration procedure is such that every 10 minutes a titration measurement cycle is performed. This cycle is started by stopping the stirrer for 1 minute in order to allow settling of the silver iodide particles. After this waiting period the titration subroutine is started. This subroutine is given schematically in fig. 4.5. The two titration boxes are handled successively. The six silver-silver iodide electrodes are scanned and each electrode is sampled 15 times in succession and the average single electrode potential is calculated. Short waiting periods are taken to avoid errors due to switching, and to average out longer fluctuations. Next, the resistance of the salt-bridge is measured. The separate electrode potentials are averaged, and electrode potentials differing more than a given value from the average potential are discarded. The way in which the titration is continued depends on the kind of titration function: surface charge (σ) or standard potential (E^o) determination. In the latter case the E^o is calculated according to

$$E^o_{Ag^+} = \bar{E}_j + 58.164 \text{ pAg} \quad (\text{if pAg} \leq \text{pI}) \tag{4.1}$$

$$E^o_{I^-} = \bar{E}_j - 58.164 \text{ pI} \quad (\text{if pI} < \text{pAg}) \tag{4.2}$$

79
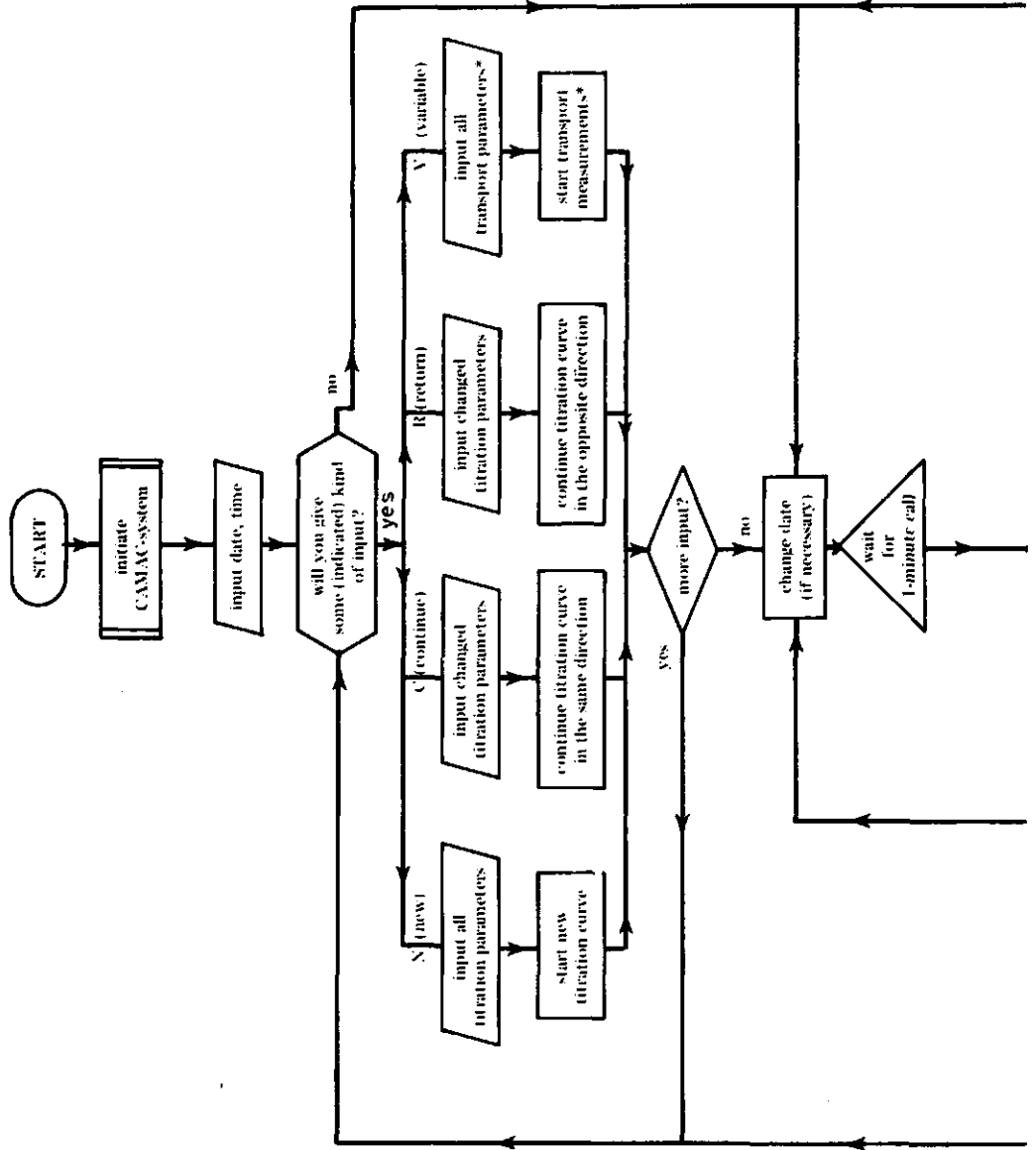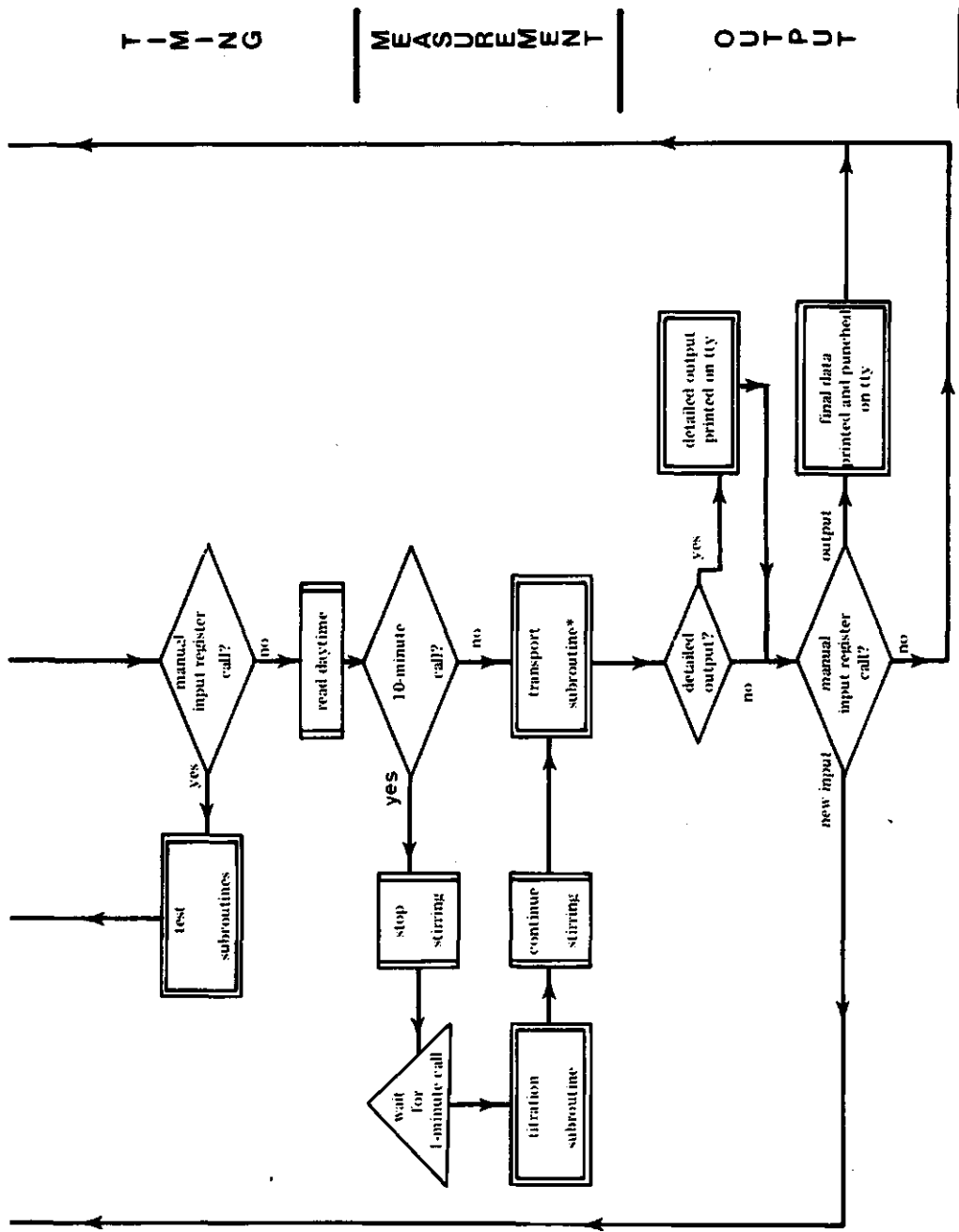
Fig. 4.4 Flow-chart for the PTS-BASIC titration programme

calculate number of buret-pulses for titrant addition

test "stop" conditions
1. converter overflow
2. salt-bridge resistance
3. end point reached
4. buret volume overflow
5. databuffer overflow

stop

go

give calculated pulses to buret and push last drop off

calculate exact μmol titrant added

RETURN

measurement of the salt-bridge resistance

(re)calculate average electrode potential $\overline{E}$

select "worst" electrode potential E_j

$|E_j - \overline{E}_i| > E_{del}$?

yes

no

delete electrode j

what kind of measurement?

σ

σ

E^0

E^0

Fig. 4.5 Flow-chart for the titration-subroutine

where $\bar{E}_j$ is the j-measurement after the previous titrant delivery. After having performed four measurements, the next delivery of titrant is calculated if the following equilibrium conditions are met:

$$\bar{E}_j - \bar{E}_{j-1} < \delta \tag{4.3}$$

$$\bar{E}_j - \sum_{i=j-3}^{j-1} E_i/3 < \delta \tag{4.4}$$

where δ is a criterion for equilibrium. The dosage is calculated from the ΔpAg given or from the ΔpAg to reach the end-point of the titration.

For the surface charge determination the actual pAg and pI are calculated from the average potential $\bar{E}_j$, using

$$pAg = (E^o_{Ag+} - \bar{E}_j)/58.164 \tag{4.5}$$

$$pI = (\bar{E}_j - E^o_{I-})/58.164 \tag{4.6}$$

Next, the relative surface charge is calculated according to

$$\sigma_j = \sigma' + \frac{(\mu mol\ titrant\ -\ \Delta\mu mol\ solution) \times 96500}{a_s \times m_{AgI}} \tag{4.7}$$

where σ' is the surface charge in the previous point (or a reference), μmol titrant follows from the delivered volume, $\Delta\mu$mol solution can be calculated from the change in concentration of potential determining ions in solution, a_s is the specific area of the AgI suspension, and m_{AgI} the mass of AgI. After four measuring cycli the equilibrium conditions are tested:

$$\bar{E}_j - \bar{E}_{j-1} < \delta_1 \tag{4.8}$$

$$\bar{E}_j - \sum_{i=j-3}^{j-1} E_i/3 < \delta_1 \tag{4.9}$$

$$\sigma_j - \sigma_{j-1} < \delta_2 \tag{4.10}$$

$$\sigma_j - \sum_{i=j-3}^{j=1} \sigma_i/3 < \sigma_2 \tag{4.11}$$

If equilibrium is obtained (or if the maximum number of measurements is reached) the amount of a new addition is computed from

the desired ΔpAg value. In doing this, the amount adsorbed in the next step is estimated from that obtained in previous steps.

Before delivering a new volume of titrant the "stop" conditions are tested. If the procedure is allowed to continue, the titrant is added and the number of μmol titrant calculated.

Detailed output is printed on the teletype when the buffer is filled or when the manual input register gives the corresponding command. The final data can be printed on the teletype by a corresponding setting of the manual input register, and a paper tape with the final data can be made in order to analyse the data on a central computer.

4.6 CONCLUSIONS

The automation of the titration procedure enables the measurement of a whole titration curve independent of human observation, also outside usual working hours. As a consequence, the overall rate of the titration will be a factor of 3 to 4 higher than in the case of manual performance of the titration. Moreover, the amount of manual labour is limited to the exchange of burette units. Besides elimination of a lot of manual labour, the automatic procedure has many advantages. More curves with more experimental points can be measured during a given period. Some experimental errors increase with the time of experimentation, e.g. evaporation of solution, shifts of standard electrode potentials etc. The reduction of the time required to complete a titration is therefore also conducive to improve the accuracy.

It appears that the hardware of the system is quite appropriate for the present kind of experiments. A limitation of the system in the given configuration was the lack of a sufficiently large storage area for data, which limited the simultaneous number of applications.

The reliability of the system is excellent. Over a period of 6 years the system has been 'down' due to technical failures for only a few days.

It may be concluded that a CAMAC data-acquisition system is very suitable in the titration experiments described and in laboratory automation in general.

4.7 SUMMARY

A laboratory automation system based on a CAMAC data-acquisition system and a PDP11 computer has been described with the purpose to perform specific potentiometric titrations of silver iodide suspensions

4.8 REFERENCES

1. H. de Bruyn, Rec.Trav.Chim. *61* 5 (1942)

2. E.L. Mackor, Thesis, 1951, Utrecht

3. J.A.W. van Laar, Thesis, 1952, Utrecht

4. J. Lijklema, Thesis, 1957, Utrecht

5. G.A. Agar, Thesis, 1961, Massachusetts Institute of Technology Cambridge USA

6. B.H. Bijsterbosch, Thesis, 1965, Utrecht

7. J.N. de Wit, Thesis, 1975, Agricultural University, Wageningen

8. L.K. Koopal, Thesis, 1978, Agricultural University, Wageningen

9. B.J.R. Scholtens, Thesis, 1977, Agricultural University, Wageningen

10. ESONE Bulletin, Issue no. 13, september 1975, Supplement A

11. G.W. Bushnell, T.K. Davies, A.D. Kirk, S.K.P. Wong, Anal. Chem. *48* 587 (1976)

12. H.K. Halling, W.J. Zwoll, CAMAC Bulletin no.6, p.15 (1973)

13. BASIC/PTS user's manual (DEC-11-LPTBA-A-D), 1973. Digital Equipment Corp., Massachusetts

14. PAL-11S Assembler and LINK-11S Linker, (DEC-11-YRWB-D and DEC-11-YRWB-DN), 1972, Digital Equipment Corp, Massachusetts

15. ESONE Committee Report EUR4100 (1972) and TID-25875

16. Borer Electronics AG, Camac, dataway uses and specifications Pub: 603.4.003.11.72

CHAPTER 5

MATERIALS, METHODS AND EXPERIMENTAL RESULTS

5.1 INTRODUCTION

This chapter is the experimental basis of chapters 6 and 7, which treat the adsorption and electrical double layer aspects of the silver iodide-electrolyte interface respectively in the presence of some quaternary ammonium ions. Some of the methods treated in this chapter in some detail recur more briefly in publication (1) which, except for minor modifications, is identical to chapter 6.

The major part of the measurements concerns the effect of the adsorption of tetrapropyl-, tetrabutyl- and tetraamyl ammonium nitrate. Some results in the presence of other quaternary ammonium compounds will also be given.

Three different experimental methods will be described: adsorption of tetraalkylammonium (TAA) ions from depletion measurements, determination of the surface charge as a function of surface potential by potentiometric titration, and measurements of the electrophoretic mobility by particle electrophoresis.

The introduction of the specific surface area can be deferred by expressing the surface quantities in units per gram AgI. A comparison of the specific surface areas as derived from adsorption and titration experiments will be given in section 5.9.

5.2 MATERIALS AND GENERAL METHODS

5.2.1 *General*

Doubly distilled water was used throughout. In all experiments the water was percolated through a column containing silver iodide precipitate prior to use to remove adsorbable impurities.

Purified nitrogen was bubbled through the water to remove O_2 and CO_2.

$AgNO_3$, KI and KNO_3 were of pro-analyse quality and were used without further purification.

Chloroform was of p.a. quality. The chloroform used was re-cycled by distillation after the adsorption determination.

Na_2HPO_4, citric acid, boric acid, and borax were all of pro analyse quality.

Bromothymol blue (Merck) was used in indicator quality.

High quality borosilicate glass was used throughout. It was cleaned by means of a chromic acid solution and rinsed successively with dilute HNO_3, tap water, and percolated water.

The volumetric glassware was recalibrated when necessary.

5.2.2 *Quaternary ammonium salts*

The following commercial salts were used:
- tetramethylammonium (TMeA) iodide,
  M = 201.05 (Merck, for polarography)
- tetraethylammonium (TEtA) iodide,
  M = 257.16 (Merck, for polarography)
- tetrapropylammonium (TPrA) iodide,
  M = 313.27 (Fluka, Purum)
- tetrabutylammonium (TBuA) iodide,
  M = 369.38 (Fluka, polarography)
- tetraamylammonium (TAmA) bromide,
  M = 425.49 (KEK,ICN Pharmaceuticals,Inc)
- phenyltrimethylammonium (PhTA) bromide,
  M = 216.13 (Fluka, Purum)
- choline (Chol) iodide, $[CH_2(OH) \cdot CH_2 \cdot N (CH_3)_3]$ I
  M = 231.08 (BDH, biochemical)
- hexamethonium (HeMe) iodide, $(CH_3)_3 \overset{+}{\underset{I^-}{N}} (CH_2)_6 \overset{+}{\underset{I^-}{N}} (CH_3)_3$
  M = 456.20 (Fluka, Purum)

All TAA^+ ions used have n-alkyl chains.

The tetraalkylammonium halides were standardized against an $AgNO_3$ solution by potentiometric titration. The halide content could be determined within 0.1%. The purity was usually within 99.5 and 100%.

In most experiments the *nitrate salt* of the quaternary ammonium compound was needed. The tetramethyl-, tetraethyl-, tetrapropyl-,

tetrabutylammonium, and the three asymmetric quaternary ammonium
solutions were prepared directly by addition of an equivalent amount
of $AgNO_3$ to a solution of the quaternary ammonium halide. This ad-
dition was potentiometrically controlled. The flocculated silver
halide sol was filtered off. The presence of remaining halide ions
can be neglected.

Tetraamylammonium nitrate was prepared in *crystalline* form
according to the following procedure (2):
Tetraamylammonium bromide (4 gram) was dissolved in 96% alcohol and
a small excess of $AgNO_3$ (dissolved in 85% alcohol) was added. The
AgI was filtered off and the excess Ag^+ was titrated with KI and
the AgI filtered off again. The dried product was recrystallized
several times from ethyl acetate and a mixture of ether and ethyl
acetate (1 : 2.5). The melting point was 113-113.8 °C (literature
115 °C).

5.2.3 *Silver iodide suspensions*

Precipitates of silver iodide were prepared by slowly adding
(ca. 50 cm^3 per hour) 2 litres of 0.1 M $AgNO_3$ to a solution of 0.1 M
KI under vigorous stirring. Purified nitrogen was bubbled through
and the whole procedure was carried out in dark. After a few hours
the rate of addition was increased to 400 cm^3 per hour. After com-
pletion the stirring was continued for a few hours. Several batches
prepared in this way were combined and stored in dark in a stoppered
bottle. The suspension was then washed with percolated water until
the specific conductivity was constant (ca. 10^{-6} Ω^{-1} cm^{-1}). Finally
the suspension was aged for 3 days at 80 °C at an initial pI of
5-5.5.

Several batches of silver iodide suspensions, each prepared
in the above way, were used for the experiments. They are desig-
nated I, II and III. The specific surface areas between these
batches differ slightly, probably because it is not easily possi-
ble to have identical drop times and stirring conditions during
the preparation and consequently it is not feasible to fully
control the relative rates of nucleation and growth.

5.2.4 *Preparation of silver-silver iodide electrodes*

The electrodes were prepared following Brown (3) and Agar (4) except for some minor modifications.

The electrodes consist of a Pt wire (diameter 0.04 cm and length 1.5 cm) sealed in a glass tube. Old electrodes covered with Ag/AgI were cleaned with a saturated solution of potassium iodide in aceton (which dissolves the AgI) during one hour and subsequent dissolution of the silver layer in concentrated HNO_3 at 60°C during three hours. The electrodes were rinsed several times with distilled water. Further cleaning was performed electrolytically by anodizing the electrodes in conc. HNO_3 during 45 minutes at ca. 2 mA/cm^2. The electrodes were carefully rinsed again with distilled water and percolated water.

The electrodes were silvered by electrolysis in a solution of 1% $KAg(CN)_2$ during 6 hours at 1.0 mA/cm^2 in a nitrogen atmosphere and in the dark. After a treatment with conc. NH_4OH during 3 hours and rinsing with distilled water, the electrodes were iodized in 0.1 M KI during 60 minutes at 0.8 mA/cm^2. After rinsing again with percolated water they were aged in the presence of some silver iodide suspension at pI = 4.5 during 3 days at 80°C.

Only electrodes with mutual differences within 1 mV were retained.

5.2.5 *Salt-bridge*

The measuring cell was connected to the reference cell by a van Laar salt-bridge (5,6) as given in fig. 4.1. The liquid junction potential of the salt-bridge is minimized by using an electrolyte mixture of 1.75 M KNO_3 and 0.25 M $NaNO_3$ at a slight overpressure and by using two capillaries in a symmetrical configuration (7). There are two crucial prerequisites for the proper operation of the salt-bridge: The outflow of electrolyte into the solution and the electrical resistance.

The outflow of the electrolyte from the salt-bridge into the measuring cell must be minimized in order to maintain a constant composition of the measuring solution. The flux of the capillary has been determined from the variation of the specific conductivity of a solution into which the electrolyte discharges. Typical values

for two different capillaries of 0.58 MΩ each at an overpressure of 20 cm Hg are 1.1×10^{-7} and 1.6×10^{-7} mol/hour respectively. The relation between the resistance and the liquid discharge is not always identical. However, the maximum increase of the indifferent electrolyte concentration amounts only to about 10^{-4} mol/month. This can be neglected in all our experiments.

If a capillary is blocked by the presence of solid particles in the narrow opening, a considerable rise in electrical resistance results. This can be remedied using different procedures: raising the pressure or cleaning with a solution of aceton-KI, concentrated nitric acid, and chromic acid/sulphuric acid. If rinsing with a cleaning solution does not help, careful polishing with a whetstone may be the last resource. The last mentioned method is also used to prepare the capillaries.

5.2.6 *Purification of nitrogen*

Technical nitrogen (3.0 technical N2, Hoek-Loos) was used throughout. Typical values for the percentage by volume of N_2, O_2 and H_2O respectively are 99.995, 5×10^{-3}, 5×10^{-3}.

Removal of traces of impurities has been performed by the following method. Nitrogen was bubbled through a solution of 10% KOH to remove CO_2 and the gas was dried by a solution of concentrated sulphuric acid and a column of silica gel respectively. Oxygen and organic gases were removed by passing them over a column of BTS catalyst (BASF) and molecular sieve (Linde, type 4A, 1/16). Normally, the gas stream was saturated again with water vapour.

5.3 DETERMINATION OF TETRAALKYLAMMONIUM ADSORPTION

5.3.1 *Determination of tetraalkylammonium ion concentration*

The concentrations of tetrapropyl-, tetrabutyl- and tetrapentyl ammonium ions are determined by extraction of a tetraalkylammonium dye complex with chloroform according to Ballard, Isaacs and Scott (8) except for some minor modifications. Cross (9) has given a review of methods to determine cationic surfactants. The principle of the method is as follows:

Tetraalkylammonium ions form a 1:1 complex with the negatively charged dye bromothymol blue. The complex is readily extracted with chloroform, but an excess of the added dye will not be extracted by the chloroform phase provided the pH is properly chosen. The colour of the complex is further stabilized by adding boric acid solution. The intensity of the coloured complex is measured with a spectrophotometer (λ = 419 mμ).

The procedure is slightly dependent on the salt concentration of the aqueous solution. The extractability differs for the three types of ions with regard to the choice of the buffer solution (and the pH) used.

The calibration procedure will be described in detail.

Apparatus
- PYE UNICAM SP 1800 spectrophotometer
- Stoppered separatory cylinders of 100 ml with a TEFLON stop-cock
- Calibrated pyrex pipettes and volumetric flasks
- The chloroform solution was filtered through a plug of glass wool to prevent aqueous droplets from entering the volumetric flask.

Solutions
- Dye solution: 0.75 g bromothymolblue and 0.75 g Na_2CO_3 in 500 ml H_2O
- Buffer solutions
  a. 7.5 ml of 0.1 M citric acid and 92.5 ml of 0.2 M sodium hydrogen phosphate pH = 7.5 (used for tetrapropylammonium ions)
  b. 0.05 M borax ($Na_2B_4O_7.10H_2O$)
      pH = 9.3 (used for tetrabutyl- and tetrapentylammonium ions)
- Boric acid solution
  16 g boric acid + 32 ml H_2O made up to 1000 ml with 96% alcohol
- Potassium nitrate solution was used to simulate the conditions in the adsorption determination
- Tetraalkylammonium salt solutions (2.10^{-4} mol/l) (see 5.2.2)

Calibration procedure
1. Pipette 25 ml boric acid solution in the 100 ml volumetric flask (not through the plug of glasswool).

92

2. Pipette 20 ml chloroform into the separatory cylinder.
3. Add accurately x ml tetraalkylammonium solution and y ml dye solution to the cylinder according to the following table.

cylinder	x	y	cylinder	x	y
1	0	0.5	4	15	2.0
2	5	1.0	5	20	2.5
3	10	1.5	6	25	3.0

4. Add 20 ml buffer solution and 1 ml 1 M KNO_3 solution to the separatory cylinder.
5. Make up the volume of the cylinder to 100 ml with the tetraalkylammonium dye complex.
6. Shake the cylinder vigorously for 2 min., thereby preventing that a too stable an emulsion is formed. Discard the chloroform very slowly into the 100 ml volumetric flask by filtration through the plug of glass-wool.
7. Repeat the extraction three times with 15, 10, 10 ml chloroform respectively.
8. Rinse the funnel with chloroform, homogenize the solution gradually, and make up to volume with chloroform accurately.
9. The extinction is measured after 1 or 2 hours and a calibration curve is plotted.

5.3.2 *Adsorption measurements*

The adsorption of tetraalkylammonium ions on silver iodide suspensions is determined from the concentration difference in solution before and after adsorption. The initial concentration is obtained from calibration measurements and the amount added; the final concentration is measured in the supernatant. The adsorbed amount is the number of moles before adsorption minus the number of moles after adsorption, divided by the weight of the silver iodide suspension. The adsorption per m² can be computed only after establishing the value of the specific surface area (section 5.9).

The weight of the suspended silver iodide is established in wet form by the following procedure:
A stoppered volumetric flask of 50 ml is filled with water and weighed (r gram). The flask is emptied and a certain amount of sil-

ver iodide slurry is added, the flask made up to volume and weighed (p gram). The amount of dry silver iodide in the slurry (a) then follows from the density of AgI (= 5.67) and water (= 0.98) : a = 1.21 x (p-r).

The supernatant is then decanted as far as possible. Successively the following solutions are added: 5 ml 1 M KNO_3, tetraalkylammonium nitrate solution, and KI or $AgNO_3$ solution. The amount of potential determining ions to be added is estimated from the final pAg desired and the measured shapes of the charge-potential curves. Finally, the volume is made up until 50 ml. The volumetric flask is then rotated end-over-end for at least 15 hours at 22 °C.

An amount of supernatant was pipetted off for the determination of the final tetraalkylammonium concentration (section 5.3.1), whereas the remainder is used for the potentiometric determination of the pAg or pI. The presence of silver iodide particles in the supernatant was negligible.

5.4 ADSORPTION OF TETRAALKYLAMMONIUM IONS: EXPERIMENTAL RESULTS

Adsorption of tetraalkylammonium ions on AgI is dependent on both the concentration of TAA^+ *and* the potential at the surface (or the pAg). In order to obtain adsorption isotherms at constant equilibrium pAg, the amount of iodide or silver ions to be added with the TAA^+ ions has to be precisely calculated à priori. As neither the equilibrium concentration of TAA^+ ions nor the charge-potential data at equilibrium concentrations is known the amount of Ag^+ or I^- cannot be estimated precisely. In order to calculate curves at a constant pAg, a two dimensional interpolation of the results is therefore necessary.

The primary adsorption results are given in detail in tables 5-1 and 5-2. Table 5-1 gives the results for AgI suspension II at different pAg values, whereas in table 5-2 the results for different tetraalkylammonium ions on AgI suspension III are given. A graphical representation of these data is given in chapter 6 (Figs. 6.1-6.3).

In order to give an estimation of the random error in the measurement of the adsorption, the data of table 5-1 have been analyzed by drawing smoothed Γ-pTBuA curves and calculating the standard deviation of the experimental points with respect to the smoothed

Table 5-1. Adsorption isotherms of tetrabutylammonium (TBuA$^+$) ions on silver iodide suspension II at different pAg (pI).

c_{KNO_3} = 0.1 M

specific area (capacitance) = 1.00 m^2/g

Γ in µmol/g.AgI
pTBuA = log [TBuA]
[TBuA] in µmol/liter

	TBuA 1			*TBuA* 2	
pI	pTBuA	Γ	pAg	pTBuA	Γ
4.4	5.835	0.077	6.2	5.425	0.050
4.3	5.015	0.373	5.9	5.073	0.143
4.3	4.706	0.498	5.6	4.710	0.247
4.3	4.274	0.591	5.4	4.488	0.333
4.3	3.840	0.686	5.2	4.187	0.461
4.3	3.471	0.697	5.1	3.815	0.559
4.3	3.269	0.698	4.9	3.460	0.616
4.2	3.196	0.738	4.8	3.265	0.650
4.3	3.137	0.769	4.8	3.194	0.684
4.3	3.079	0.721	4.8	3.138	0.723
4.3	3.031	0.745	4.8	3.081	0.761
			4.8	3.034	0.765
			5.3	3.459	0.627

	TBuA 3			*TBuA* 4			*TBuA* 5	
pI	pTBuA	Γ	pAg	pTBuA	Γ	pI	pTBuA	Γ
3.95	5.775	0.075	9.2	6.143	0.087	4.5	5.630	0.061
3.95	5.471	0.206	9.2	5.314	0.192	4.5	5.393	0.200
3.95	4.984	0.368	8.8	5.144	0.410	4.5	5.009	0.370
3.95	4.661	0.494	7.7	4.811	0.542	4.5	4.667	0.483
3.95	4.295	0.567	8.4	4.330	0.668	4.5	4.263	0.544
3.95	4.048	0.602	8.6	4.071	0.699	4.5	4.050	0.606
3.95	3.824	0.638	8.3	3.843	0.710	4.5	3.839	0.660
3.95	3.626	0.718	8.1	3.476	0.774	4.5	3.622	0.737
3.95	3.470	0.705	7.4	3.276	0.794	4.5	3.474	0.739
3.95	3.270	0.753	7.7	3.203	0.754	4.5	3.275	0.775
3.95	3.198	0.732	7.9	3.137	0.742	4.5	3.202	0.773
3.95	3.136	0.721	7.2	3.079	0.650	4.5	3.081	0.724
4.0	4.435	0.522	8.4	3.029	0.676	4.5	3.035	0.832
4.0	4.246	0.548	7.2	3.463	0.695	4.46	4.430	0.535
						4.46	4.270	0.574

Table 5-1. (cont.)

TBuA 6			TBuA 7			TBuA 8		
pAg	pTBuA	Γ	pAg	pTBuA	Γ	pAg	pTBuA	Γ
4.06	5.033	-0.016	4.50	4.753	0.030	5.2	5.123	0.008
4.04	4.708	0.004	4.57	4.470	0.072	5.2	4.785	0.043
4.02	4.409	0.011	4.56	4.325	0.157	5.1	4.553	0.156
4.02	4.031	0.077	4.52	4.117	0.299	5.1	4.394	0.243
3.99	3.764	0.335	4.51	3.780	0.438	5.0	4.153	0.370
3.95	3.443	0.483	4.48	3.452	0.612	4.9	3.801	0.516
3.95	3.254	0.496	4.47	3.258	0.563	4.9	3.456	0.612
3.95	3.123	0.548	4.49	3.124	0.594	4.8	3.260	0.646
3.94	3.071	0.582	4.50	3.072	0.670	4.9	3.127	0.667
			4.52	3.028	(0.483)	4.9	3.072	0.682
			4.48	3.262	0.645	5.3	3.459	0.627
			4.47	3.451	0.547			
			4.47	3.445	0.518			

TBuA 9			TBuA 10			TBuA 11		
pAg	pTBuA	Γ	pAg	pTBuA	Γ	pAg	pTBuA	Γ
6.51	5.463	0.057	8.3	5.853	0.081	9.8	6.010	0.092
6.26	5.120	0.156	8.0	5.466	0.210	9.6	5.582	0.206
5.98	4.739	0.283	7.9	5.004	0.377	9.2	5.133	0.403
5.84	4.521	0.365	7.0	4.689	0.480	9.4	4.745	0.525
5.57	4.238	0.508	6.5	4.264	0.578	9.3	4.309	0.588
5.45	3.819	0.603	6.0	3.823	0.645	9.3	3.843	0.694
5.31	3.459	0.665	5.9	3.463	0.676	9.5	3.469	0.710
5.42	3.264	0.662	5.6	3.270	0.715	9.7	3.271	0.729
5.46	3.130	0.724	5.6	3.132	0.694	9.6	3.132	0.739
5.55	3.078	0.723	5.8	3.078	0.724	8.2	3.077	0.721
6.4	3.457	0.625	6.53	3.463	0.667	9.6	4.289	0.611
6.4	4.273	0.577	6.4	4.033	0.608	9.4	3.465	0.705

Table 5-2. Adsorption isotherms of different tetraalkylammonium nitrates on silver iodide suspension III at different pAg (pI).
c_{KNO_3} = 0.1 M Γ in µmol/g.AgI
Specific area (capacitance) = 0.80 m^2/g   pTAA = - log [TAA]
[TAA] in mol/liter

TBuA 12			TBuA 13		
pI	pTBuA	Γ	pI	pTBuA	Γ
4.0	5.647	0.069	4.0	3.453	0.543
4.0	5.216	0.176	4.0	3.344	0.564
4.0	4.849	0.325	4.0	3.260	0.541
4.0	4.550	0.396	4.0	3.122	0.468
4.0	4.199	0.449	4.0	3.069	0.505
4.0	3.796	0.503	4.0	3.453	0.583
4.0	3.455	0.553	4.0	3.348	0.559
4.0	3.261	0.570	4.0	3.263	0.596
4.0	3.121	0.482	4.0	3.188	0.533
4.0	3.074	0.528	4.0	3.127	0.570
			4.0	3.073	0.596

TPrA 1			TPrA 2		
pAg	pTPrA	Γ	pI	pTPrA	Γ
9.8	4.828	0.061	4.6	5.172	0.014
9.6	4.323	0.138	4.6	4.846	0.070
9.6	4.074	0.177	4.6	4.499	0.100
8.7	3.751	0.252	4.6	4.300	0.117
9.3	3.432	0.313	4.6	4.065	0.163
9.2	3.330	0.329	4.6	3.747	0.241
8.8	3.250	0.366	4.6	3.430	0.307
9.2	3.183	0.393	4.6	3.249	0.318
8.7	3.119	0.389	4.6	3.118	0.355
9.1	3.064	0.323	4.6	3.066	0.366

TAmA 1			TAmA 2			TAmA 3		
pI	pTAmA	Γ	pI	pTAmA	Γ	pI	pTAmA	Γ
4.55	6.899	0.229	4.5	6.473	0.258	4.5	5.016	0.483
4.55	4.860	0.478	4.5	5.177	0.413	4.5	4.221	0.485
4.55	4.302	0.496	4.5	4.202	0.486	4.5	3.791	0.511
4.55	3.864	0.521	4.5	3.806	0.505	4.5	3.447	0.528
4.55	3.508	0.580	4.5	3.449	0.542	4.5	3.337	0.540
4.55	3.397	0.582	4.5	3.341	0.520	4.5	3.258	0.583
4.55	3.318	0.586	4.5	3.263	0.569	4.5	3.183	0.511
4.55	3.245	0.574	4.5	3.189	0.535	4.5	3.124	0.588
4.55	3.176	0.582	4.5	3.127	0.604	4.5	3.065	0.505
4.55	3.125	0.600	4.5	3.072	0.526	4.5	3.253	0.540
						4.5	3.180	0.493
						4.5	3.117	0.457

curve. For pTBuA values exceeding 3.7 (in general below the plateau
value) the standard deviation calculated from isotherms TBuA1 to
TBuA11 amounts 0.013 µeq/g.AgI, whereas for pA lower than 3.7
(around the plateau value) the standard deviation amounts to 0.03
µeq/g.AgI (or ± 4%). Linear regression of the calibration curves
indicates that the relative errors of the slopes are between 0.2
and 0.4%. On the average, the error in the concentration determina-
tion is amplified by a factor between 6 and 16 for pTBuA
values higher than 3.7 when calculating the amount adsorbed from
the relatively small concentration change upon adsorption. Hence,
the reproducibility of the analytical procedure, and particularly
of the spectrophotometer readings explains to a large extent the
value of the random error calculated above.

The plateau values for the adsorption of TBuA$^+$ ions on AgI can
be estimated from a direct extrapolation of the adsorption iso-
therms. From the adsorption isotherms at negative surface charges,
an average plateau value of 0.75 ± 0.02 µmol/g.AgI is obtained for
suspension II. The plateau values can also be estimated by fitting
the adsorption isotherms to a Langmuir model and calculating $\Gamma(c \to \infty)$.
In this way a value of 0.69 ± 0.03 µmol/g.AgI is obtained. However,
for purposes of estimating the surface area the first value is pre-
ferred, as the Langmuir isotherm suffers from the neglect of
lateral interaction etc.

Plateau values for the adsorption of the three tetraalkylam-
monium ions at suspension III have also been estimated by direct
extrapolation. We obtained 0.39, 0.58 and 0.56 µmol TAA/g.AgI for
TPrA$^+$, TBuA$^+$ and TAmA$^+$ ions respectively. The value of tetrapropyl-
ammonium will be relatively inaccurate because the higher concen-
trations cannot be measured accurately.

In tables 5-1 and 5-2 also the specific surface area of the
suspension used has been indicated. This value has been obtained
from titration experiments on the corresponding suspension by com-
parison with a standard curve as described in sections 5.5 and 5.6.
The values given have been computed by averaging 4 titrations for
both suspensions. It must be realized that the surface areas ob-
tained from titrations are taken *after* several titration cycli,
whereas in the adsorption experiment the pAg value immediately
assumes its final value.

5.5 DETERMINATION OF THE SURFACE CHARGE

The automation aspects of the titration, the description of the cell, and the preparation of the electrodes have been described before.

A complete titration cycle was performed with one batch of ca. 20 g of AgI suspension. After the measurement of a base curve in the absence of adsorbate, a set of 4 to 7 charge-potential curves were measured at different adsorbate concentrations. Before and after such a cycle several calibrations were performed.

The temperature of the titration cell was kept constant within 0.05 °C. Purified nitrogen saturated with water vapour was led slowly over the measuring solution to maintain a low oxygen and carbon dioxide level in the solution. Due to evaporation or condensation the final volume after a complete titration cycle (base curves + the curves with adsorbate) could differ by about 1 ml from the calculated final volume. At extreme pAg values this can result in an error for the surface charge between 0.01 and 0.05 $\mu C/cm^{-2}$ for the latter curves in the measuring cycle.

The potential was calibrated against a Weston cell having a well-known potential. The accuracy of the potential measurement amounted to 0.1 mV. The burettes were calibrated by weighing the delivered volume using a mechanical relay to tick off the last drop. The reproducibility was 1 μl. It is likely that the long-term accuracy will be less due to minor leakages, room temperature fluctuations, heat developed by the motor of the burette, and evaporation. An error between 1 and 3 μl seems a quite realistic estimate.

The silver and iodide concentrations are determined from the cell potential according to Nernst's law (4.5 and 4.6). As described in chapter 4, the standard potentials, E^o_{Ag+} and E^o_{I-}, are determined by a titration procedure giving standard potentials at different pAg's (or pI's). Due to the limitations set by the accuracy of the burettes, silver and iodide concentrations are subject to large errors between pAg 5.5 and 10.5 so that standard potentials cannot be determined between these values. Outside these limits the standard potentials do not depend on the pAg or pI within experimental error. The same conclusion has also been reached by

Bijsterbosch (7). As the reference potential (due to calomel elec-
trode and salt-bridge) can vary a little in different experimental
set-ups, a check on the reliability of the standard potentials
follows from the calculation of the solubility product. The solu-
bility product is a property of silver iodide and the solution
phase and follows from the difference between the two standard
potentials which, accordingly, must be constant. The negative
logarithm of the solubility product amounted usually to 16.16±0.01.

Standard potentials have also been measured in the presence
of mixtures of 0.099 M KNO_3 and 10^{-3} M tetrapropyl- or tetrabutyl-
ammonium nitrate respectively. The shifts due to the presence of
TAA^+ ions of both E^o_{Ag+} and E^o_{I-} were less than 0.3 mV. Although stan-
dard potentials have not been evaluated in the presence of tetra-
amylammonium nitrate, it is expected that the influence of $TAmANO_3$
on E^o is in the same order or less, because the concentrations used
are lower as for the other ions. It can be concluded that the in-
fluence of tetraalkylammonium ions on the standard potentials can
be neglected in the concentration range used.

The ionic strengths of the two titrants ($AgNO_3$ and KI) were
kept the same as that of the measuring solution by maintaining
in them a KNO_3 concentration of 0.099 M.

Silver iodide suspensions in the absence of adsorbate were
titrated several times by addition of 0.01 M $AgNO_3$ or 0.01 M KI
until the charge-potential curves obtained did not vary any more.
The ratio between a reference curve (given in $\mu C/m^2$) (7.12) and
the experimental curve (in $\mu C/gram$) is calculated. A typical result
of this ratio is given in fig. 5.1, which shows the reduction of
the apparent specific surface area with successive titrations. It
appears that after 4 or 5 titrations constancy of the surface area
has been established. The effect is probably due to a kind of aging
of the surface. If at the end of a complete titration cycle in the
presence of adsorbate titrations were repeated, it appeared that
the reduction of surface area is absent within experimental error.

After the establishment of the base curve, the titration was
stopped at pAg = ca. 8.0 and an amount of adsorbate was added. The
titration was then continued to the negative side. Although hyster-
esis effects are neglectible within experimental error, charge po-
tential curves as given in the results were taken only from titra-

100
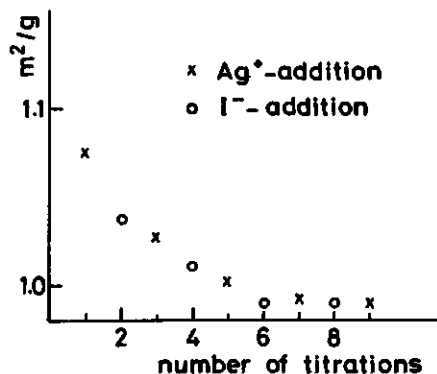
Fig. 5.1 Decrease of the apparent specific surface area upon successive titrations.

tions of the extreme negative side to the extreme positive side in order to maximize the mutual reproducibility.

A preliminary calculation of the surface charge, expressed in $\mu C/g.AgI$, was performed by the PDP11/10 computer. This has been described in chapter 4. The relevant data are punched at a Teletype.

In order to analyze the titration data in more detail a separate computer programme was used. This programme compared the base curve with three ICT (International Critical Tables) curves (12) in which σ values are expressed in $\mu C/cm^2$, so that the (relative) specific surface area could be evaluated. The ICT curves were obtained from refs. 7, 10 and 11. It appears that the curve obtained from reference 7 matches best with our base curves and therefore this one will be used throughout.

The programme calculates polynomial regression coefficients from the experimental data. Usually 4th- to 9th-order regression analysis is performed. The charge-potential curves are expressed by the following equation

$$\sigma = \sum_{i=0}^{N} B_i x^i \qquad (5.1)$$

where x is given by

$$x = \frac{(pAg - 8)}{3} \tag{5.2}$$

Standard deviations are calculated from the difference between
the experimental points and from the corresponding points calculated
from the polynomial regression coefficients. The standard deviation
depends on the order of regression and on the composition of the
solution. For 4th- or 5th-order regression base curves the standard
deviation usually amounts to $0.01 - 0.02$ $\mu C/cm^2$, whereas for the
9th-order curves this value is usually between 0.003 and 0.005
$\mu C/cm^2$.

5.6 CHARGE-POTENTIAL CURVES: EXPERIMENTAL RESULTS

5.6.1 *General*

Charge-potential data are given in the presence of tetraalkyl-
ammonium ions, where alkyl = methyl, ethyl, propyl, butyl, and amyl
respectively, and three other quaternary ammonium ions. For propyl
and butyl two sets of data are given. Data are designated as
TPrA1, TPrA2, TBuA1 etc.

5.6.2 *Tetrapropylammonium ions*

Two sets of charge-potential curves at ± 7 TPrA$^+$ concentra-
tions are presented. The results are given in Table 5-3 as poly-
nomial regression coefficients, described in the previous section.
An impression of the overall reproducibility is given in fig. 5.2
where the surface charge is given as a function of the logarithm of
the TPrA$^+$ concentration at pAg = 6 for the two titrations. It ap-
pears that the reproducibility is very good, especially if we real-
ize that differences can occur because of different amounts of AgI
and correspondingly a different depletion of concentration upon ad-
sorption.
A graphical representation of the titration TPrA2 is given
in fig. 5.3.
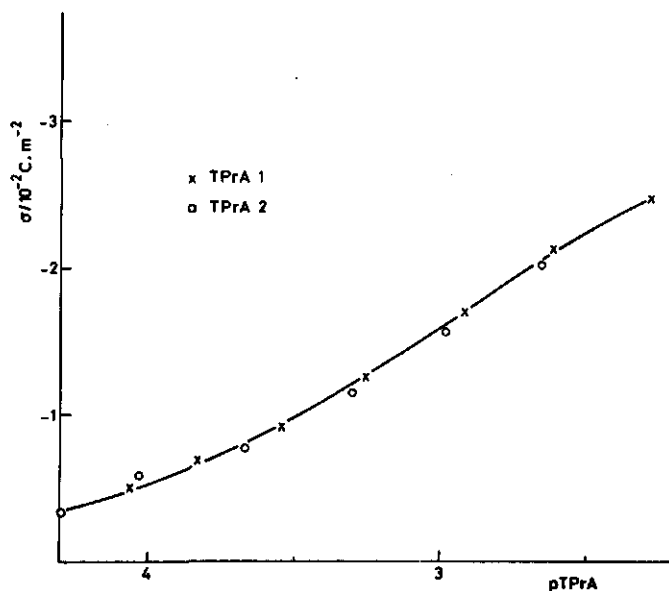
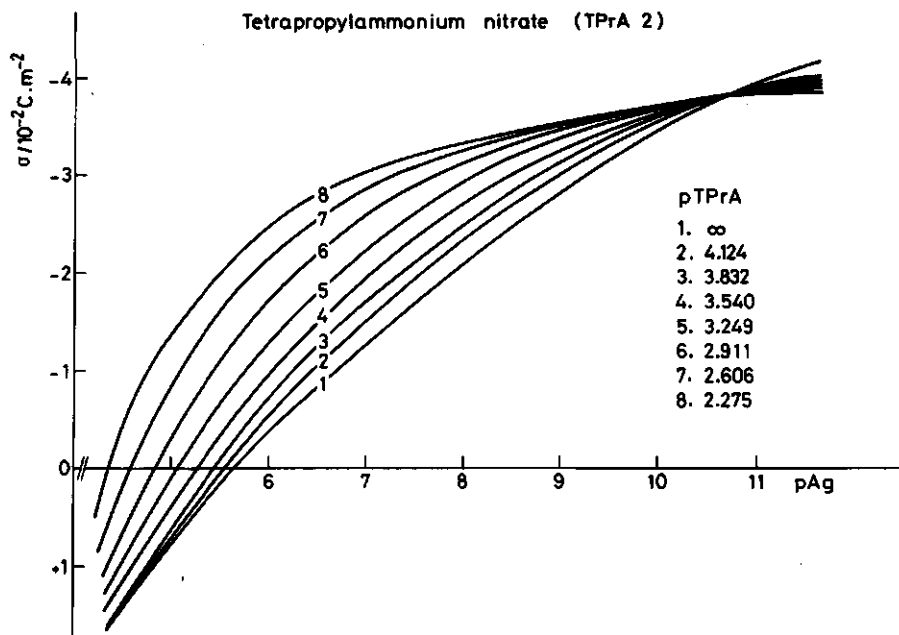Fig. 5.2 Surface charge of AgI in the presence of TPrA at pAg = 6 for two independent titrations.

Fig. 5.3 Surface charge on silver iodide as a function of pAg at different initial concentrations of tetrapropylammonium nitrate (titration TPrA2). Electrolyte: 0.1 M KNO$_3$, T = 20.0 °C, pH ≅ 7, specific surface area of AgI (from capacitance) = 1.00 m^2/g.

Table 5-3. Regression coefficients according to eqs. 5.1 and 5.2 for charge-potential curves of AgI in the presence of tetrapropylammonium nitrate.

Titr.	Susp.	a_s	g.AgI	pTPrA	B0	B1	B2	B3	B4	B5	B6
TPrA1	I	0.87	21.27	∞	-2.072	-2.369	0.1243	0.0019	0.6020	-0.0161	-0.2937
				4.504	-2.197	-2.397	0.1995	1.2954	0.9894	-3.7034	1.8972
				4.032	-2.392	-2.189	0.7404	-0.1670	-3.9780	0.1765	
				3.672	-2.617	-2.011	1.0226	-0.3295	-0.1177	0.2224	
				3.299	-2.847	-1.678	0.7810	-0.5549	0.5551	0.2432	-0.2685
				2.983	-3.066	-1.321	0.8381	-0.8127	0.3146	0.2883	0.0079
				2.648	-3.263	-0.922	1.0258	-0.8457	-0.3119	0.2218	0.3587
TPrA2	II	1.00	24.93	∞	-2.072	-2.300	0.3495	-0.0478	0.1496		
				4.124	-2.320	-2.267	0.6198	-0.0408	0.1002		
				3.832	-2.484	-2.116	0.7157	-0.1424	0.1364		
				3.540	-2.693	-1.959	0.9365	-0.1598	0.0284		
				3.249	-2.907	-1.657	0.9749	-0.3130	0.0766		
				2.911	-3.122	-1.264	0.8862	-0.4948	0.1787		
				2.606	-3.240	-0.904	0.5965	-0.6237	0.3181		
				2.275	-3.314	-0.674	0.3463	-0.5756	0.3806		

Table 5-4. Regression coefficients according to eqs. 5.1 and 5.2 for charge-potential curves of AgI in the presence of tetrabutylammonium nitrate.

Titr.	Susp.	a_s	g.AgI	pTBuA	B0	B1	B2	B3	B4	B5	B6
TBuA1	I	0.92	20.14	∞	-2.098	-2.238	0.3817	-0.1818	0.1032	0.0813	
				4.503	-2.673	-1.293	0.3784	-0.4490	0.7869	-0.0308	-0.2521
				4.209	-2.908	-0.709	0.4517	-0.6404	0.3372		
				4.040	-3.066	-0.340	0.4959	-0.9955	0.2147	0.2182	
				3.824	-3.129	-0.231	-0.1173	-0.7414	0.9160	0.1267	-0.3008
				2.822	-3.243	-0.354	-0.0111	0.0537	0.1379	-0.2011	
TBuA2	II	0.96	23.03	∞	-2.097	-2.242	0.3280	-0.1633	0.2597	0.0870	
				4.951	-2.408	-1.735	0.5049	-0.7129	0.4880	0.3253	-0.1330
				4.561	-2.667	-1.269	0.4741	-0.6277	0.6817	0.1193	-0.2141
				4.268	-2.810	-0.469	0.8078	-0.4327	0.0766	-0.2163	0.1337
				4.099	-2.993	-0.132	0.4248	-1.3991	0.4456	0.4121	-0.0219
				3.883	-2.940	-0.108	0.0854	-0.6627	0.5469	0.0267	-0.0152
				3.419	-3.031	-0.137	-0.1901	0.0273	0.2449	-0.2395	0.1716

Table 5-5. Regression coefficients according to eqs. 5.1 and 5.2 for charge-potential curves of AgI in the presence of tetraamylammonium nitrate.

Titr.	Susp.	a_s	g.AgI	pTAmA	B0	B1	B2	B3	B4	B5	B6
TAmA1	III	0.806	17.57	∞	-2.069	-2.342	0.2879	-0.0321	0.1687		
				5.660	-2.247	-2.236	0.2618	-0.0655	0.2554		
			·	5.007	-2.502	-1.527	0.3217	-0.1557	0.2640		
				4.693	-2.754	-0.714	0.0949	-0.3158	0.3873		
				4.449	-2.757	-0.457	0.1909	0.2909	-0.4551	-0.3894	0.4880
				4.097	-2.771	-0.371	-0.0123	-0.0473	0.1427		
				3.445	-2.827	-0.368	-0.0588	-0.0400	0.1756		

It appeared that the intersection points of the charge-potential curves at increasing adsorbate concentrations with the base curve shift somewhat to more positive potentials. The c.i.p. for TPrA1 (pAg = 10.55) is lower than the averaged c.i.p. for TPrA2 (pAg = 10.70). This difference is a consequence of the accuracy of the charge-potential curves. From these results and a third titration not given here the c.i.p. for TPrA can be taken as pAg = 10.70 ± 0.15 or σ = -3.80 ± 0.05 $\mu C/cm^2$.

5.6.3 *Tetrabutylammonium ions*

Two sets of titration curves of a silver iodide suspension in the presence of TBuA$^+$ ions are given in Table 5-4 in terms of poly-nomial regression coefficients as described above. A graphical rep-resentation of titration TBuA2 is given in fig. 5.4.

The overall reproducibility as follows from the results of TBuA1 and TBuA2 seems somewhat less than for titrations in the presence of the propyl compound.

The 'common' intersection point is less defined than in the propyl case, and the shift of the intersection points with the base curve is much more pronounced. Above pA = 4.5 an average c.i.p. can be obtained as pAg = 9.9 ± 0.1 or σ = -3.60 ± 0.05 $\mu C/cm^2$. For concentrations between pA = 4 and 4.5 a c.i.p. of pAg = 9.6 ± 0.2 or σ = -3.2 ± 0.1 $\mu C/cm^2$ is obtained. The average value for the posi-tion of the common intersection point can be assumed equal to pAg = 9.75 ± 0.20 or σ = -3.3 ± 0.1 $\mu C/cm^2$.

In contradistinction to charge-potential curves in the pres-ence of TPrA$^+$ ions, for TBuA$^+$ ions the concentration level and the affinity of the adsorbate are such that considerable concentration changes in solution at the given available surface area do occur. Thus, in order to obtain titration curves at constant equilibrium concentrations, recalculations using adsorption data are necessary. This is described in chapter 7.

Fig. 5.4 Surface charge on silver iodide as a function of pAg at different initial concentrations of tetrabutylammonium nitrate (titration TBuA1). Electrolyte: 0.1 M KNO_3, T = 20.0 °C, pH $\cong$ 7, specific surface area of AgI (from capacitance) = 0.92 m^2/g.
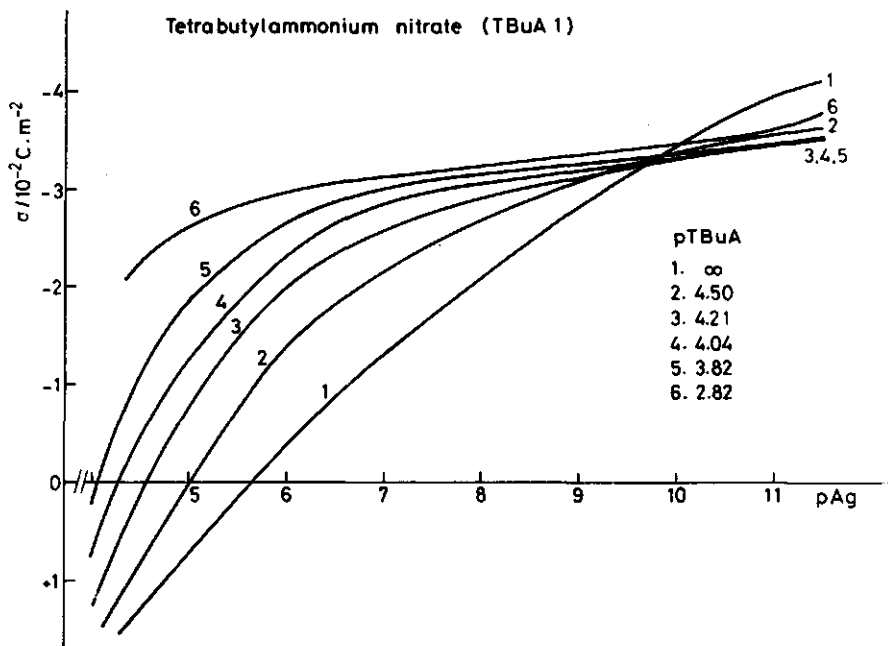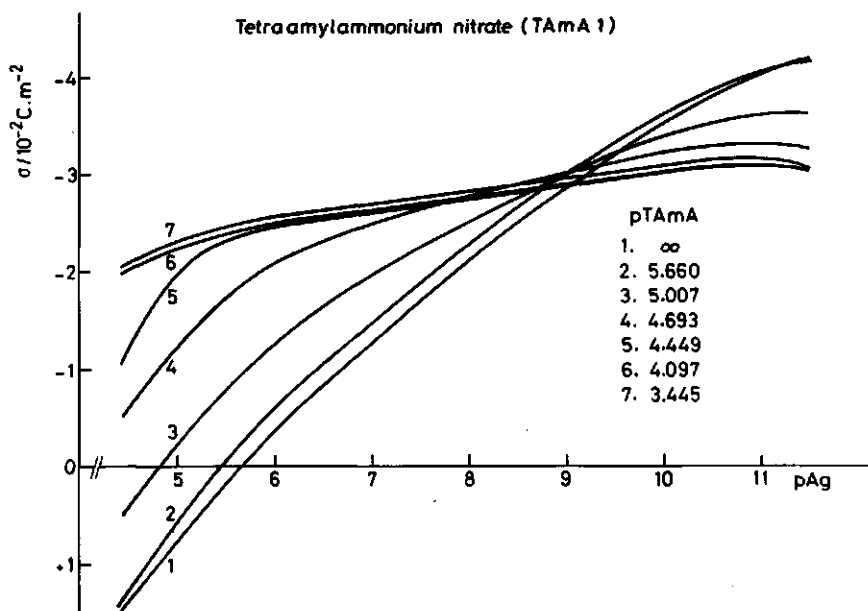

Fig. 5.5 Surface charge on silver iodide as a function of pAg at different initial concentrations of tetraamylammonium nitrate (titration TAmA1). Electrolyte: 0.1 M KNO_3, T = 20.0 °C, pH $\cong$ 7, specific surface area of AgI (from capacitance) = 0.806 m2/g.

106

5.6.4 *Tetraamylammonium ions*

Charge-potential curves at a few *initial* concentrations of tetraamylammonium nitrate are given in Table 5-5 and in fig. 5.5. The 'common' intersection point is again less defined than for tetrapropylammonium ions and it is located at pAg = 9.1 ± 0.3 or σ = -2.9 ± 0.2 $\mu C/cm^2$.

5.6.5 *Other quaternary ammonium ions*

As an extension of the measurements on the three tetraalkylammonium ions given above, titrations were also performed for tetramethyl- and tetraethylammonium ions. The results are given in figs. 5.6 and 5.7. It appears that the adsorption of tetramethylammonium ions is hardly measurable, a finding that follows also from measurements of the electrophoretic mobility. Tetraethylammonium ions assume an intermediate position between $TMeA^+$ and $TPrA^+$ ions. A common intersection point is observed at pAg = 11.5 ± 0.3 or σ = -4.4 ± 0.2 $\mu C/cm^2$.

Some preliminary results have been obtained for three asymmetrical quaternary ammonium salts, viz. phenyltrimethylammonium nitrate, choline nitrate and hexamethonium nitrate. They are given in figs. 5.8, 5.9, and 5.10 respectively.

5.7 DETERMINATION OF THE ELECTROPHORETIC MOBILITY

Electrophoretic mobilities of silver iodide sols in the presence of TAA^+ ions have been measured at 22.0 ± 0.2 °C in a Rank Brothers MKII microelectrophoresis apparatus using a cylindrical cell. The sol was prepared as described by Koopal (13). The sol concentration was in the order of 5×10^{-5} mol AgI/liter. The apparatus was equipped with four electrodes of which the outer ones were platinized and connected to a constant current source, whereas the inner two were silver-silver iodide electrodes measuring the potential difference across the cell.

The electrophoretic mobilities are measured at 1/7 and 6/7 of the depth. The diameter of the capillary was $1.868 ± 0.002 \times 10^{-3}$ m, whereas the thickness of the glass wall was in the order of

Fig. 5.6 Surface charge on silver iodide as a function of pAg at different initial concentrations of tetramethylammonium nitrate. Electrolyte: 0.1 M KNO_3, T = 20.0 °C, pH $\cong$ 7, specific surface area of AgI (from capacitance) = 1.00 m^2/g.

Fig. 5.7 Surface charge on silver iodide as a function of pAg at different initial concentrations of tetraethylammonium nitrate. Electrolyte: 0.1 M KNO_3. T = 20.0 °C, pH $\cong$ 7, specific surface area of AgI (from capacitance) = 1.00 m^2/g.
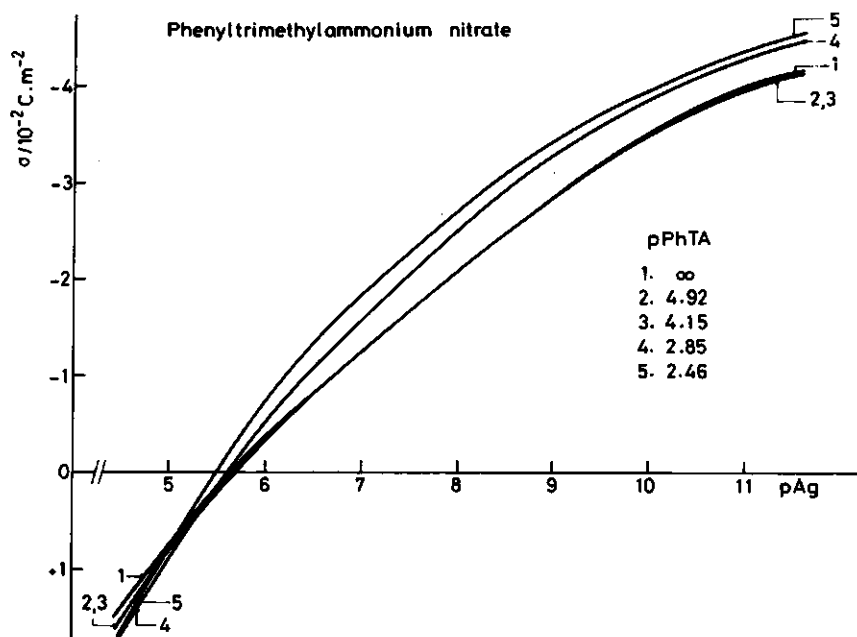
Fig. 5.8   Surface charge on silver iodide as a function of pAg at different initial concentrations of phenyltrimethylammonium nitrate. Electrolyte: 0.1 M KNO$_3$, T = 20.0 °C, pH $\cong$ 7, specific surface area of AgI (from capacitance) = 0.794 m^2/g.
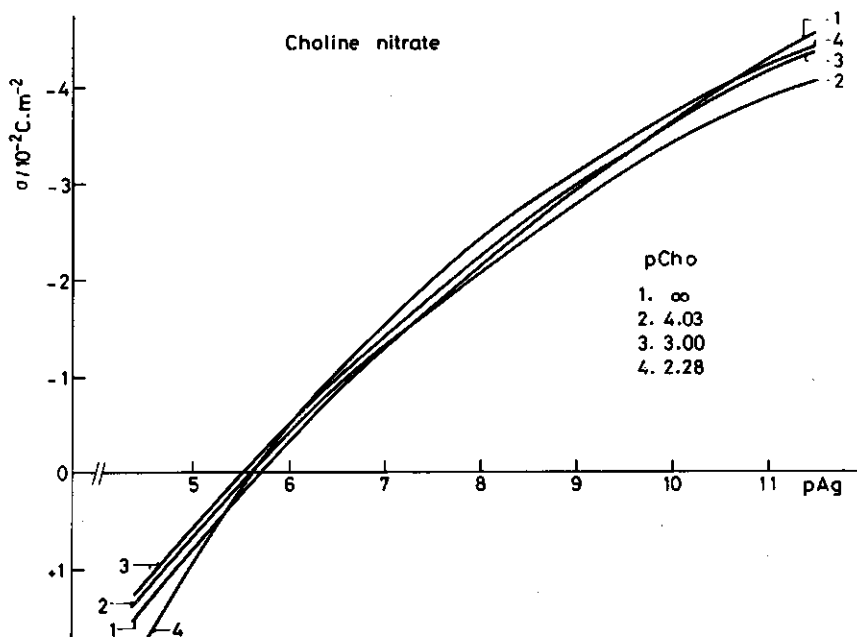
Fig. 5.9   Surface charge on silver iodide as a function of pAg ar different initial concentrations of choline nitrate. Electrolyte: 0.1 M KNO$_3$, T = 20.0 °C, pH $\cong$ 7, specific surface area of AgI (from capacitance) = 1.02 m^2/g.
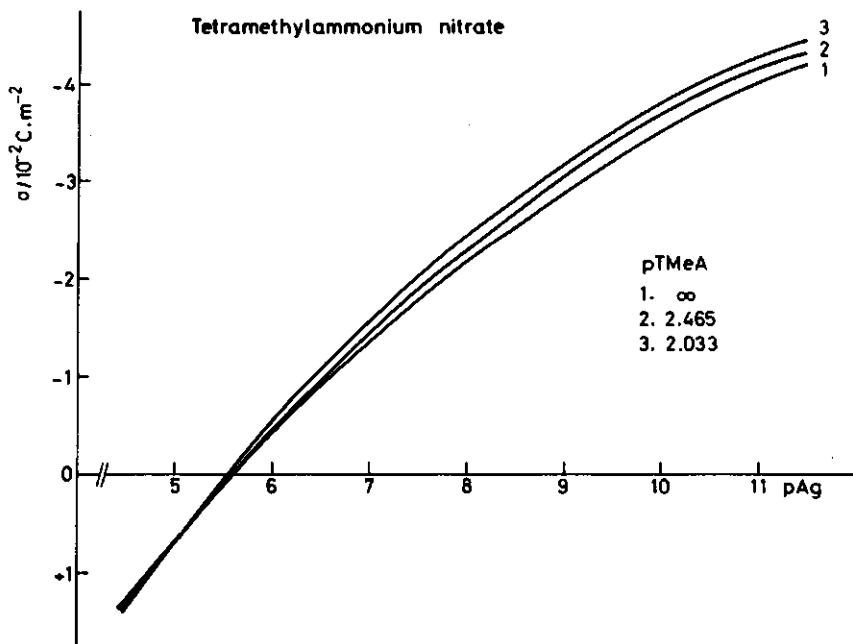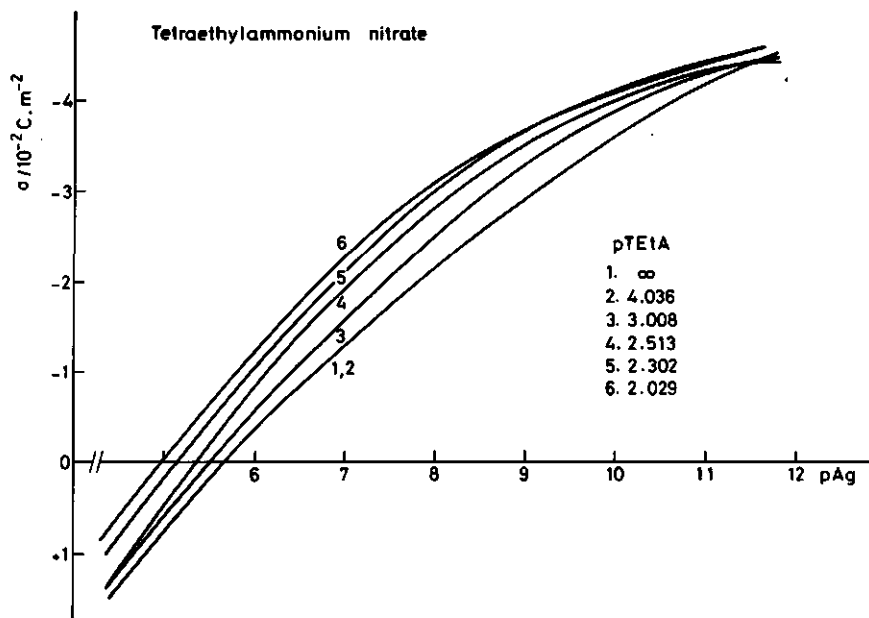
109
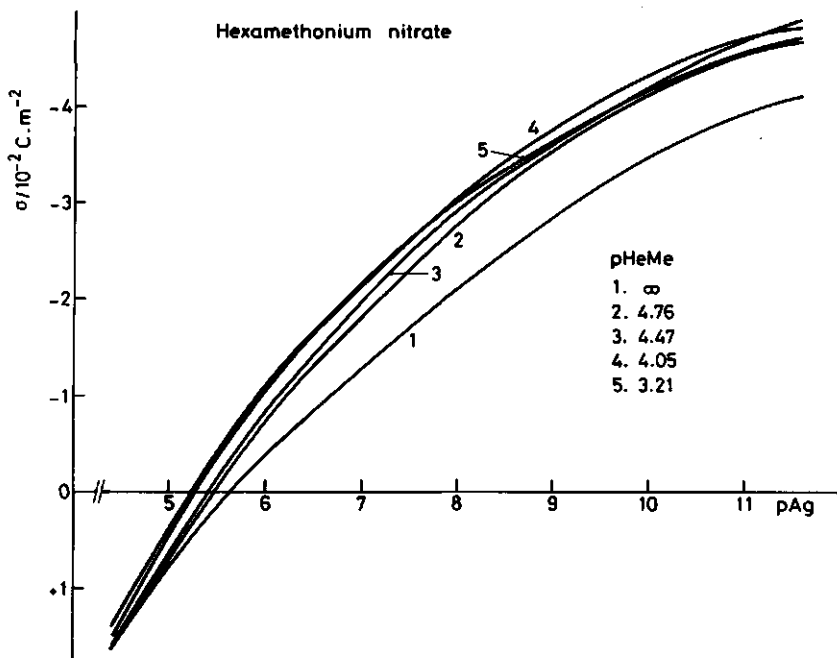
Fig. 5.10 Surface charge on silver iodide as a function of pAg at different ini-
tial concentrations of hexamethonium nitrate. Electrolyte: 0.1 M KNO_3,
T = 20.0 °C, pH ≅ 7, specific surface area of AgI (from capacitance) = 0.802 m2/g.

8×10^{-5} m. The latter value warranted that the optical distor-
tion by the difference in the radii of the inner and outer wall
may be neglected.

The cell was calibrated with solutions of potassium nitrate
and nitric acid by leading a constant current (i) through it and
measuring the potential difference (V) between the electrodes,
whereas the specific conductivity (κ_{sp}) was measured separately.
The effective length followed from

$$ 1 = \kappa_{sp} \; 0 \; \frac{i}{V} $$

where O is the cross-section of the cylinder. The effective dis-
tance between the inner electrodes was 7.40 ± 0.03 cm for solutions
of 0.001, 0.01 and 0.1 M KNO_3, whereas a value of 7.33 ± 0.03 cm
was obtained for 10^{-3} M HNO_3. The difference between the two values
is within 1% and can be neglected for the calculation of the elec-
trophoretic mobilities.

The experiments have been performed at pH = 3 to minimize the
effect of adsorbing silicates (14). The profile of the particle

110

velocity over the cross-section had a parabolic shape within exper-
imental error.

The experimental points were obtained from 40 measurements,
20 at each depth. The applied potential was reversed after each
reading. Mobilities from separate readings were averaged and the
standard deviation of the measurements was calculated. The standard
deviation of the mobility at a fixed depth amounted to 1-3%. The dif-
ference between the two measuring positions in the cell can be as
high as 10%. The average overall reproducibility may be estimated
as 5%.

5.8.   ELECTROPHORETIC MOBILITIES: EXPERIMENTAL RESULTS

The electrophoretic mobilities of silver iodide particles at
pI = 4.5 are determined at 10^{-3} M HNO_3 and 10^{-1} M KNO_3. The results
are given in figs. 5.11 and 6.9.
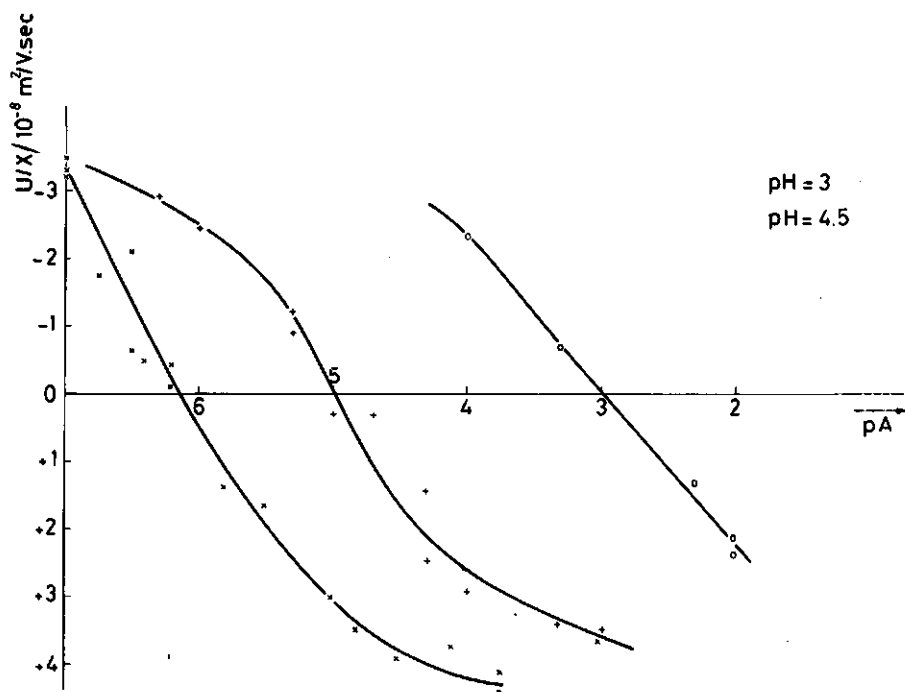
Fig. 5.11   Electrophoretic mobilities of silver iodide sol particles in the
presence   of different concentrations of tetraalkylammonium nitrates. Electro-
lyte: 0.001 M HNO_3, T = 22.0°C, pH = 3, pAg = 11.6.

5.9   SPECIFIC SURFACE AREA OF SILVER IODIDE

In order to express the adsorption values or surface charges per unit area, the specific surface area of the suspension must be known. Unfortunately, many problems still exist in comparing values obtained from different methods. Recently this has been discussed in some detail by Koopal (13).

Three methods are compared in the present study in which the area is obtained (i) from comparison of the capacitance on AgI and Hg, (ii) from the plateau value of tetraalkylammonium ions.

Standard charge-potential curves according to the capacitance method are given in the International Critical Tables (12). However, as discussed before, in our case it was found more expedient to compare the curve in $\mu C/cm^2$ according to (7) with the experimental charge-potential curves in $\mu C/gram$. The specific surface areas were in general reproducible within 2 à 5%.

The measured plateau values for adsorption of methylene blue on AgI amounted to 0.84 ± 0.01 and 0.70 ± 0.01 $\mu mol/g.AgI$ for suspensions II and III respectively. The effective molecular area of a methylene blue molecule is rather uncertain and depends on the nature of the surface. The area of a single flatly adsorbed molecule is 1.08 nm^2. Based on a thorough comparison of different experimental results, Koopal (13) assumed a value of 0.60 nm^2 corresponding to a flat adsorption of dimers. This value has been used in this study.

The adsorption of tetraalkylammonium ions was thought very useful for the determination of the specific surface area of solid particles because the molecules are almost perfect spheres and they form neither micelles nor aggregates (15). The molecular areas can be estimated from the ionic radii (15,16). For $TBuA^+$, it amounted to 0.80 nm^2.

Some results are summarized in table 5-5 for suspensions II and III.

Table 5-5. Specific surface areas of silver iodide suspension

	Capacitance	Methylene blue adsorption		$TBuA^+$ adsorption	
Suspension	S_{cap}	S_{MB}	S_{MB}/S_{cap}	S_{TBuA}	S_{TBuA}/S_{cap}
II	1.00	0.302	3.0	0.360	3.6
III	0.80	0.255	3.2	0.278	3.5

It appears that the differences between the methylene blue method and the TBuA$^+$ method amount to 10 till 20%. However, a difference of a factor 3 – 3.5 is found with the capacitance method. The large factor is obviously not due to experimental errors.

A potential solution for the previous problem could have been obtained from the ratios of the plateau values of TPrA$^+$, TBuA$^+$ and TAmA$^+$ ions if the ions would be in direct contact at saturation. However, from the experimental results given in section 5.4 it follows that the plateau values for TBuA$^+$ and TAmA$^+$ are equal within experimental error, whereas the value for TPrA$^+$ is probably lower. Hence, on these grounds we are not able to exclude the possibility that the capacitance area is correct, and consequently that in the adsorption maximum tetraalkylammonium ions are situated at relative large distances due to e.g. adsorption on specific sites only. It must be concluded that a simple interpretation of the adsorption results of tetraalkylammonium ions may give a better insight into the value of the cross-section of a methylene blue molecule. However, it does not solve the problem of the large difference between capacitance and adsorption specific surface areas.

Some progress can be made by comparing a number of electrochemical and adsorption properties between the mercury-electrolyte interface and the silver iodide-electrolyte interface. This will be discussed in the next chapter.

5.10 SUMMARY

In this chapter a detailed description of the experimental methods and results used in this study is given. Adsorption results are given for tetrapropyl-, tetrabutyl, and tetraamylammonium ions at a charged AgI-electrolyte interface.

Charge-potential curves are given in the presence of $(C_{4n} H_{8n+4} N)^+$-ions for n=1 to 5, and for choline nitrate, hexamethonium nitrate, and phenyltrimethylammonium nitrate.

Electrophoretic mobilities of silver iodide sol particles in the presence of adsorbed tetrapropyl-, tetrabutyl- and tetraamylammonium ions are also reported.

A survey of the specific surface areas of a silver iodide suspension according to different methods is given.

5.11 REFERENCES

1. A. de Keizer and J. Lyklema, J. Colloid Interface Sci. *75* 171 (1980)

2. R.M. Fuoss and C.A. Kraus, J. Am. Chem. Soc. *55* 21 (1933)

3. A.S. Brown, J. Am. Chem. Soc. *56* 646 (1934)

4. G.A. Agar, Thesis, 1961, M.I.T., Cambridge, USA

5. J.A.W. van Laar, Thesis, 1952, Utrecht

6. J.A.W. van Laar, Dutch Patent 79, 472, November 15th, 1955

7. B.H. Bijsterbosch, Thesis, 1965, Utrecht

8. C.W. Ballard, J. Isaacs, P.G.W. Scott, J. Pharm. Pharmacol. *6* 971 (1954)

9. J.T. Cross, in E. Jungermann, Cationic Surfactants, M. Dekker, New York, 1970, p. 447

10. J. Lijklema, Thesis, 1958, Utrecht

11. B.H. Bijsterbosch and J. Lyklema, J. Colloid Sci. *20* 665 (1965)

12. J. Lyklema, in International Critical Tables, 3rd Report, contract no. CST 1265 (1967)

13. L.K. Koopal, Thesis, 1978, Agricultural University, Wageningen

14. H.W. Douglas and J. Burden, Trans. Faraday Soc. *55* 350 (1959)

15. W.-Y. Wen, in Water and aqueous solutions, R.A. Horne Ed., Wiley-Interscience, New York, 1972

16. J. Kůta and I. Smoler, Collection Czechoslov. Chem. Commun. *40* 225 (1975)

ADSORPTION OF TETRAALKYLAMMONIUM IONS AT THE SILVER
IODIDE-ELECTROLYTE INTERFACE*

6.1 INTRODUCTION

In this article we focus our attention to the cooperation of electrical and nonelectrical effects in the adsorption on solids from aqueous solution.

More often than not, solid surfaces in contact with an aqueous solution bear a surface charge. (The surface charge is absent only if special precautions are taken, for instance, if the surface is at its point of zero charge (p.z.c.) or in the unlikely absolute absence of any adsorbable ionic species.) As a consequence, molecules adsorbing on such a surface adsorb in an electric field, and as the magnitude of this field affects the competition between ionic, dipolar, quadrupolar, and apolar but polarizable components, the adsorbed amount Γ is as a rule dependent on the surface charge and/or surface potential.

The model system is in our case tetraalkylammonium (TAA$^+$) salts, adsorbing on silver iodide. The electrochemistry of the AgI/aqueous electrolyte interface has been studied in great detail (1). An important feature is that the surface charge density σ and the potential $\Delta\phi$ across the interface (except for a constant) can be controlled, also in the presence of adsorbed TAA$^+$. This enables us to analyze the electrostatic component in the adsorption free energy in some detail. A second property of AgI is that it has a hydrophobic surface, with a hydrophobicity depending on σ or $\Delta\phi$ (2) and that AgI smokes are powerful cloud seeders (3,4). It is an interesting feature of TAA$^+$ ions that the length of the hydrocarbon chain can be changed. In our study, we have worked with tetrapropylammonium (TPrA$^+$), tetrabutylammonium (TBuA$^+$), and tetraamyl-

---

* Published in J. Colloid Interface Sci. 75, 171 (1980) except for some minor modifications.

ammonium (TAmA[+])ions. Lengthening of the hydrocarbon chain can be
changed. In our study, we have worked with tetrapropylammonium
(TPrA[+]), tetrabutylammonium (TBuA[+]), and tetraamylammonium (TAmA[+])
ions. Lengthening of the hydrocarbon chain does not only render the
ion more hydrophobic, it also leads to changes in the adsorption
free energy in that the charged group has to remain at a greater
distance from the surface (reducing the coulombic component of the
interaction) and in providing more CH_2 groups that can exchange
against adsorbed water dipoles.

In this study, the adsorption of the three TAA[+] ions on AgI
has been measured, thereby systematically measuring also σ and
$\Delta\phi$. Moreover, electrophoretic mobilities have been obtained; in
combination with the σ data they provide additional information
on the amount of charge in the Stern layer, i.e., they give indi-
cations on the extent of coadsorption of anions. Combining all
this information, and using some procedures from the field of
interfacial electrochemistry, an attempt will be made to obtain
detailed information on the electrostatical and molecular aspects
of the adsorption system under consideration.

6.2   MATERIALS AND METHODS

All chemicals were analytical grade, unless stated otherwise.
The used double-distilled water was percolated over a column of
AgI suspension to remove any adsorbable impurities, and purified
nitrogen was led through to remove oxygen and carbon dioxide.
Silver iodide suspensions were made and aged in the usual way
(1,5).

Solutions of TAA[+] nitrates were prepared from the commer-
cially available corresponding halides: tetrapropylammonium iodide
(Fluka, purum), tetrabutylammonium iodide (Fluka, polarography),
and tetraamylammonium bromide (KEK). Tetrapropyl- and tetrabutyl-
ammonium nitrate were prepared by adding equimolar amounts of the
required tetraalkylammonium iodide and $AgNO_3$ adjusting the pAg
(= -log c_{Ag+}) to 8.0 and filtering off the suspended silver
iodide. Tetraamylammonium nitrate was prepared in crystalline
form. To that end, tetraamylammonium bromide was dissolved in
distilled alcohol and the bromide was precipitated with a 1%
excess of $AgNO_3$ (in 85% ethyl alcohol). AgBr was filtered off

116

and the solution was titrated with KI to the equivalence point. After filtering and drying, the crystals were recrystallized from ethyl acetate and from a 1:4 (v/v) mixture of ethyl acetate and ether. The melting point is 113.2-113-8°C. Some experiments with $TPrA^+$ and $TBuA^+$ were repeated with the corresponding recrystallized nitrates. No differences in the adsorption properties could be detected.

Concentrations of TAA^+ ions were analytically determined by chloroform extraction as a TAA^+ dye complex and subsequent spectrophotometric determination of the color intensity. Except for some minor modifications we followed the method of Ballard, Isaacs, and Scott (6). The detailed procedure is given in (5). The analytical determination has a repeatability of approximately 0.2% for the highest concentrations.

Adsorption isotherms of TAA^+ ions on silver iodide were determined analytically. An aqueous slurry of silver iodide was delivered to a 50-ml volumetric flask, which was made up to volume with water and weighted to determine the amount of AgI added. After decanting and addition of the desired solutions of TAA^+ nitrate, KNO_3, KI, and/or $AgNO_3$, the flask was rotated end over end for at least 15 hr at 22.0 ± 0.5°C in the dark. The concentration of TAA^+ in the supernatant was determined as described before. The pAg was measured potentiometrically. The amount of TAA^+ adsorbed at some value of the equilibrium concentration and the equilibrium pAg can then be calculated.

Surface charge against pAg curves have been obtained by potentiometric titration of the AgI suspension with potential determining (p.d.) ions (I^- or Ag^+), following essentially the procedure described by Lyklema and Overbeek (7). The procedure has been automated by a PDP 11/10 computer (Digital Equipment Corp.) and a CAMAC data acquisition system (Borer Electronics AG) as described in detail elsewhere (5). The surface charge σ is defined through

$$\sigma = F(\Gamma_{Ag^+} - \Gamma_{I^-}), \tag{6.1}$$

where F is the Faraday constant and Γ is the surface excess of the ionic species named. The pAg follows from the measured cell potential according to Nernst's law. The obtained surface charge is reproducible within 0.05-0.1 $\mu C/cm^2$.
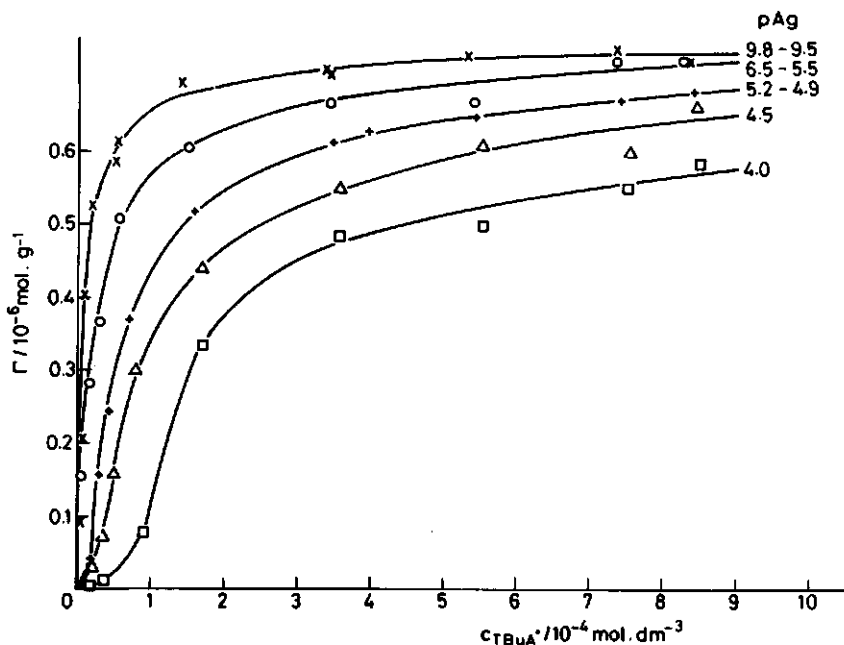
Fig. 6.1. Some typical adsorption isotherms of tetrabutylammonium ions on silver iodide. Electrolyte: 0.1 M KNO_3, T = 22.0°C, pH ≅ 7, specific surface area (capacitance) = 1.00 m^2/g. The pAg range over each isotherm is given.

Electrophoretic mobilities of silver iodide sols in the presence of TAA^+ ions have been measured at 20.0 ± 0.2°C in a Rank Brothers MKII microelectrophoresis apparatus, using a cylindrical cell. The apparatus was equipped with four electrodes. Two of them were platinized and connected to the constant-current source, whereas the inner two silver-silver iodide electrodes measured the potential difference across the cell. The experiments have been performed at pH = 3 to minimize the effect of adsorbing silicates (8). There is no indication that the pH influences the adsorption of TAA^+ ions nor the surface charge.

6.3 RESULTS

The adsorption of TAA^+ ions has been determined as a function of the equilibrium concentration $c_{TAA}+$ and the equilibrium pAg. Upon the adsorption of TAA^+, generally a shift of pAg is observed.

118
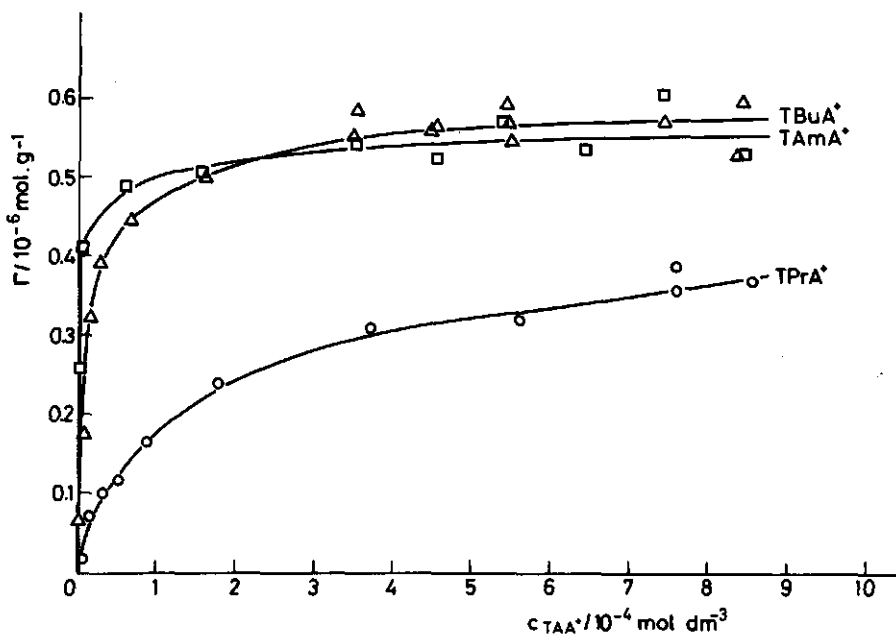
Fig. 6.2. Adsorption isotherms of tetrapropylammonium, tetrabutylammonium, and tetraamylammonium ions. Electrolyte: 0.1 M KNO_3, T = 22.0°C, pH $\cong$ 7, pAg $\cong$ 12, specific surface area of AgI (from capacitance) = 0.81 m^2/g.

Hence, interpolation of the adsorption data is required to obtain isotherms at constant pAg. Alternatively, isotherms can be replotted at constant σ. Below, we return to the implications of this choice. At high or low pAg, the variation of this quantity upon adsorption of TAA^+ is negligible, so that under these conditions no interpolation is necessary.

In Fig. 6.1 adsorption isotherms of $TBuA^+$ ions are given. These are a representative selection of directly measured isotherms without interpolation, i.e. pAg varies somewhat along the isotherm. The experimental error in Γ_{TAA}^+ is on the order of 0.01 µmole/g AgI for concentrations below 4×10^{-4} M, whereas at higher concentrations the error rises up to 0.05 µmole/g AgI. In Fig. 6.2 adsorption isotherms of three different TAA^+ ions are compared at pAg $\cong$ 12. At this high pAg value no interpolation is needed.
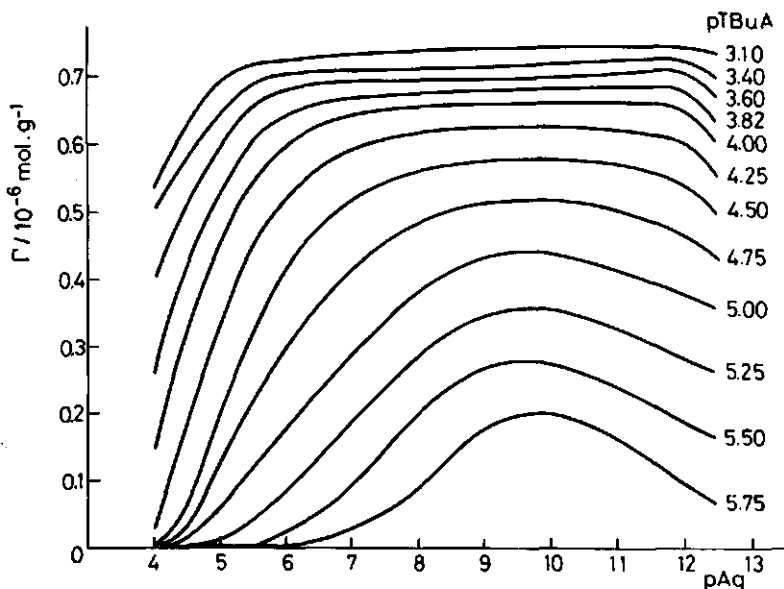
Fig. 6.3. Dependence of the adsorption of tetrabutylammonium ions on the pAg. Electrolyte: 0.1 M KNO_3, T = 22.0°C, pH $\cong$ 7, specific surface area of AgI (from capacitance) = 1.00 m^2/g.

The adsorption data of $TBuA^+$ have been interpolated and smoothed by computer using spline functions. The result is given in Fig. 6.3, which is obtained from 11 adsorption isotherms with approximately 12 datapoints each. From pAg = 4 to 8 the surface changes from positive to negative; the p.z.c. itself is a function of the amount of TAA^+ adsorbed. It is seen that first the adsorption of the positive ions increases with increasing negative surface charge, but after a specific value of pAg it decrease again. The adsorption maximum can be located at pAg 9.5 ± 0.5. At high TAA^+ concentrations adsorption is close to saturation and the maximum is broad.

In Fig. 6.4 curves of the surface charge σ against the pAg at a fixed value of the equilibrium concentration of $TBuA^+$ are given. Upon addition of Ag^+ or I^- during the titration procedure c_{TBuA}^+ shifts because its adsorption changes according to Fig. 6.3. The directly measured σ-pAg data have been recalculated by computer to yield curves at constant pTBuA, using the data from Fig. 6.3. Original data and details are given elsewhere (5, 9). From Fig. 6.4 it can be seen that the curves have a well-defined common

120
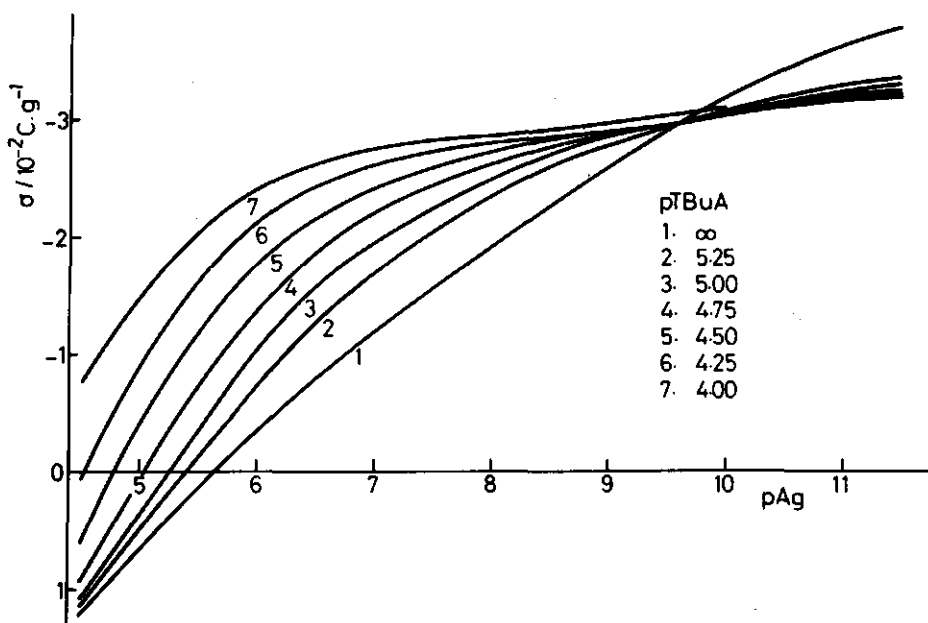
Fig. 6.4. Surface charge on silver iodide as a function of pAg at different equilibrium concentrations of tetrabutylammonium nitrate. Electrolyte: 0.1 M KNO_3, T = 20.0°C, pH ≅ 7, specific surface area of AgI (from capacitance) = 0.92 m^2/g.

intersection point (c.i.p.) at low concentrations. This is also the case for $TPrA^+$, while for $TAmA^+$ the c.i.p. is much less defined. At low concentrations the c.i.p.'s are located at pAg values of 10.7 ± 0.15, 9.6 ± 0.2, and 9.1 ± 0.3, for $TPrA^+$, $TBuA^+$, and $TAmA^+$ respectively.

Both the amount adsorbed of TAA^+ and σ are expressed per gram AgI, in order to exclude any problems in attributing absolute specific surface areas to the silver iodide suspensions (10). This is adequate as long as conclusions are drawn in which the absolute molecular area is unimportant. In other cases the electrochemical specific surface area, which ultimately stems from negative adsorption measurements, is taken (1, 11). The specific surface areas of the suspensions used were 1.00 ± 0.3 (Fig. 6.1 and 6.3)*, 0.92 ± 0.1 (Fig. 6.4), and 0.81 ± 0.3 m^2/g AgI (Fig. 6.2).

The smoothed adsorption data at fixed pAg values have been recalculated to the correponding curves at fixed σ values. The results are plotted in Fig. 6.5 and 6.6. The slope of the dashed

---

* Erratum: In the original publication an incorrect value has been reported for the specific surface area of suspension II (0.92 m^2/g).
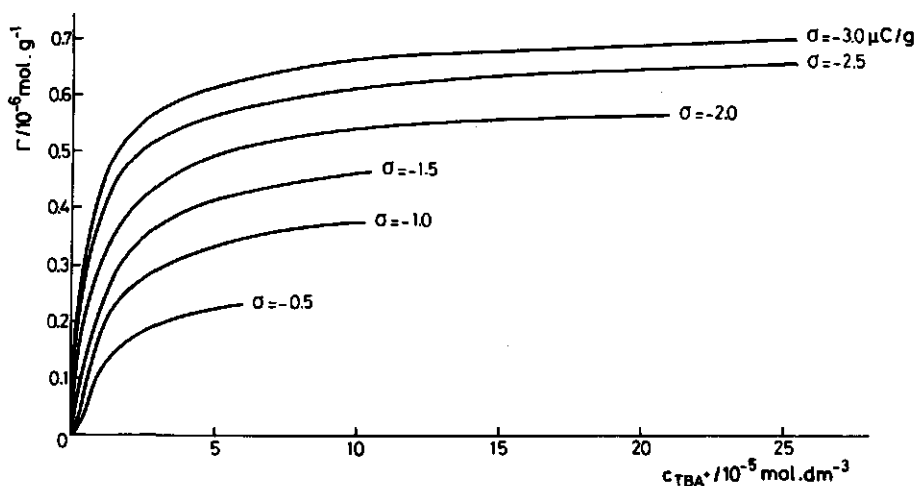
Fig. 6.5. Interpolated adsorption isotherms of tetrabutylammonium ions at fixed σ. Electrolyte: 0.1 M KNO_3, T = 22.0°C, pH ≅ 7, specific surface area of AgI (from capacitance) = 1.00 m²/g.
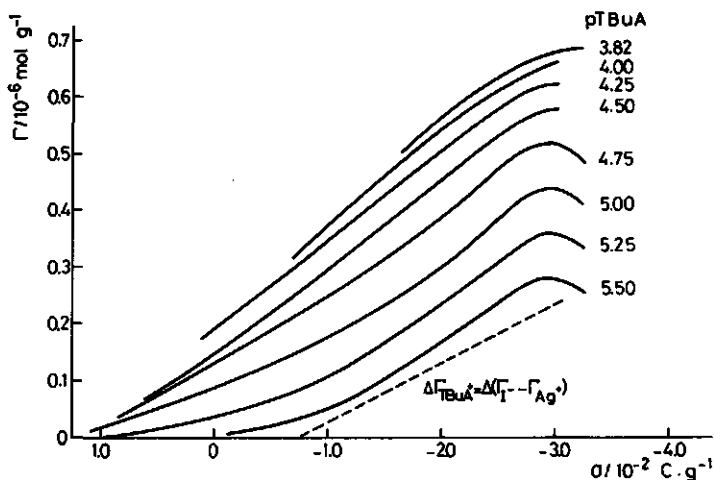
Fig. 6.6. Dependence of the adsorption of tetrabutylammonium ions on σ. Electrolyte: 0.1 M KNO_3, T = 22.0°C, pH ≅ 7, specific surface area of AgI (from capacitance) = 1.00 m²/g.

line in Fig. 6.6 indicates the situation in which the increase in surface charge would equal the charge increase imparted by adsorbed TAA[+] ions. In Fig. 6.7 and 6.8 the adsorption isotherms at fixed pAg and σ respectively have been plotted as a function of pTAA ($= -\log c_{TAA}+$).

In Fig. 6.9 we have given a plot of the electrophoretic mobility at c_{KNO_3} = 0.1 M as a function of pTAA. Around the isoelectric point (i.e.p.) the measurements are relatively less certain, because the silver iodide sol is not colloidally stable. The estimated values of the i.e.p.'s for $TPrA^+$, $TBuA^+$, and $TAmA^+$ are 3.00 ± 0.10, 4.45 ± 0.20, and 5.50 ± 0.20, respectively.
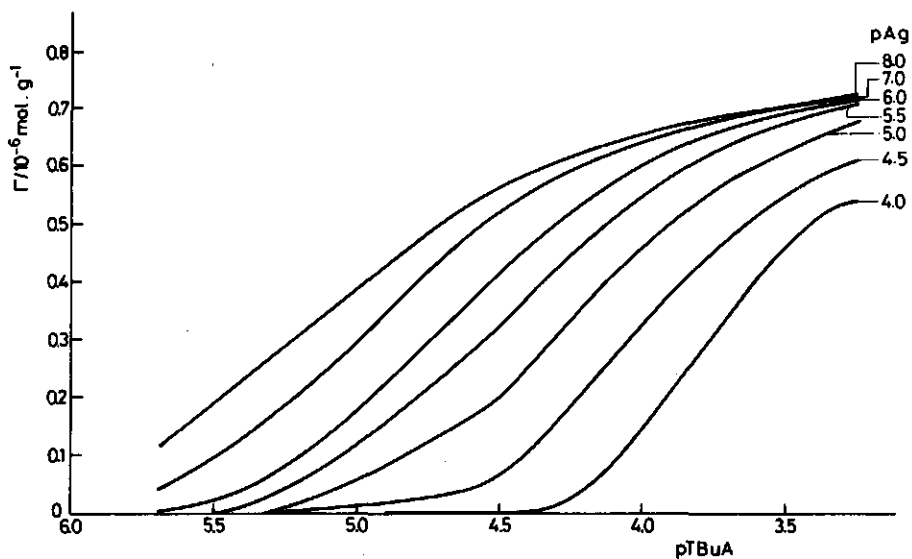
Fig. 6.7. Semilogarithmic plot of the adsorption of $TBuA^+$ ions on silver iodide at fixed pAg. c_{KNO_3} = 0.1 M, specific surface area = 1.00 m^2/g.
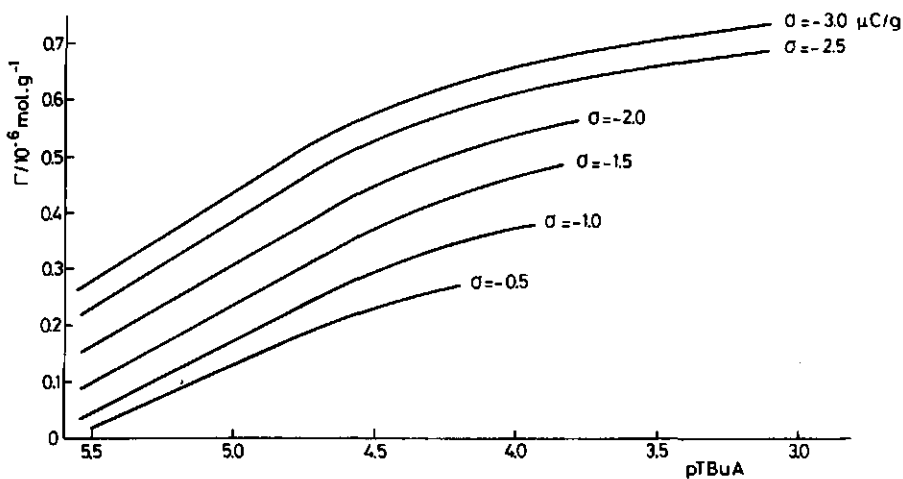
Fig. 6.8. Semilogarithmic plot of the adsorption of $TBuA^+$ ions on silver iodide at fixed σ. c_{KNO_3} = 0.1 M, specific surface area = 1.00 m^2/g.
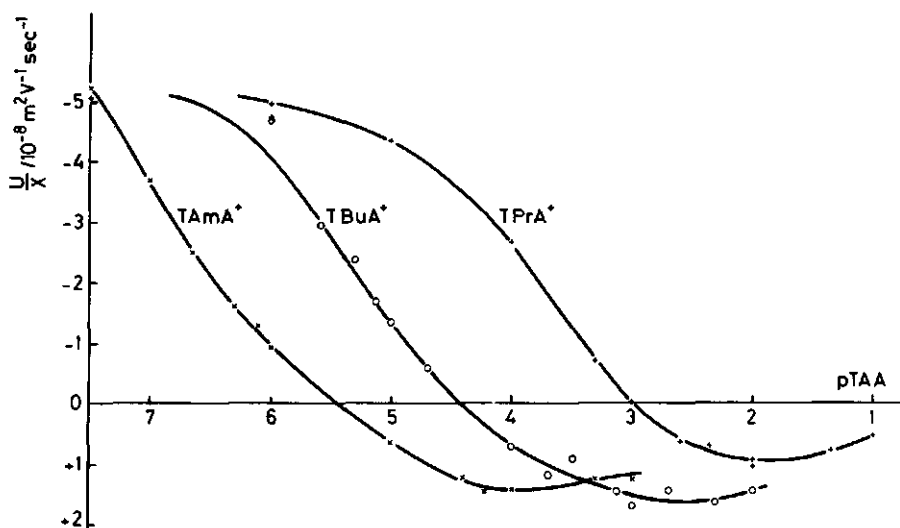
Fig. 6.9. Electrophoretic mobilities of silver iodide sol particles in the presence of different concentrations of tetraalkylammonium nitrates. Electrolyte: 0.1 M KNO_3, T = 22.0°C, pH = 3, pAg = 11.6.

6.4 DISCUSSION

6.4.1 *Some Experimental Indications for the Composite Behaviour of* ΔG^O_{ads}

At negatively charged surfaces (high pAg) the adsorption isotherms of $TBuA^+$ on silver iodide (Fig. 6.1) have a typical "Langmuirian" shape: a strongly increasing adsorption at low concentrations and a single plateau value. However, on positively charged silver iodide surfaces (low pAg) a sigmoidal adsorption isotherm is obtained. At first sight this shape could suggest cooperativeness due to lateral attracting forces (12). However, this conclusion is premature, because the AgI interface is *charged*, and it is necessary to analyze the electrical contributions before conclusions may be drawn. Specifically, it is mandatory to describe the adsorption isotherm at fixed electrical contribution to the adsorption free energy ΔG^O_{el} before any conclusions concerning the nonelectrical parameters may be drawn. In order to analyze adsorption data it is therefore necessary to

124

separate the electrical from the chemical contributions to the adsorption free energy. The choice of the electrical parameters is an important problem and automatically introduces the matter of congruency.

A qualitative comparison of the adsorption isotherms of TAA^+ at $pAg \cong 12$ (Fig. 6.2) shows that the affinity increases in the order $TPrA^+$, $TBuA^+$, and $TAmA^+$. As both the pAg and σ are almost equal for the three curves, this is an indication that this increase in affinity is mainly due to an increase in the chemical contribution ΔG_{chem}^0.

The maximum in the adsorption of $TBuA^+$ as a function of pAg (Fig. 6.3) indicates that at high pAg the gain in adsorption free energy due to coulombic interaction between the positive and the negative surface must be outweighed by another interaction dependent on the pAg. The latter effect must be due to displacement of water dipoles from the surface. This emphasizes once more the importance of separating the components of ΔG_{ads}^0, in order to arrive at a molecular interpretation of adsorption phenomena.

6.4.2 Components of ΔG_{ads}^0

The adsorption of TAA^+ ions from aqueous solutions at the silver iodide-electrolyte interface is really an exchange process:

$$(TAA^+)_{sol} + v(H_2O)_{ads} \qquad (TAA^+)_{ads} + v(H_2O)_{sol}. \qquad (6.2)$$

Below, the standard free energy ΔG_{ads}^0 of adsorption will be separated into an electrical and a chemical component. The electrical component will be subdivided into a coulombic and a dipolar part:

$$\Delta G_{ads}^0 = \Delta G_{chem}^0 + \Delta G_{dip}^0 + \Delta G_{coul}^0. \qquad (6.3)$$

This given decomposition of ΔG_{ads}^0 is arbitrary, because the chemical contribution is not completely independent of the electrical field. In order to avoid this arbitrariness, we define two terms rigorously, viz., ΔG_{dip}^0 and ΔG_{coul}^0. In doing so the remaining terms are automatically defined as ΔG_{chem}^0.

The definitions are

$$\Delta G^0_{coul} \equiv zF\Delta\phi_{ads} \qquad (6.4)$$

$$\Delta G^0_{dip} \equiv \Sigma \ \Delta n_j \ \vec{\mu}_j \cdot \vec{E}_{ads}, \qquad (6.5)$$

where z is the valency of the adsorbed ion, $\Delta\phi_{ads}$ the electrical potential at the locus of adsorption with respect to the potential in bulk, Δn_j the change in the number of adsorbed molecules j due to process (6.2), $\vec{\mu}_j$ the dipole moment of j, and $\vec{E}_{ads}$ the field strength at the locus of adsorption. In our case, in view of exchange reaction (6.2) only the dipole moment of the displaced water molecules has to be taken into account , and Δn_j is related to n in (6.2) and to the mode of attachment of the hydrocarbon chains on the AgI surface.

From a phenomenological point of view, it has been established that at constant temperature and ionic strength for the silver iodide-electrolyte interface the adsorption can generally be described with four variables, viz., σ, pAg, Γ_A, and c_A, where the index A stands generally for adsorbate. However, only two of these variables are independent. Hence, an adsorption isotherm equation can be quite generally written as (13)

$$F'(pAg,\Gamma_A) \cdot c_A = f'(\Gamma_A) \qquad (6.6)$$

or

$$G'(\sigma,\Gamma_A) \ \cdot c_A = g'(\Gamma_A), \qquad (6.7)$$

where F', G', f', and g' are mathematical functions of the parameters indicated. An adsorption isotherm can be classified as congruent in charge or potential provided the functions F' and G' are separable into a product of two functions, one depending on the electrical parameter only, and the other depending on Γ_A only. In that case (6.6) and (6.7) can be rewritten as

$$F(pAg) \cdot c_A = f(\Gamma_A) \qquad (6.8)$$

and

$$G(\sigma) \ \cdot c_A = g(\Gamma_A). \qquad (6.9)$$

These equations are directly applicable to verify if in a given case potential or charge congruency applies. Plots of Γ_A vs pA (= $-\log c_A$) at different pAg's (or σ's) must coincide by shifting along the pA axis, if the adsorption is potential or charge

126

congruent respectively. If one of such congruencies is found a shift in pA equals a shift 2.3 ln F(pAg) or 2.3 ln G(σ) respectively (14, 15). If the standard adsorption free energy ΔG^0_{ads} is the part of the adsorption free energy that is not dependent of Γ_A, we may write

$$\Delta G^0_{ads} = -RT \ln F(pAg) \qquad (6.10)$$
or
$$\Delta G^0_{ads} = -RT \ln G(\sigma). \qquad (6.11)$$

All components of the adsorption free energy that depend on Γ_A (e.g., lateral interactions) are included in f or g, respectively (16), hence they do not occur in ΔG^0_{ads}.

In Fig. 6.7 and 6.8 the adsorption of TBuA$^+$ ions on silver iodide is given as a function of pTBuA at constant pAg and constant σ respectively. The congruency in the potential (i.e., in pAg) seems rather poor, especially at low pAg. The congruency in the charge σ is not perfect either; deviations occur especially at low surface charges and at high coverage. Apparently, our system does not completely obey perfect charge congruency or perfect pAg congruency.

The molecular interpretation of the congruence matter is as follows. The adsorption is congruent in some electrical parameter if the electrical component of the adsorption free energy, written in terms of this parameter, is constant. In ideal cases ΔG^0_{el} would depend on the field strength $\vec{E}_{ads}$ near the surface only, if the adsorption process were a dipole displacement, but it would depend on the electrical potential $\Delta\phi_{ads}$ only in the case of adsorption of ions. As in first approximation $\Delta\phi_{ads}$ is related to pAg and $\vec{E}_{ads}$ to σ (by virtue of Gauss' law), prevalence of the second term in (6.3) would lead to charge congruency, whereas prevalence of the third term in (6.3) would promote pAg congruence. However, there are complications. First, $\Delta\phi_{ads}$ is lower than $\Delta\phi$, and as the difference between these two potentials depends on σ, "pure" cases of potential congruence do not exist. Second, as in our system both coulombic and dipolar electric energies play a role, it is not surprising that neither fit is perfect. However, the regions of applicability give some information on the relative prevalence of the two electrical contributions.

Deviations from these limiting (ideal) congruency models may also occur if components of the adsorption free energy that are dependent on Γ_A (included in f or g) are also dependent on the electrical parameter. As $f(\Gamma_A)$ and $g(\Gamma_A)$ depend on the particular adsorption model, deviations from ideal congruency change these functions into functionalities $f(\Gamma_A, pAg)$ and $g(\Gamma_A, \sigma)$ respectively.

As a model to describe the adsorption of TAA$^+$ ions on silver iodide, we use the Frumkin-Fowler-Guggenheim (FFG) adsorption isotherm (17, 18),

$$\ln\{\theta/(1 - \theta)\} + A\theta = \ln \beta c_A/55.5, \tag{6.12}$$

where θ is the degree of occupation (Γ_A/Γ_{max}). β is identical with either F or G in (6.10) and (6.11) depending on the nature of the congruency. The FFG isotherm is derived from the following premises: the adsorption is localized and reversible, the surface is energetically homogeneous, and adsorption is limited to a mono-layer. Nonidealities due to lateral interaction are taken into account through the parameter A. Usually, only β is dependent on the electrical parameter. However, in more complex situations, for instance in the case of the lateral interaction between adsorbed TAA$^+$ ions, A may also be a function of the surface charge. In such cases, the FFG isotherm is no longer congruent in one of the electrical parameters, because the electrical part and the θ part cannot be separated.

A convenient way to analyze the FFG adsorption isotherm equation makes use of its first and second derivative:

$$\frac{d\theta}{d \ln c_A} = \frac{\theta(1 - \theta)}{1 + A\{\theta(1 - \theta)\}} \tag{6.13}$$

$$\frac{d^2\theta}{d(\ln c_A)^2} = \frac{\theta(1 - \theta)(1 - 2\theta)}{1 + A\{\theta(1 - \theta)\}^3} . \tag{6.14}$$

It follows that the slope has a maximum at $\theta = 0.5$:

$$\left(\frac{d\theta}{d \ln c_A}\right)_{max} = \frac{1}{4 + A} . \tag{6.15}$$

This maximum slope of the $\theta - \ln c_A$ curve is experimentally always well accessible. It amounts to 0.25 if the lateral interaction vanishes; under that condition the FFG isotherm

reduces to the Langmuir isotherm. Moreover, at $\theta = 0.5$ it follows from (6.12) that

$$\ln \beta = A/2 - \ln c_A/55.5 \qquad\qquad (6.16)$$

which can also easily be applied to experimental results.

Application of (6.15) and (6.16) to the results given in Figs. 6.7 and 6.8 leads to the data in Table 6-1.

Table 6-1 Parameters of the Frumkin-Fowler-Guggenheim Equation for the Adsorption of TBuA+ Ions on Charged Silver Iodide Surfaces

Electrical parameter pAg			Electrical parameter σ	
pAg	A	$\ln \beta$	σ	A
8.0	0.11	15.78	-3.0	1.49
7.0	-0.31	15.16	-2.5	1.20
6.0	-0.43	14.57	-2.0	0.78
5.5	-0.55	14.10	-1.5	(0.37)
5.0	-0.78	13.47		
4.5	-0.97	12.80		
4.0	-1.39	12.00		

If the pAg is used as the electrical parameter in the FFG isotherm, an increasingly negative interaction parameter A is found if the surface becomes more positive, while à decreasingly positive interaction parameter is found for σ as the electrical parameter. For TBuA$^+$ ions it is more likely that lateral interaction is repulsive (A > 0) than attractive. Hence, this consideration supports charge congruency. The decrease of the repulsion with decreasing negative charge points to an increase of lateral screening in this direction. This may in the first place be attributed to differences in the amount of coadsorbed NO_3^- ions. For the pAg as the electrical parameter, a quadratic dependence of $\ln \beta$ on the pAg is observed. This is a general indication that permanent and induced dipolar effects prevail. Unfortunately, β values cannot be easily calculated for the charge congruence case, because the apparent plateau value decreases with decreasing negative σ and the curves do not cover the full concentration range. Some indication on the relative position of the plateau values can be obtained by extrapolating the curves of Fig. 6.8 according to (6.12). Then a decrease in plateau value with in-

creasing σ is found, which is surprising. One explanation could be that sites with adsorbed Ag^+ ions are less favourable. This is due to a strong repulsion between Ag^+ and the adsorbed TAA^+ ions. Moreover, it is likely that Ag^+ sites are strongly hydrated.

The mutual positions of the (apparent) plateau values in the adsorption isotherms of $TPrA^+$, $TBuA^+$, and $TAmA^+$ at pI = 4 (Fig. 2) are unexpected but well established. Apparently, the molecular dimensions of the ions do not completely determine the effective molecular cross section. A more detailed analysis to explain this effect is necessary. This significance of the specific surface area may be related to this issue.

6.4.3 *Electrophoresis*

The electrophoretic mobility of AgI particles in the presence of TAA^+ ions at pAg = 11.6 and c_{KNO_3} = 0.1 M is given in Fig. 6.9. Upon adsorption of TAA^+ ions the mobility decreases because (i) these ions neutralize the surface charge, and (ii) the surface of shear is displaced outwardly. At high adsorbate concentration the surface charge σ is overcompensated by adsorbate ions. The shift in i.e.p. follows the trend in affinity of these ions. The maximum resulting mobility of the positive particles is much lower than the same of the naked negative particles, indicating that the maximum charge within the surface of shear is much lower than for the naked particle. This is partly due to the fact that the charge attributed by adsorbed TAA^+ ions has a maximum lower than twice the surface charge, and partly because of co-adsorption of nitrate ions. The relative maximum values of the positive mobilities for $TPrA^+$, $TBuA^+$, and $TAmA^+$ are in the same order as the apparent plateau values in the isotherms. This indicates that coadsorption of nitrate within the surface of shear does not or not strongly increase with increasing ion size of TAA^+.

A semiquantitative estimate of the change of ΔG^0_{chem} with increasing hydrocarbon chain length is obtainable from the relative positions of the i.e.p.'s. At the i.e.p., ΔG^0_{el} and the numbers of molecules adsorbed per unit area are both roughly equal for the three TAA^+ ions. This follows from the independ-

ently obtainable fact that at the three i.e.p.'s the surface charge is also approximately the same, hence in view of the foregoing the electrical conditions are very similar. Moreover, as at the i.e.p. the surface charge is just compensated by the charge of TAA$^+$ ions, Γ_{TAA}^+ is also identical if coadsorption of nitrate is equal too. Assuming the adsorption to follow the FFG picture with the same interaction parameter and constant ΔG_{el}^0, a shift of 2.3 pA equals the shift in $-\Delta G_{chem}^0/RT$. In our system, $pA_{i.e.p.}$ amounts to 3.00, 4.35, and 5.50 for TPrA$^+$, TBuA$^+$ and TAmA$^+$ respectively. The average shift of 1.25 in the i.e.p. can be compared with the change of 0.48 in the adsorption affinity within a homologous series upon increasing the hydrocarbon chain length by one -CH$_2$ group (Traube's rule)(19, 20) suggesting that upon increasing the four hydrocarbon chains in the TAA$^+$ ion each by one CH$_2$ group, only 2.6 of them contribute to the increased activity. This, in turn, suggests that the TAA$^+$ ion is in contact with the hydrophobic silver iodide surface by 2-3 alkyl chains. The experimental fact that the difference in i.e.p. between TBuA$^+$ and TAmA$^+$ is smaller than that between TPrA$^+$ and TBuA$^+$ could indicate that for TPrA$^+$ not all five CH$_2$ groups of each chain contribute equally to the value of ΔG_{chem}^0. These results indicate that ΔG_{chem}^0 is mainly determined by the liberation of structuralized water molecules, similar to the hydrophobic dehydration at the air-water interface.

In principle it is possible to estimate the amount of nitrate coadsorbed within the surface of shear. At the isoelectric point,

$$\sigma + \sigma_{TAA+} + \sigma_{NO3-} = 0. \tag{6.17}$$

Here, σ and σ_{TAA}^+ are known from experiments. Unfortunately, for TBuA$^+$ and TAmA$^+$ a slight uncertainty in the choice of the i.e.p. gives rise to a large uncertainty in σ_{TAA}^+, because the isotherms are steep under these conditions. However, for TPrA$^+$ a reliable estimate can be made. The value of σ_{TPrA}^+, is 4.54 μC/cm^2; for σ 3.90 μC/cm^2 is found (5, 9). It follows that the charge contribution of the nitrate ions within the surface of shear amounts to -0.64 μC/cm^2 for TPrA$^+$ ions, corresponding with 14% of the number of adsorbed TPrA$^+$ ions.

A reliable estimate for the amount of nitrate ions within the surface of shear at saturation values can be made by calculating the electrophoretic charge from Smoluchowski's equation (high κa) for the values of maximum electrophoretic mobility. The electrophoretic charge is 1.5 ± 0.2 $\mu C/cm^2$ for $TAmA^+$ and $TBuA^+$; for these ions the contribution of NO_3^- amounts to -1.4 $\mu C/cm^2$ corresponding with 20% of the number of adsorbed TAA^+ ions. For $TPrA^+$ a smaller value is obtained, but an accurate estimate is difficult because the adsorption at 10^{-2} mole/dm^3 has not been measured. It may be concluded that the coadsorption of NO_3^- is much smaller than the TAA^+ adsorption. It is likely that coadsorbed NO_3^- ions are located in the Stern layer between TAA^+ ions, screening their lateral interaction.

6.4.4 *Model Considerations of the Adsorption Maximum*

The surface charge versus pAg for various pTAA values is related to the adsorption of TAA^+ ions by an equation that can be derived from the Gibbs adsorption equation (1, 5):

$$\Gamma_{TAA+}^{(s)} - \Gamma_{TAA+}^{(s)*} = \frac{1}{F} \int_{pAg*}^{pAg} \left(\frac{\partial\sigma}{\partial pTAA}\right)_{T,pAg,\mu_{KNO_3}} dpAg, \qquad (6.18)$$

where $\Gamma_{TAA+}^{(s)}$ is the Gibbs excess adsorption of the TAA^+ ions with the solid-liquid boundary as the Gibbs dividing plane, $\Gamma_{TAA+}^{(s)*}$ is the adsorption in some reference point (e.g., the adsorption maximum), T is the temperature, and μ_{KNO_3} the chemical potential of KNO_3, which is approximately constant, because the KNO_3 concentration is relatively high. Application of (6.19) to the data of Fig. 6.4 shows immediately the coincidence of the (common) intersection point with the adsorption maximum. The adsorption maximum (Figs. 6.3 and 6.6) agrees within experimental error with the location of the common intersection point (Fig. 6.4).

A molecular interpretation of the adsorption maximum will be given in more detail elsewhere (5, 9). Here we shall briefly review the principles.

The potential difference between the solid and the bulk of
the solution is the Galvani potential (difference) $\Delta\phi$ which is
related to the pAg by Nernst's law. At the common intersection
point, characterized by values σ_m and ϕ_m of the surface charge
density and Galvani potential respectively, the conditions

$$\left(\frac{\partial\Delta\phi}{\partial\theta}\right)_{\sigma=\sigma_m} = 0 \tag{6.19a}$$

or

$$\left(\frac{\partial\sigma}{\partial\theta}\right)_{\phi_o=\phi_m} = 0 \tag{6.19b}$$

must be satisfied. The whole problem to interpret the common inter-
section point thus reduces to describing the Galvani potential $\Delta\phi$
in terms of σ and θ. This problem can be simplified by assuming as
an adsorption model either the parallel capacitors model (21) or
the series capacitors model (22). From a thermodynamic analysis
(5, 14) it can be shown that the parallel capacitors model corres-
ponds to adsorption congruent in the potential, while the series
capacitors model corresponds to adsorption congruent in the charge.
Because our system is probably closer to charge congruence than to
potential congruence, we use the series capacitors model. However,
it can easily be shown (5) that the same expression for σ_m results
if the parallel capacitors model would be used. In our model the
Galvani potential is written as

$$\Delta\phi = \Delta\phi^C \theta + \Delta\phi^0 (1 - \theta) \tag{6.20}$$

in which $\Delta\phi^C$ and $\Delta\phi^0$ are the Galvani potentials of the completely
covered and uncovered parts, respectively. Applying (6.19a) to
(6.20) gives $\Delta\phi^C = \Delta\phi^0$ at $\sigma = \sigma_m$. In order to obtain an expression
for σ_m (or ϕ_m) we need double layer models for the covered and the
uncovered part.

The Galvani potentials $\Delta\phi^C$ and $\Delta\phi^0$ are composed of a diffuse-
layer potential (described by the Poisson-Boltzmann equation), a
Stern-potential decay (following the Poisson equation), and a χ
potential originating from the adsorbed dipoles and from polari-
zation in the solid. It is assumed that polarization effects are
incorporated in the Stern potential through the value of the
effective dielectric constant. Let the χ potential of a completely
covered surface be χ_2^0 (independent of $\Delta\phi$ or σ and approximately

133

zero for TAA$^+$ adsorption) and let it be χ_1^0 for the uncovered surface *at the p.z.c.* There must exist some reference surface charge σ_R at which the χ potential of the uncovered surface is zero. We asssume that for σ values not too far from the c.i.p. the χ potential changes linearly with σ. To a first approximation, we neglect specific adsorption of K^+ and NO_3^- ions. Then the following equations result:

uncovered surface

$$\Delta\phi^0 = \frac{\sigma}{\varepsilon\varepsilon_0\kappa} + \frac{\sigma\,\delta^0}{\varepsilon_s^0\varepsilon_0} + \chi_1^0\,(1 - \frac{\sigma}{\sigma_R})\ , \tag{6.21}$$

completely covered surface

$$\Delta\phi^c = \frac{\sigma + F\Gamma_A^{max}}{\varepsilon\varepsilon_0\kappa} + \frac{\sigma\,\delta^c}{\varepsilon_s^c\varepsilon_0} + \chi_2^0. \tag{6.22}$$

Here, ε, and ε_s^0, and ε_s^c are the effective relative dielectric constants of the solution, of the Stern layer without and completely covered with adsorbate respectively, ε_0 is the dielectric permittivity in vacuum, δ^c and δ^0 are the corresponding thicknesses of the two types of Stern layer, Γ_A^{max} is the maximum adsorption of adsorbate, and κ is the reciprocal thickness of the diffuse double layer. The first term of (6.21) and (6.22) is the diffuse layer term in the linear approximation. This may be applied in the underlying case, because $\Delta\phi$ (diff) is low due to the high electrolyte concentration. The second term is the Stern-potential drop and the third term is caused by the presence of dipoles. Combining (6.19a), (6.20), (6.21), and (6.22) leads to this expression for σ_m:

$$\sigma_m = \frac{\chi_1^0 - \chi_2^0 - F\Gamma_A^{max}/\varepsilon\varepsilon_0\kappa}{(\chi_1^0/\sigma_R) - (\delta^0/\varepsilon_s^0\varepsilon_0) + (\delta^c/\varepsilon_s^c\varepsilon_0)}\ . \tag{6.23}$$

The same equation applies for the parallel capacitors model. Accounting for specific adsorption would lead to a term $F\Gamma_T/\varepsilon\varepsilon_0\kappa$, in which Γ_T is the amount of specifically adsorbed ions. However, this term is much smaller than $F\Gamma_A^{max}/\varepsilon\varepsilon_0\kappa$. Moreover, the latter term is small because κ is large, so neglecting specific adsorption causes only a small error. In (6.23) σ_m is independent of

θ, hence a *common* intersection point is obtained. However, in real systems the relation $\Delta\phi(\sigma,\theta)$ could be more complicated; for instance, the simple linear relation of θ in (6.20) could break down and then the adsorption maximum would become dependent on θ. This has been observed in a few cases.

According to a very simplified picture, the c.i.p. would coincide with the point where in the absence of an adsorbate the water molecules are randomly oriented ($\sigma_m = \sigma_R$) resulting in a position of the c.i.p. which is independent of the nature of the adsorbate. From (6.23) it can be seen that this situation only occurs at high salt concentration ($F\Gamma_A^{max} << \varepsilon\varepsilon_0\kappa$) and at high Stern capacitances (δ^0/ε_s^0 and δ^C/ε_s^C small). However, in general the changes in Stern-layer and diffuse-layer capacitances also contribute use the position of the maximum.

The trend in the c.i.p.'s for TPrA$^+$, TBuA$^+$, and TAmA$^+$ is readily explained according to (6.23) in terms of the change in Stern-layer thickness for different ionic radii. Figure 6.3 proves the existence of an adsorption maximum, and its position (pAg = ± 9.5) corresponds well with the position of the c.i.p. in Fig. 6.4 (pAg = 9.6). As far as we know this is the first experimental verification of the existence of such a maximum. The identity of the directly measured adsorption maximum and the same derived from σ(pAg) by thermodynamics underscore the self-consistency of the picture and support the applicability of equilibrium thermodynamics to these systems.

6.5 CONCLUSION

Thus, the combination of various techniques allowed us to develop a self-consistent picture of the adsorption of TAA$^+$ ions on AgI.

6.6. SUMMARY

This chapter described the adsorption of tetrapropyl-, tetrabutyl-, and tetraamylammonium ions on charged silver iodide surfaces. Adsorption isotherms are obtained at various values of the surface charge density and the surface potential. In addition,

electrophoretic mobilities of silver iodide sols in the presence
of adsorbed tetraalkylammonium ions have been measured. As a
function of charge or potential, the adsorbed amount passes
through a maximum. This maximum can also be obtained from separa-
tely measured surface charge-surface potential curves, and a mole-
cular interpretation is offered. Upon adsorption, not all CH_3
groups of the tetraalkylammonium ions attach themselves to the sur-
face. Congruence analysis shows that the adsorption is better
charge congruent than potential congruent. The system is nonideal,
the lateral interaction parameter has been established as a func-
tion of the surface charge. The adsorption of tetraalkylammonium
ions is accompanied by a nonnegligible coadsorption of nitrate
ions that probably contributes to the lateral screening.

6.7   REFERENCES

1.   B.H. Bijsterbosch, and J. Lyklema, Advan.Colloid Interface
      Sci. *9* 147 (1978)

2.   D.F. Billet, D.B. Hough, and R.H. Ottewill, J. Electroanal.
      Chem. *74* 107 (1976)

3.   A.C. Zettlemoyer, (Ed.) in "Nucleation", Dekker, New York,
      (1969)

4.   A.C. Zettlemoyer, in "Hydrophobic Surfaces" (F.M. Fowkes,
      Ed.), p. 1. Academic Press, New York, 1969)

5.   This thesis, chapter 7

6.   C.W. Ballard, J. Isaacs, and P.G.W. Scott, J. Pharm.
      Pharmacol. *6* 971 (1964)

7.   J. Lyklema, and J.Th.G. Overbeek, J. Colloid Sci.,
      16 595 (1961)

8.   H.W. Douglas, and J. Burden, Trans. Faraday Soc. 55 350
      (1959)

9.   A. de Keizer, and J.Lyklema, to be published

10.   L.K. Koopal, Thesis, Commun, Agricultural University,
      Wageningen, The Netherlands, 75-14, 1975

11.   H.J. van den Hul, and J. Lyklema, J. Amer.Chem.Soc.
      90 3010 (1968)

12.   J.J. Kippling, "Adsorption from Solution of Non-Electrolytes",
      p. 130. Academic Press, New York, 1965

13.   S.K. Rangajaran, J. Electroanal.Chem. *45* 279 (1973)

14.   R. Payne, in "Progress in Surface and Membrane Science"
      (J.F. Danielli, M.D. Rosenberg, and D.A. Cadenhead, Eds.),
      Vol.6, p. 51. Academic Press, New York, 1973

15. S. Trasatti, J. Electroanal.Chem. *53* 335 (1974)

16. S.K. Rangarajan, J. Electroanal.Chem. *45* 283 (1973)

17. A.N. Frumkin, Z. Phys.Chem. *116* 466 (1925)

18. R.H. Fowler, and E.A. Guggenheim, "Statistical Thermo-
     dynamics", p. 558. Cambridge Univ. Press, London/New York,
     1965

19. I. Traube, Ann. *265* 27 (1891)

20. A.W. Adamson, "Physical Chemistry of Surfaces", 2nd ed.,
     p. 101. Interscience, London, 1967

21. B.B. Damaskin, and A.N. Frumkin, J. Electroanal.Chem. *34*
     191 (1972)

22. R. Parsons, J. Electroanal.Chem. *5* 397 (1963)

CHAPTER 7

THE EFFECT OF THE ADSORPTION OF TETRAALKYLAMMONIUM IONS ON
THE ELECTRICAL DOUBLE LAYER ON SILVER IODIDE

7.1 INTRODUCTION

The electrical double layer on silver iodide can be investi-
gated by several experimental methods. The most basic information
on double layer properties is the relation between the surface
charge and the surface potential. Using interfacial thermodynamics,
the effect of the adsorption of tetraalkylammonium ions on this
relation can be applied to obtain the dependence of this adsorp-
tion on the electrical parameter.

As the adsorption of tetraalkylammonium ions can also be
measured *directly*, the comparison between these results and the
adsorption derived from titration curves is now possible. In the
present field of study this comparison can be considered a unique
cheque on the validity of Gibbs' adsorption law or, more generally,
as a check on the applicability of equilibrium thermodynamics to
the silver iodide-electrolyte system. To my knowledge, this is the
first direct check for the silver iodide system.

One of the most intrigueing properties of charge-potential
curves at different adsorbate concentrations is probably the pre-
sence of a *common intersection point*. It has been observed with
most adsorbates investigated till now. In the previous chapter
a model was developed to explain the occurrence and position of
this point. The discussion will now be extended and the picture
developed will be used to interpret quantitatively the dependence
of the common intersection point on the nature of the TAA^+ ion.

The electrical double layers on mercury and silver iodide are
qualitatively very similar in most experimental cases. However, the
quantitative differences appear to be quite pronounced. Some typ-
ical differences will be given for the adsorption of n-butanol and

139

TAA$^+$ ions on both interfaces, and a discussion will be presented.

A recurrent problem in the interfacial electrochemistry of silver iodide is the ambiguity in the choice of the specific surface area of a suspension. As discussed in section 5.9, surface areas obtained from different methods can be different by a factor of 3. Investigation of the electrosorption of tetraalkylammonium ions on silver iodide adds new arguments to the discussion on the difference between adsorption and capacitance areas. This matter will be treated in some detail, and a suggestion for a new adsorption model will be made.

7.2 MATERIALS, METHODS AND RESULTS

The materials have been described in section 5.2. The titration procedure is given in chapter 4 and in section 5.5, whereas the titration results are given in section 5.6.

7.3 SOME ASPECTS OF CHARGE-POTENTIAL CURVES IN THE PRESENCE OF QUATERNARY AMMONIUM IONS

In this section a qualitative discussion of charge-potential curves in the presence of symmetrical tetraalkylammonium ions and some other quaternary ammonium ions as given in chapter 5 will be offered. A quantitative analysis for TPrA$^+$ and TBuA$^+$ follows in sections 7.5 and 7.6 respectively.

Qualitatively, the σ-pAg curves in the presence of TPrA$^+$ ions in 0.1 M KNO$_3$ very much resemble the corresponding curves as usually obtained in the presence of neutral compounds, such as n-butanol (1). The most noteworthy common feature is the occurrence of a more or less well-defined *common intersection point*. As discussed in detail in chapter 2, this common intersection point corresponds to an adsorption maximum of the organic compound as a function of the pAg (potential). At first glance, it seems unlikely that beyond a given surface potential positive ions are adsorbed in smaller amounts if the surface is made more negative. This decrease of adsorption suggests that tetraalkylammonium ions are really present as neutral ion pairs rather than as charged entities. However, it follows from electrophoretic mo-

140

bilities of silver iodide sol particles in the presence of TPrA$^+$ ions, that the organic ions are mainly present in the dissociated state both on negative and positive surfaces. The explanation must be sought in the fact that the TPrA$^+$ adsorption is actually the result of a competition with water dipoles (cf. ch. 6). More specifically, beyond the c.i.p. bonding of H_2O dipoles in the Helmholtz layer is more favourable than adsorbing TPrA$^+$ ions.

The slope of the charge-potential curves in the presence of TPrA$^+$ (i.e. the *differential capacitance*) decreases with increasing Γ_A, at least around the c.i.p., analogous to many corresponding curves with neutral compounds, e.g. n-butanol. As the indifferent electrolyte concentration is high, the effect is mainly due to a decrease in the capacitance of the inner layer. This decrease can be explained by realizing that at increasing adsorption of TPrA$^+$ ions (i) the number of adsorbing water dipoles decreases, (ii) the dielectric constant of the Stern layer decreases, and (iii) the thickness of the Stern layer will increase. All these effects contribute positively to the decrease of the inner layer capacitance. Away from the c.i.p. the value of the capacitance is to an increasing extent determined by the desorption of the tetra-alkylammonium ions, if the curves are given at a constant equilibrium concentration. As a consequence, at low pAg the slope of the charge-potential curves of TPrA$^+$ ions increases with increasing Γ_A.

In the presence of neutral compounds, the shift of the *point of zero charge* is usually interpreted in terms of the exchange of dipoles. In the presence of tetraalkylammonium ions the shift is due both to dipolar effects and to the contribution of the diffuse double layer facing the TAA charge. Thus, the shift in positive direction is composed of (i) the displacement of water molecules adsorbed with their negative sides, and (ii) the increase of $\Delta\phi$ (Stern) with increase of Γ_A.

A very characteristic feature of the charge-potential curves with TPrA$^+$ ions is the fact that they tend to *merge* at positive potentials implying complete desorption of TAA$^+$. For low molecular weight substances like n-butanol (1), any indication of convergence at positive potentials is absent, although at the negative surface there are some vague indications of merging at extreme negative potentials. However, for adsorption of n-butanol at the

mercury-electrolyte interface (2) the charge-potential curves do merge both at positive and at negative potentials, albeit that the applied potential range is much larger. It is likely that also n-butanol (and other butanols) at AgI would desorb completely at high positive and high negative potentials which are experimentally inaccessible.

The merging of charge-potential curves in the presence of tetrapropylammonium ions and, correspondingly, the complete desorption at potentials which are experimentally (almost) accessible, enables the calculation of absolute adsorption values from titration data according to Gibbs' law. This unique feature allows comparison with direct adsorption data as mentioned in 7.1.

In the behaviour of charge-potential curves for a series of symmetrical tetraalkylammonium ions (where alkyl stands for methyl, ethyl, propyl, butyl, and amyl) some trends emerge (figs. 5.3-5.7). (i) The adsorption increases from methyl to amyl, indicating that hydrophobic bonding is an important factor in the interaction energy with the surface.
(ii) The common intersection points shift to more positive potentials with increasing alkyl length. This trend was already qualitatively explained in the previous chapter.
(iii) Finally, it appears, that the extent of desorption with respect to the c.i.p. decreases from methyl to amyl if the pAg decreases.

In chapter 5 also the results of three asymmetrical quaternary ammonium ions were given. Trimethylphenylammonium ions (fig. 5.8) appear to desorb already completely at small positive potentials. A common intersection point at the negative side is absent. Probably the phenyl group is the origin of this deviation from the usual behaviour. The effect of choline nitrate (fig. 5.9) on σ-pAg curves is not very pronounced. The concentration range corresponds to that used in the tetramethylammonium curves (fig. 5.6). It is likely that the three methyl groups are attached to the surface with the hydrophilic OH group pointing to the solution side. This OH-group has a strong dipole moment, replacing the H_2O dipoles oriented in the same way so that the net effect is small. The tendency of the shift of the p.z.c. to *negative* potentials may also be

explained in this way. Qualitatively, the effect of hexamethonium
nitrate (fig. 5.10), having 12 methyl groups in total, is of the
same order as that of tetrapropylammonium nitrate, which has also
12 methyl groups, as long as pAg < 8. However, at more negative
potentials the two behaviours differ largely. For hexamethonium ni-
trate a c.i.p. is absent. This is likely due to the presence of two
positive charges in the adsorbate, giving rise to a stronger Cou-
lombic contribution than in the case of tetrapropylammonium ions.

7.4   CALCULATION OF ADSORPTION FROM CHARGE-POTENTIAL DATA

In principle, the adsorption of an organic compound can be
calculated from charge-potential curves according to eq. 2.39.
Before carrying out these computations we must realize that the
primary data as given in chapter 5 are measured at fixed initial
concentrations of the adsorbate and not at constant equilibrium
concentrations. Hence, in order to apply eq. 2.39, the data at
fixed initial concentrations have to be transformed to the same
at fixed equilibrium concentrations using adsorption data.
The transformation can be performed along two different
routes dependent on the source of the adsorption data.
(i) If adsorption data at different pAg values are available
from depletion measurements, the initial concentrations can be
directly transformed to equilibrium concentrations after several
interpolations of the titration and adsorption data. This proce-
dure will be followed for the adsorption of tetrabutylammonium
ions. The results are given in section 7.6.
(ii) If no direct adsorption data are available, a first guess
of the adsorption can be obtained by application of (2.39) to the
uncorrected charge-potential data using extrapolation of the σ-pAg
curves to complete desorption. The equilibrium concentrations are
then obtained by using an iteration procedure. This method is ap-
plied to the adsorption of tetrapropylammonium ions and the re-
sults are given in section 7.5.

Calculations of the adsorption according to Gibbs' law have
been performed with the central computer (DEC 10) using IMSL sub-
routines (International Mathematical and Statistical Libraries, Inc.,
Houston, USA) in a FORTRAN programme. The programme (ISOPOL.FOR)

143

is given schematically in fig. 7.1. The programme can accept data
according to the routes (i) and (ii) as described above.
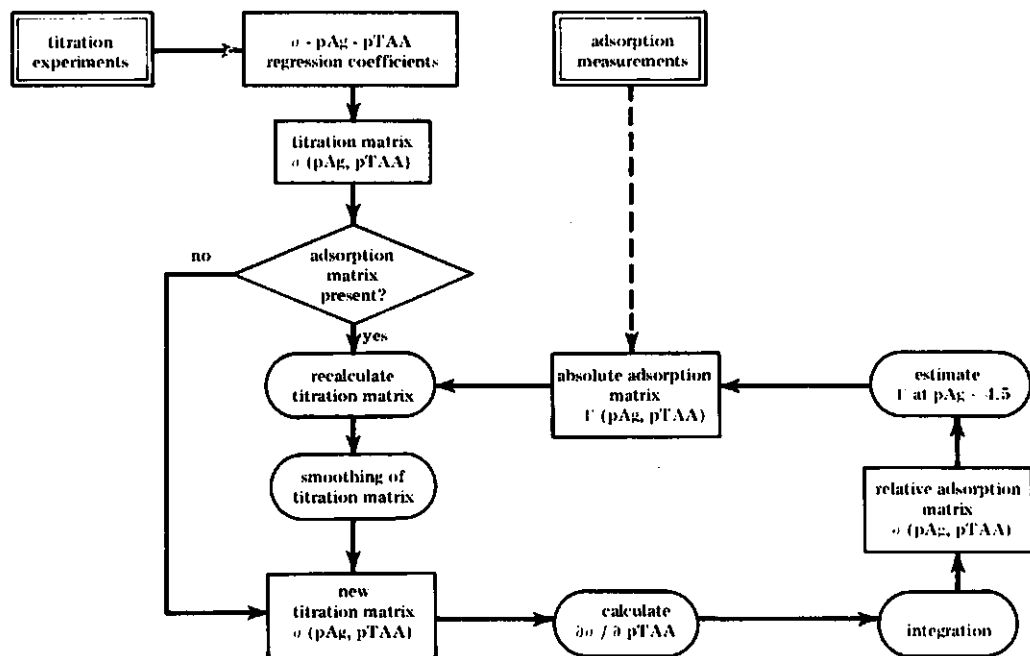
Fig. 7.1   Calculation of adsorption from titration. Flow-chart of
          programme ISOPOL.FOR

The explanation of the flow-chart of the computer programme
(fig. 7.1) will be given below. Titration data are in our case
available as polynomial regression coefficients. These regression
coefficients are used to calculate a matrix σ(pAg, pTAA) of surface
charges as a function of pAg and pTAA using interpolation pro-
cedures based on spline mathematics. The σ values in the matrix
are given relative to the initial TAA$^+$ concentration and can be
recalculated to the corresponding values at equilibrium concen-
trations. A new σ matrix is then obtained at the original set
of pAg and pTAA values by interpolation and smoothing of the
recalculated results. Either from the primary σ matrix (first
loop in route(ii)) or from the recalculated matrix, a matrix
of derivatives $(\partial\sigma/\partial pTAA)_{pAg, T}$ is calculated. The matrix of
derivatives can be integrated from pAg = 4.5 to any other pAg
using (2.39). In this way, adsorption values relative to the
adsorption at pAg = 4.5 are obtained. If the adsorption at

144

pAg = 4.5 can be estimated by other arguments, absolute adsorption
values can then be calculated at any pAg. In applying route (ii)
several loops (iterations) can be performed to obtain equilibrium
concentrations within the desired accuracy.

7.5   INFERENCE OF THE ADSORPTION OF TPrA$^+$ IONS FROM DOUBLE LAYER
         DATA AND COMPARISON WITH DIRECT MEASUREMENTS

Charge-potential curves for tetrapropylammonium ions on AgI
can be rather unambigously extrapolated until the curves merge.
Thus, absolute adsorption values can be evaluated from these data
only according to the iteration procedure described in the previ-
ous section. It appeared that adsorptions calculated from titration
curves at initial concentrations differed only by about 1 to 2%
from the equilibrium values. Specific surface areas obtained by the
capitance method (or by negative adsorption) are used throughout in
this section. The results given below are obtained from the titra-
tion TPrA2 (Table 5-3).

A comparison of the adsorption obtained from titration at
pAg = 11.5 and the directly measured adsorption values at pI = 4
(pAg $\cong$ 12.2) is given in fig. 7.2. The difference between the two
curves is about 20%. It is reasonable to consider this discrepancy
to be within experimental error by realizing that it includes
differences in the effective surface area of the suspensions used
and that errors in adsorption depend linearly on the errors in the
derivative $\partial\sigma/\partial$TPrA, which may be substantial.

The result obtained is very important from a fundamental
point of view because it is an experimental verification of the
applicability of Gibbs' law to the underlying system.

In fig. 7.3 the adsorption of TPrA$^+$ ions is given as a func-
tion of the pAg at different pTPrA values. These curves resemble
the corresponding curves for n-butanol (1) and ethylene glycol (3),
albeit that the adsorption maximum at TPrA$^+$ is much more to the
negative side, so that the parabolic behaviour of the curves is
less pronounced. The presentation of the curves is different. For
n-butanol and ethylene glycol the curves are given relative to an
adsorption maximum, whereas the TPrA data are absolute. The shapes
of the desorption curves of n-butanol are markedly dependent on
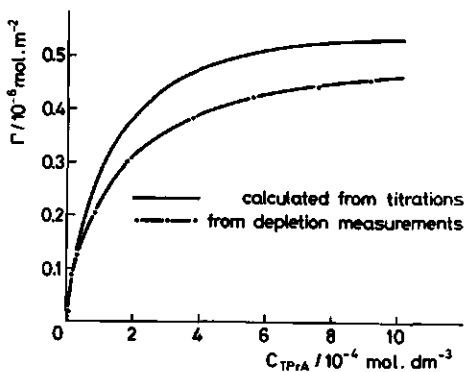
Fig. 7.2 Comparison of Gibbs' and direct adsorptions for TPrA$^+$ ions at pAg = 11.5
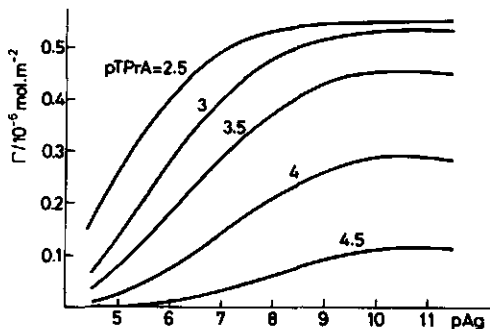
Fig. 7.3 The electrical dependence of the adsorption of TPrA$^+$ ions on AgI.

the alcohol concentration in solution. For low concentrations the (absolute) slope of these desorption curves increases with concentration up to a maximum beyond which it decreases again. This phenomenon occurs also for TPrA$^+$ ions. The explanation is that the decrease in adsorption from the plateau value is relatively slower than at lower adsorption values. Stated otherwise, a small shift in either pTPrA or pAg has a relatively smaller effect on the amount adsorbed if the monolayer coverage is reached.

Quantitatively, the results obtained for TPrA$^+$ ions differ significantly from those reported for neutral compounds (1,3). For instance, for n-butanol the maximum desorption between pAg 6.5 and 11 amounts to ca. 0.8×10^{-6} mol/m^2. Assuming for the complete monolayer coverage a value of about 4×10^{-6} mol/m^2, the maximum desorption in the pAg range given is 20% of the monolayer coverage. For ethylene glycol only 5% has been calculated (3). From these data it would follow that the desorption of TPrA$^+$ ions over a corresponding pAg difference from the c.i.p. is *much* higher than that for neutral compounds. This leads us to the conclusion that the Coulombic repulsion plays an important role in the desorption of the organic compound. However, the quantification of the difference between TPrA$^+$ and n-butanol deserves further attention.

146

The assumed adsorption at saturation for n-butanol has never been verified experimentally. As the specific surface area calculated from the monolayer coverage of, say, TBuA$^+$ ions assuming a realistic molecular cross section differs by about a factor of 3 with the capacitance (or negative adsorption) area (section 5.9), we realize that the real monolayer coverage for n-butanol is very uncertain. More specifically, it is not known if perhaps always some water molecules are present between the molecules of the organic compound at saturation coverage. If we would assume that for n-butanol adsorption also the factor 3 must be taken into account, the desorption between pAg 6.5 and 11 would amount to 60%. Hence, with this assumption the desorption would be considerable. There are some additional arguments which support this higher desorption.

(i) The charge-potential curves with n-butanol at AgI for higher alcohol concentration tend to converge at the negatively charged surface (1).

(ii) For the mercury-electrolyte interface complete desorption occurs at a potential of about 700 mV to the negative side of the adsorption maximum. The potential range covered from the adsorption maximum to pAg = 11.5 amounts to 280 mV. Ignoring for this purpose the difference in charging mechanism, we would for n-butanol on AgI expect a considerable desorption in the potential range covered and a decrease in adsorption between the c.i.p. and pAg 11 which is higher than 20% and being probably between 40 and 60% of monolayer coverage.

(iii) The fact that TPrA$^+$ adsorption has a maximum as a function of pAg is an indication that the dipolar water contribution to the adsorption free energy is able to compensate the Coulombic contribution. Neglecting for this purpose the dipolar contribution of alcohol dipoles, it is reasonable to suppose that complete desorption of butanol molecules is reached if we extend the experimentally accessible potential range by a factor of about 2. Finally, it must be realized that the desorption of 20% is relative to the saturation value. The relative decrease in adsorption with respect to that at the c.i.p. is always higher. It follows that it is very likely that the desorption with respect to the c.i.p. is also appreciable in the case of n-butanol.
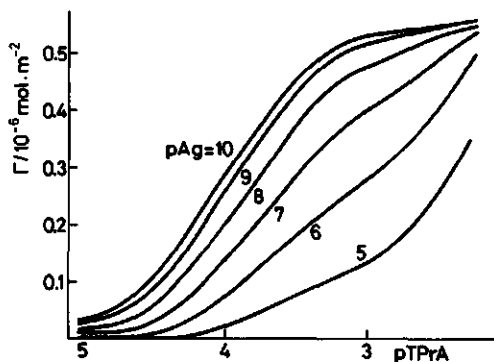
Fig. 7.4 Adsorption of TPrA$^+$ ions on AgI.
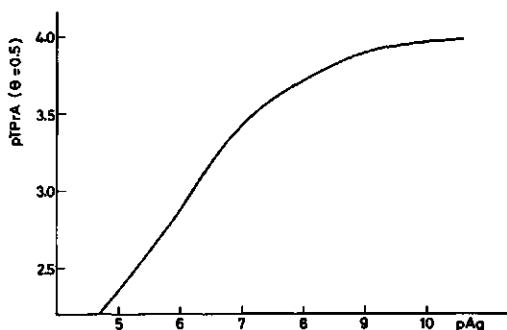
Fig. 7.5 Dependence of pTPrA ($\theta = 0.5$) on the pAg.

The adsorption results for TPrA$^+$ ions on AgI are plotted semi-logarithmically in fig. 7.4 in order to examine if congruency in potential is present. There exists a close correspondence between fig. 6.7 and fig. 7.4. It follows that the mechanism of the adsorption of tetrapropyl- and tetrabutylammonium ions is likely the same. The adsorption of tetrapropylammonium ions is not congruent in the potential and probably, as follows from the correspondence with TBuA$^+$, not congruent in the charge either. The shift in pTPrA at $\theta = 0.5$, which would be proportional to ΔG^0_{ads} in the case of potential congruency, has been given in fig. 7.5. The parabolic or, rather bell-shaped curve indicates to a significant dipolar contribution to the adsorption free energy, the Coulombic contribution being proportional to the surface potential (or pAg).

7.6 INFERENCE OF THE ADSORPTION OF TBuA$^+$ IONS FROM DOUBLE LAYER DATA AND COMPARISON WITH DIRECT MEASUREMENTS

The extent of desorption with respect to the adsorption maximum for TBuA$^+$ on AgI at pAg = 4.5 is less than that for TPrA$^+$. Consequently, extrapolation of charge-potential curves in order to find the point of complete merging (that is: to the point of full desorption) is too inaccurate. On the other hand, a complete set of adsorption data as a function of pTBuA and pAg has been obtained

148

from depletion measurements, so that comparison between Gibbs'
and direct adsorptions is still possible.

All calculations and comparisons are performed with titration
TBuAl (Table 5-4) and adsorption isotherms TBuAl-TBuAll (Table 5-1).
Smoothing and interpolation of adsorption isotherms are performed
with IMSL subroutines. The result of this procedure has been given
in section 6.3.

The affinity of TBuA$^+$ ions for AgI is higher than that of
TPrA$^+$ ions. As a consequence, equilibrium concentrations are lower
and the concentration changes in the titration vessel are larger.
This is illustrated in fig. 7.6. These shifts have been calculated
with the computer programme described in section 7.4. It follows
that recalculation of the titration data is necessary.
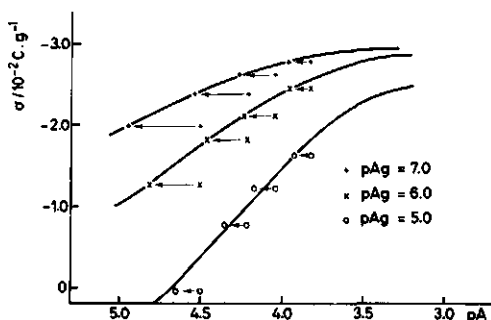
Fig. 7.6 Shift of initial to final concentration of TBA$^+$ in the
          titration procedure.

Adsorptions relative to the same at pAg = 4.5 have been cal-
culated from titration curves and compared with the direct adsorp-
tion data given in fig. 6.4. By way of example, we plot the differ-
ences in adsorption between pAg = 11.0 and pAg = 4.5 in fig. 7.7
and those between pAg = 9 and pAg = 6 in fig. 7.8. The most reli-
able concentration traject is between the two vertical dashed
lines. It appears that in this range the differences vary from
0 to 30% for both figs. 7.7 and 7.8. The maximum difference is
in the same order (and in the same direction) as that found for
TPrA$^+$ ions. In view of the potential errors in the experimental
results, it is not allowed to draw physical conclusions from the
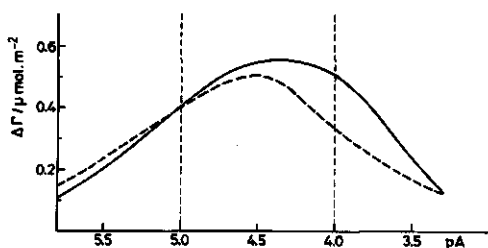
Fig. 7.7 Adsorption of tetrabutyl-
ammonium ions on silver iodide. Com-
parison of analytically determined
adsorption (——direct measurements)
with adsorption evaluated from sur-
face charge-pAg curves (---Gibbs-
adsorption) c_{KNO_3} = 0.1 M.

$\Delta\Gamma = \Gamma_{TBuA}(pAg = 11) - \Gamma_{TBuA}(pAg = 4.5)$.
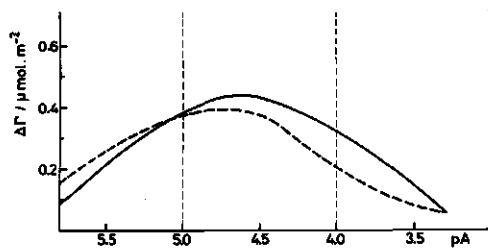
Fig. 7.8 Adsorption of tetrabutyl-
ammonium ions on silver iodide. Com-
parison of analytically determined
adsorption (——direct measurements)
with adsorption evaluated from sur-
face charge-pAg curves (---Gibbs-
adsorption) c_{KNO_3} = 0.1 M.

$\Delta\Gamma = \Gamma_{TBuA}(pAg = 9) - \Gamma_{TBuA}(pAg = 5)$.

differences. If we realize that the direct adsorption values and
those from integration are obtained by completely different pro-
cedures, the correspondence between the two sets of data may be
considered as solid evidence for the applicability of chemical
thermodynamics to the underlying system.

7.7 A SEMI-QUANTITATIVE ANALYSIS OF THE COMMON INTERSECTION POINT FOR TAA$^+$ IONS

In the previous chapter a model was developed to describe the
presence and the position of the common intersection point. This
led ultimately to an equation for σ_m (6.23). In the derivation a
number of more or less drastic approximations have been made. Never-
theless, it may be illustrative to apply this equation to our data
in some more detail than has been done in the previous chapter.
     Information on a number of molecular properties can be ob-
tained by comparing the positions of c.i.p.'s for different adsor-
bates and a constant medium, or for different media and the same
adsorbate according to the parameters of eq. 6.23. Here we will
limit ourselves to the trend in the position of the common inter-
section points for a homologous series of tetraalkylammonium ions.

150

The common intersection points of the TAA$^+$ ions are summarized in table 7-1. These data are taken from chapter 5. The c.i.p. shifts to more positive potentials, or to lower σ values, with increasing radius of the ions (r_{TAA+}). In order to formulate the relationship between σ_m and r_{TAA+} in terms of our model eq. 6.23 can be rewritten as

$$\frac{\chi_1^0 - \chi_2^0 - F\Gamma_{max}/\varepsilon\varepsilon_0\kappa}{\sigma_m} = \frac{\chi_1^0}{\sigma_R} - \frac{\delta^0}{\varepsilon_s^0\varepsilon_0} + \frac{\delta^c}{\varepsilon_s^c\varepsilon_0} \tag{7.1}$$

or

$$\frac{1}{\sigma_m} = k_1 + k_2 r_{TAA+} \tag{7.2}$$

if it can be assumed that $\delta^c = r_{TAA+} + r_{I-}$. The parameters are defined in chapter 6. In fig. 7.9 $1/\sigma_m$ has been plotted against r_{TAA+}. Considering the inaccuracy of the c.i.p.'s a satisfactory linear behaviour exists. This may be considered as an indication that the theory is basically correct as far as the thickness of the Stern layer is concerned.

From the experimental values of k_1 and k_2 two unknown parameters can be solved. We consider σ_R and ε_s^c as the unknowns and assign definite values to the other parameters. It follows from (7.1) and (7.2) that

$$\varepsilon_s^c = \frac{1}{\varepsilon_0 \cdot (k_2 . \alpha)} \tag{7.3}$$

$$\frac{\chi_1^0}{\sigma_R} = (k_1 . \alpha) + \frac{\delta^0}{\varepsilon_s^0\varepsilon_0} - \frac{r_{I-}}{\varepsilon_s^c\varepsilon_0} \tag{7.4}$$

where

$$\alpha = \chi_1^0 - \chi_2^0 - F\Gamma_{max}/\varepsilon_0\varepsilon\kappa \tag{7.5}$$

The computations of the σ_R and ε_s^c values are given in table 7.2. The estimated values for the various parameters are mainly taken from chapter 3. The value of Γ_{max} is taken from chapter 5. The choice of this parameter is not critical.

The values obtained for ε_s^c appear quite reliable, although the value obtained from the solid curve seems most appropriate as it corresponds best with the values usually taken for the dielectric constant of the Stern layer in the presence of an organic compound.
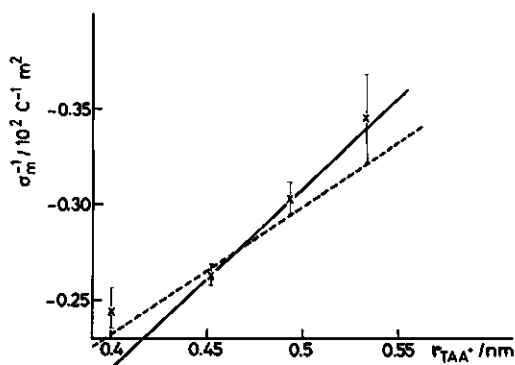
Fig. 7.9 Linearization of eq. 6.23 for a homologous series of TAA[+] ions.

The reliability of the σ_R values is low. The main reason follows from the values for the different terms in eq. 7.4. Specifically, the value for σ_R derived from the solid curve (-.106) is much higher than σ_R (ϕ(dip)=0) obtained from the theory in chapter 3 (-0.043). This theoretical value can be obtained by substituting r_{I-} = 0.07 nm. This may be realistic, as TAA[+] ions can also adsorb to some extent *between* the adsorbed p.d. ions.

Table 7-1 Common intersection points of charge-potential curves of AgI for a homologous series of tetraalkylammonium ions

	TEtA[+]	TPrA[+]	TBuA[+]	TAmA[+]
pAg_m	11.5 ± 0.3	10.7 ± 0.15	9.75 ± 0.20	9.1 ± 0.3
σ_m (10^{-2} C.m^{-2})	- 4.1 ± 0.2	- 3.80 ± 0.05	-3.3 ± 0.1	-2.9 ± 0.2
r_{TAA+} (nm)*	0.400	0.452	0.494	ca. 0.54

---

*   For TEtA[+], TPrA[+] and TBuA[+] the crystal radius has been given according to ref. 8. The value for TAmA[+] has been obtained by extrapolation.

Table 7-2 Derivation of σ_R and ε_s^c from fig. 7.9. The parameters were chosen as follows:

$$\chi_1^0 = -0.2 \text{ V} \qquad\qquad \kappa = 1 \text{ nm}^{-1}$$
$$\chi_2^0 = 0 \text{ V} \qquad\qquad \varepsilon = 78$$
$$\Gamma_{max} = 0.83 \times 10^{-6} \text{mol/m}^2 \qquad\qquad \varepsilon_0 = 8.85 \times 10^{-12} \text{ CV}^{-1}\text{m}^{-1}$$

parameter/term	dimension	solid line	dashed line
k_1	$C^{-1}m^{-2}$	15.8	3.7
k_2	$C^{-1}m$	-9.3×10^{10}	-6.7×10^{10}
$k_1\alpha$	$C^{-1}m^2.V$	-3.32	-0.78
$k_2\alpha$	$C^{-1}m.V$	1.95×10^{10}	1.41×10^{10}
ε_s^c	-	5.8	8.0
$\delta^0/\varepsilon_s^c\varepsilon_0$	$C^{-1}m^2 \text{ V}$	9.41	9.41
$r_{I^-}/\varepsilon_s^c\varepsilon_0$	$C^{-1}m^2 \text{ V}$	4.20	3.05
χ_1^0/σ_R	$C^{-1}m^2 \text{ V}$	1.89	5.58
σ_R	$10^{-2}C.m^{-2}$	-10.6	-3.6

Thus, within experimental error, it is possible to explain quanti-
tatively the shift of the c.i.p. by the theory given in the previous
chapter.

7.8 COMPARISON OF THE DOUBLE LAYER OF MERCURY AND SILVER IODIDE IN THE PRESENCE OF n-BUTANOL, TPrA$^+$, AND TBuA$^+$

The adsorption of tetraalkylammonium ions at the mercury-elec-
trolyte interface has been studied by many workers. A survey has
been given in section 1.6. In order to make reliable quantitative
comparisons between the mercury and the silver iodide system, the
medium in which the experiments are performed must be similar. Kůta
and Smoler (4) have obtained charge-potential curves on Hg for
tetrapropyl- and tetrabutylammonium ions in a medium of 0.1 M HClO$_4$.
If we assume that both HClO$_4$ and KNO$_3$ can be treated as an inert
1:1 electrolyte, quantitative comparison between Kůta et al. and
our data is allowed.

Using the Lippmann equation, Kůta and Smoler (4) obtained
charge-potential curves from electrocapillary curves.

153

In order to avoid co-adsorption of iodide ions, as occurred in the work of Devanathan and Fernando (5), they conducted their measurements of the perchlorate salts of TAA-ions in a medium of either 0.1 M HClO$_4$ or 0.05 M H$_2$SO$_4$. Perchlorate anions adsorb also specifically at the mercury-electrolyte solution interface, although to a smaller extent than halides. At very positive potentials the adsorption of the surface-active cations increases due to this co-adsorption of perchlorate. This follows from a comparison with the corresponding sulphates, which are relatively inactive.

In table 7-3 several properties of the mercury- and silver iodide-electrolyte interface as obtained from Kûta and Smoler (4) and from the present investigations respectively are compared. Comparative data for n-butanol (1,2) are also included in the table. A strong correlation is found between the positions of the c.i.p.'s of n-butanol and TAA$^+$ ions on AgI and Hg. Considering the widely differing absolute values, the near-constancy of the ratio is very striking indeed. The ratio calculated for the potential is in the order of unity. For the surface charge a ratio of 2 is calculated. Assuming that this is not due to specific surface area effects, it could be a consequence of the localized behaviour of charges on AgI as contrasted to the smeared-out behaviour of charges on Hg. The differential capacitance at the p.z.c. in 10^{-1} M KNO$_3$ differs by a factor of 1.4. This must be due to different properties of the Stern layer or, more specifically, the ratio ε_s^0/δ^0 on Hg is about 40% in excess of that on AgI. Finally, the monolayer coverage differs by a factor of 3-4. In the next section, a model will be postulated explaining that ratio in terms of the difference in mobility of the adsorbate on AgI and Hg respectively. However, it may not be completely excluded that a specific surface area for AgI different from the "capacitance" area used would be more appropriate. Equalization of the c.i.p.'s for Hg and AgI would remove the major part of the difference of monolayer between the two systems, but in that case the capacitances of AgI and Hg at low salt concentrations would differ. Although, it is believed that the data given are a good starting point for a more definite solution of the specific surface area problem, more specific experiments are needed before final conclusions can be drawn.

154

Tabel 7-3 Comparison of some electrosorption properties of n-butanol, TPA$^+$ and TBuA$^+$ on silver iodide and mercury

Physical property	n-butanol			TPA$^+$			TBA$^+$		
	Hg(2)*	AgI(1)	ratio	Hg(4)	AgI	ratio	Hg(4)	AgI	ratio
Common intersection point									
- Surface charge (in 10^{-2} C/m²)	2.0	1.05	1.9	-8.21	-3.8	2.2	-6.73	-3.3	2.0
- potential relative to pzc (θ=0)(in Volts)	-0.073	-0.070	1.04	-0.370	-0.293	1.26	-0.280	-0.237	1.18
Differential capacitance									
- in p.z.c. at θ=0	0.243	0.130(?)	-	.254	.176	1.4	.254	.176	1.4
Adsorption isotherms:									
- Monolayer coverage (μmol/m²)	-	-	-	2.4	0.5	(4.8)	2.2	0.75	2.9
- Potential relative to cip to obtain complete desorption (in Volts)	ca..700	-	-	ca..800	ca..400	-	-	-	-

* The number added to Hg and AgI indicate the reference

Recently, Hamdi et al. (6) studied the adsorption of tetra-alkylammonium halides on the mercury-electrolyte interface. They concluded that TAA^+ ions in excess of those required to neutralize the surface are adsorbed as neutral entities. However, from the experimental results for the AgI-electrolyte interface it follows definitely that TAA^+ ions are mainly adsorbed in the inner layer as single ions. Before comparing these results, one must realize that Hamdi et al. used halides, whereas in our study nitrate is the main anion. If we compare the potential ranges to obtain complete desorption relative to the c.i.p. of TAA^+ ions for mercury (4) and AgI, we find a ratio of 2. Hence, it appears that the desorption due to an increasing positive potential is weaker for Hg (in the presence of ClO_4^-) than for AgI (in the presence of NO_3^-). This fact is in agreement with the apparent differences in ion pairing at the AgI and Hg surface. Moreover, it seems consistent that the potential range for TAA^+ ions on mercury is not very different from that for n-butanol, indicating that the charge of the adsorbate is not very important. It is not clear if the differences between the Hg and AgI system are due to different properties of the surface itself (e.g. charging mechanisms) or to the different properties of the anions, although in our opinion the former is preferred.

7.9   SOME ADDITIONAL REMARKS ON THE SURFACE AREA OF AgI

The specific surface area of AgI has been extensively studied by van den Hul (6). Recently, Koopal (7) has discussed in some detail the problems about the difference existing in the specific surface areas as derived from titration and adsorption measurements respectively. The difference between the two methods amounts to a factor of 3 to 3.5. Koopal concluded that in electrochemical studies the capacitance area is acceptable, whereas for (polymer) adsorption the area obtained by adsorption methods is preferred. Only in this way different kinds of measurement were comparable. From a scientific point of view this conclusion is unsatisfactory, as no physical explanation is offered for this difference. On the basis of the present results new arguments can now be added to this discussion.

They are summarized below.

(i) The adsorption if expressed per gr. of AgI calculated from charge-potential data according to Gibbs' law is within experimental error identical to the adsorption values obtained from depletion measurements. This result implies that it is not allowed to use different surface areas for titration and adsorption experiments.

(ii) If the capacitance area is used for AgI, the adsorption of TAA$^+$ ions on mercury is about a factor of 3 higher than on AgI. However, if the BET-area would be used for AgI (6), the TAA$^+$ ion adsorption would be the same on both surfaces, but then the double layer capacitance at the p.z.c. in 10^{-3} M KNO$_3$ would exceed the diffuse D.L. capacitance by a factor of 3.

As the capacitance area of AgI corresponds with the area obtained by negative adsorption (6), it seems more appropriate to choose the capacitance area of AgI as the physically realistic surface area. However, in that case we have to explain the difference in monolayer coverage between AgI and mercury and we must find the physical reason for the low plateau value on AgI.

As far as the monolayer coverage concerns, the main difference between AgI and Hg is the degree of localization of the adsorbate. Mercury is a *liquid* metal and the adsorption can be assumed to be non-localized (mobile adsorption). Silver iodide, on the other hand, is a crystalline material, and a higher degree of localization is very likely. This difference in localization may be a potential cause of the difference in monolayer coverage.

Let us first consider the concept of localization. Localized adsorption, as follows from the Langmuir theory, is related to a definite number of adsorption sites. For the AgI-electrolyte interface it is unlikely that the surface has only a *limited* number of widely spaced adsorption sites. The result that molecules with a different molecular area (including BET) give (almost) the same surface area in adsorption experiments, pleads also against this assumption. For convenience, the site area is usually set equal to the molecular area of the adsorbed molecule. However, it is not unlikely that the effective number of sites (which is determined by the surface structure of the crystal) is much higher than the number of most adsorbed organic molecules. Let us assume that the surface of silver iodide contains a very large number of adsorption

sites and that the adsorbate is fully localized. Stated otherwise, if a molecule collides with the (empty) surface it will stick to the crystal without lateral movement. The question is now: do these adsorbed molecules form a saturated monolayer?

The Langmuir equation can be derived either by a kinetic or by a statistical reasoning. To analyse the consequences of the alternative site model proposed, a kinetic reasoning will be followed, although by statistical means the same result must be obtained.

In our model the rate of desorption is proportional to the number of molecules adsorbed, completely analogous to the Langmuir reasoning. However, in our model the adsorption is not equal to the unoccupied surface area, but is less than that. This follows from the consideration that a molecule can only adsorb between two other molecules if their centres are a distance 4r apart. This means that if the centres of two molecules are less than a distance 4r apart the area is not available for adsorption at a time t (fig. 7.10).
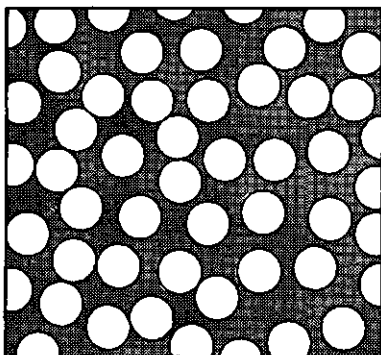
Fig. 7.10 Saturated monolayer for a model with an infinite number of sites and complete localization

In the unlikely case that at monolayer coverage *all* molecules are a distance of almost 4r apart, this would decrease the available surface area by a factor of about 4. However, on the average there will be a distribution of distances probably leading to a factor between 2 and 3. In principle this factor could be calculated from a more advanced statistical model.

It may be concluded that the difference in the degree of localization between a solid-liquid and a liquid-liquid interface is a potential factor in accounting for a difference in effective mole-

cular area of a factor 3. This will apply especially if no strong
lateral attractive interaction is present, as is the case for
tetraalkylammonium ions.

However, it must be realized that the explanation for the low
saturation coverage is tentative and that it is based on strong
localization without lateral movement.

7.10 CONCLUSIONS

The electrosorption of tetraalkylammonium ions is a process
to which equilibrium interfacial thermodynamics can be applied. The
model developed for the c.i.p. is applicable with reasonable values
for the different parameters.

Several properties of the AgI-solution interface in the pres-
ence of neutral adsorbates can be better understood from the re-
sults in the presence of TAA^+ ions.

7.11 SUMMARY

In this chapter electrosorption properties of tetraalkylam-
monium ions and some other quaternary ammonium ions are discussed,
especially in relation to the experimental charge potential curves.

The adsorptions of $TPrA^+$ and $TBuA^+$ were calculated from charge-
potential curves and compared with the outcome of direct measure-
ments. This comparison proved within experimental error that equi-
librium interfacial thermodynamics is applicable to the system used.

A quantitative analysis of the trend of the c.i.p.'s of a
homologous series of TAA^+ ions resulted in an estimate of the value
for the dielectric constant of the Stern layer in the presence of
TAA^+ ions, which seems quite reasonable. From the value calculated
for σ_A it followed that TAA^+ ions probably can approach the sur-
face closer than the sum of the TAA^+ and I^- radii.

An adsorption model was introduced to explain the difference
in monolayer coverage between AgI and Hg from the difference in
lateral mobility for the adsorbate in the two systems.

7.12 REFERENCES

1. B.H. Bijsterbosch and J. Lyklema, J. Colloid Sci. *20* 665 (1965)

2. E. Blomgren, J.O'M. Bockris and C. Jesch, J. Phys. Chem. *65* 2000 (1965)

3. J.N. de Wit and J. Lyklema, J. Electroanal. Chem. *41* 259 (1973)

4. J. Kůta and I. Smoler, Collection Czechoslov. Chem. Commun. *40* 225 (1975)

5. M. Hamdi, R. Bennes, D. Schuhmann and P. Vanel, J. Electroanal. Chem. *108* 255 (1980)

6. H.J. van den Hul and J. Lyklema, J. Colloid Interface Sci. *23* 500 (1967)

7. L.K. Koopal, Thesis, Agricultural University, Wageningen, 1978

8. W-Y Wen, in Water and aqueous solutions (R.A. Horne, ed.), Wiley-Interscience, London, 1972, p.622.

SUMMARY

The object of the present investigations was to study the effect of the adsorption of *charged* organic ions on electrically charged, solid-liquid interfaces. To that end, symmetrical quaternary ammonium ions were adsorbed on a silver iodide-electrolyte interface at various surface charges. The electrochemistry of this model interface is well developed in comparison with other solid-liquid interfaces and it is very suited for fundamental electrosorption studies. Special attention was paid to some *general* problems in the field of electrosorption:

- The effect of solvent- and other dipoles on interfacial properties.
- The presence of a maximum as a function of the surface potential in the adsorption of organic compounds.
- The applicability of equilibrium interfacial thermodynamics.
- The discrepancy between the specific surface areas obtained according to different methods.

It appears that the study of the adsorption of tetraalkylammonium (TAA) ions contributes to the solution of some of these general problems.

Electrosorption of TAA^+ ions has been investigated in 0.1 M KNO_3 in order to maintain a constant ionic strength and to suppress diffuse double layer effects. The electrical properties are obtained from experimental charge-potential curves and from measurements of the electrophoretic mobility. Adsorption of TAA^+ ions at various values of the surface potential has been measured analytically.

This thesis can be subdivided into three more or less separate parts: the theoretical chapters 2 and 3, the automation chapter 4, and the experimental chapters 5, 6 and 7 on the electrosorption of TAA^+ ions.

Interfacial thermodynamics has been elaborated for a system containing strongly adsorbing organic ions. Ionic components have been introduced into Gibbs' adsorption equation, and the solid-liquid boundary was taken as Gibbs' dividing plane. Interfacial excess quantities were related to the temperature, concentrations

of the potential determining ions, concentration of the organic compound, and the ionic strength. A discussion has been given on the definition of the surface charge. It was shown that a consistent thermodynamical definition of the surface charge eliminates non-thermodynamic terms in the equations for the temperature dependency of the surface charge. The adsorption isotherm for a binary solution was derived from a quasi-thermodynamic approach. It was discussed how electrical effects can be introduced in the adsorption isotherm. The occurrence of congruency in the potential or the charge facilitates the evaluation of the adsorption Gibbs energy.

A new approach of the contribution of *dipolar-* or χ potentials to the properties of a solid-electrolyte interface in the absence of an organic adsorbate has been described. It was assumed that dipolar potentials at the solid-liquid boundary arise as a consequence of local properties of the interface (hydration) and not from the action of a homogeneous electrical field. The hydration of solid particles is thus treated as a patchwise phenomenon, in which the orientation of water dipoles varies in a patchwise fashion along the surface. The idea is applied to the AgI system, where besides the neutral surface, Ag^+ patches and I^- patches are distinguished. A first-order elaboration is offered including an analysis of the relation between overall macroscopic quantities and local properties. It was assumed that the large difference in hydration free energies of Ag^+ and I^- leads to a difference in the contribution of the adsorbed Ag^+ and I^- to the dipolar potential across the interface. The model offers an interpretation of two characteristics of double layers on silver iodide: the asymmetry of its p.z.c. and the conspicuous capacitance rise on the positive side, and it may serve as a starting point for a better description of the typical differences between the double layers on AgI and Hg.

The surface charge of a silver iodide suspension can be determined as a function of the surface potential (or pAg) by potentiometric titration with Ag^+ and I^- ions. This determination is very important, because the charge-potential relation can be considered as a "finger-print" in electrosorption studies. However, the manual procedure is very time-consuming. Therefore, the procedure has been *automatized* with a PDP11-computer and a CAMAC data acquisition sys-

tem. This laboratory automation system enables the measurement of one complete titration curve independent of human observation. The reliability of the system appears to be excellent.

The major part of the experimental study was concerned with the *electrosorption* of tetrapropyl-, tetrabutyl-, and tetraamylammonium ions on AgI. The results enabled the development of a self-consistent picture of the adsorption mechanism.

Charge-potential curves in the presence of TAA^+ ions are rather similar to those obtained for e.g. n-butanol, except that the curves tend to merge at the positive side, implying complete desorption of TAA^+ at increasing positive potentials. The most noteworthy common feature is the occurrence of a more or less well-defined common intersection point. According to interfacial thermodynamics this point corresponds to an adsorption maximum as a function of the surface potential. This result may appear surprising. From the coulombic interaction between a positive ion and an increasingly negative surface we would expect an increase in affinity. The observation that, after surpassing a certain surface potential, the affinity *decreases* is an indication that the dipolar contribution due to the energy of displacement of water molecules is able to overcompensate even the coulombic interaction.

The desorption at increasing positive potentials enables a quantitative test of Gibbs' law by comparing calculated adsorption values with those measured analytically. It has been shown that both for tetrapropyl- and tetrabutylammonium ions the agreement between calculated and direct values is within about 20%. This is probably within experimental error. This basically is a very important result, because it is the first quantitative verification of the applicability of Gibbs' law to the AgI system. It proves that adsorption of both potential determining ions and tetraalkylammonium ions is reversible and obeys the thermodynamic laws.

Tetraalkylammonium nitrates are strong electrolytes. The presence of an adsorption maximum could suggest that TAA^+ ions are (mainly) adsorbed as neutral entities, as was suggested for tetraalkylammonium halides on mercury. However, from measurements of the electrophoretic mobility of silver iodide sols it follows, that the major part of the ions are adsorbed as non-paired ions.

It appears that the adsorption Gibbs energy of tetraalkylammonium ions consists of three contributions of an approximately comparable order. The dipolar and the coulombic contributions were already mentioned above. Hydrophobic bonding is the third contribution, the operationality of which can be inferred from comparison of the adsorption of the homologous series of TAA^+ ions and the effect of an increasing number of CH_2 groups.

Analysis of the adsorption data shows that the isotherms are neither perfectly congruent in the surface charge nor in the surface potential. However, from interpretation according to the Frumkin, Fowler-Guggenheim isotherm equation congruency in the charge seems more probable because only in that case a positive interaction parameter is found. Congruency in charge implies that the field strength at the adsorption site is more relevant than the potential.

Significant progress has been made in the interpretation of the presence and the position of the adsorption maximum (or common intersection point). An equation for the position of the common intersection point has been derived both for the case of congruency in charge and in potential taking into account the effect of the adsorption of an organic ion on the various contributions to the total Galvani potential. According to the equation derived, the shift of the common intersection point with increasing length of the alkyl chains of the TAA^+ ions is correctly accounted for if the thickness of the Stern layer and the radius of the tetraalkylammonium ion are identical.

Several properties of the silver iodide-electrolyte interface were compared with the mercury interface in the presence of adsorbed n-butanol, tetrapropylammonium and tetrabutylammonium ions. It appears that the potential of the common intersection point is about the same for both systems with the three adsorbates, whereas the charge of that point is a factor of 2 higher for mercury. The monolayer coverage for $TBuA^+$ is about a factor of 3 higher for mercury. These results are not completely understood but may be related to the difference in the natures of the surface charges for both systems or to the problems in choosing a proper specific surface area for silver iodide.

The specific surface area as determined with the adsorption of tetraalkylammonium ions or dyes differs by about a factor of 3 to 3.5 from the area obtained by comparing double layer capacitances of AgI and Hg at low salt concentrations. The difference must either be due to a failure in the comparison of double layer capacitances of both surfaces or to a different behaviour in the adsorption of the organic adsorbate. As by negative adsorption also the capacitance area is obtained, the latter factor was chosen. An adsorption model was introduced to explain the difference in monolayer coverage between AgI and Hg in terms of differences in lateral mobility of the adsorbate.

Resuming, it can be concluded that the electrosorption of tetraalkylammonium ions on silver iodide has given new insight into some general and specific interfacial properties. Significant progress has been made in the experimental verification of Gibbs' law, in the description of the adsorption maximum, and in the behaviour of water dipoles on the surface.

LIST OF SYMBOLS AND ABBREVIATIONS*

a_i	activity of component i in solution (2.35)
a_i	molar area (2.74)
a_s	specific surface area (4.7)
A	interaction parameter in the FFG equation (6.12)
A_s	area of the interface (2.3)
B_i	polynomial regression coefficient (5.1)
c	electrolyte concentration in solution (3.35)
c_i	concentration of component i in solution (2.35)
c_i^α	concentration of component i in phase α (solid phase) (2.14)
c_i^β	concentration of component i in phase β (solution) (2.14)
C	differential capacitance of the double layer (2.48)
d	thickness of the Stern layer (3.2)
E_{Ag+}^o	standard potential with respect to Ag^+ of an AgI electrode (4.1)
E_{I-}^o	standard potential with respect to I^- of an AgI electrode (4.2)
E_i	potential of electrode i (4.4)
$\bar{E}_j$	averaged potential difference at the jth-measurement (Ch.4)
$\vec{E}_{ads}$	field strength at the locus of adsorption (6.5)
f_i	activity coefficient of component i in solution (2.35)
F	Faraday constant (2.24)
F	free energy of the system (2.68)
$F(pAg)$	equilibrium constant of adsorption process in the case of pAg congruence (2.91)
$G(\sigma)$	equilibrium constant of adsorption process in the case of congruence in charge (2.95)
ΔG_{ads}^0	total standard Gibbs energy of adsorption (2.87, 6.3)
ΔG_{chem}^0	chemical part of ΔG_{ads}^0 (2.87, 6.3)

---

* Relevant equations are given between brackets

167

ΔG^0_{coul}	Coulombic part of ΔG^0_{ads} (6.3)
ΔG^0_{el}	electrical part of ΔG^0_{ads} (2.87)
ΔG^0_{dip}	dipolar part of ΔG^0_{ads} (6.3)
$G^{h,L}_i$	hydration Gibbs energy of component i in solution (3.28)
$G^{h,I}_i$	hydration Gibbs energy of component i at the surface (3.28)
G^{cov}_{AgI}	covalent part of the Gibbs energies of bonding for Ag^+ and I^- (3.28)
ΔG^0_{Ag+}	standard affinity of Ag^+ ions for the AgI surface (3.28)
ΔG^0_{I-}	standard affinity of I^- ions for the AgI surface (3.29)
i	electrical current (5.3)
k_1, k_2	linearization constants (7.2)
k_{Ag+}	coefficient proportional to the net degree of orientation of H_2O at an Ag^+ patch (3.14)
k_{I-}	id. at an I^- patch
k'_i	measure for the effective patch area per adsorbed ion (3.11)
K	constant in (3.26)
K_a	equilibrium constant in adsorption process or in the Langmuir equation (2.65, 2.87)
K^{chem}_a	chemical part of K_a (2.87)
K^{el}_a	electrical part of K_a (2.87)
$K_a(\sigma)$	$\equiv G(\sigma)$ (p.40)
$K_a(pAg)$	$\equiv F(pAg)$ (p.40)
l	effective length of electrophoresis cell (5.3)
L	solubility product of AgI (3.31)
m_{AgI}	mass of AgI (4.7)
M	molecular weight (chapter 5)
n_i	number of *moles* of component i in the total system (2.2)

n_i^α	id. in phase α (2.2)
n_i^β	id. in phase β (2.2)
n_i^L	number of moles of component i in the solution (2.68)
n_i^I	number of moles of component i in the interface (2.68)
n_0	number of adsorption sites (2.75)
$n^\perp$	effective number of normally oriented water molecules (3.1, 3.7)
$n_i^\perp$	effective number of normally oriented water molecules at patch i (3.7)
$\bar{n}_{Ag+}^\perp$	averaged number of oriented water dipoles per nm^{-2} at Ag^+ patches (p.55)
$\bar{n}_{I-}^\perp$	id. at I^- patches (p.55)
$\bar{n}_{AgI}^\perp$	id. at AgI patches (p.55)
Δn_j	change in the number of adsorbed molecules j due to adsorption (6.5)
N_p	number of patches (3.6)
O	cross-section of the capillary of the electrophoresis cell(5.3)
p	pressure in the system (2.68)
pX	$\equiv -\log c_X$ (2.37)
pAg_b	pAg (= potential) at the uncovered surface (2.95)
pAg_c	pAg (= potential) at the complete covered surface (2.96)
pAg^*	pAg in some reference point (2.39)
r_i	radius of i
R	gas constant (2.30)
s^σ	surface excess entropy per surface area (2.3)
s^α	molar entropy in phase α (2.9)
s^β	molar entropy relative to H_2O in phase β (2.6)
$s^{(s)}$	relative surface excess entropy (2.11)

s_i^0	standard entropy of component i (2.45)
s_i^ϕ	id. including activity coefficient of i (2.45)
S	entropy of the system (2.3)
S^α	entropy of phase α (2.3)
S^β	entropy of phase β (2.3)
T	absolute temperature (2.1)
V	volume of the system (2.68)
V	applied potential in the electrophoresis cell (5.3)
x_i	mole fraction of component i in solution (2.7)
x	reduced pAg (5.2)
x_i^1	mole fraction after adsorption (2.41)
β	Esin–Markov coefficient (2.55)
γ	interfacial tension (2.1)
Γ_i	(excess) adsorption of component i (3.24)
Γ_i^{max}	id. at saturation (3.24)
Γ_T	amount of specifically adsorbed counterions
Γ_i^σ	surface excess concentration (Gibbs convention) (2.2)
$\Gamma_i^{(s)}$	relative surface excess concentration (relative adsorption) (2.12)
$\Gamma_i^{(s)*}$	id. in a reference point (2.39)
$\Gamma_{i,max}^{(s)}$	id. at saturation (2.62)
δ	criterion for equilibrium in the titration procedure (4.3, 4.4)
δ_1	id. (4.8, 4.9)
δ_2	id. (4.10, 4.11)
δ^0	thickness of the Stern layer at the uncovered surface (6.21)

δ^C	thickness of the Stern layer at the completely covered surface (6.22)
ε_0	dielectric permittivity of vacuum = 8.854×10^{-2} C/Vm
ε^L	dielectric constant of the bulk solution (3.34)
ε_s^C	dielectric constant of the Stern layer completely covered with adsorbate (6.22)
ε_s^0	dielectric constant of the Stern layer in the absence of adsorbate (6.21)
ε^S	dielectric constant of the Stern layer (3.5)
ε^M	molecular part of ε^S (3.5)
ε^O	orientational part of ε^S (3.5)
ε^H	effective relative dielectric constant applicable to the Helmholtz equation (3.1)
ε_i	relative dielectric constant in the fluid at patch i (p.50)
ε_∞	dielectric constant at high frequencies (p.51)
θ	degree of occupation of the organic component (2.62,2.63)
θ_i	fraction of the surface covered with patches i (3.6)
κ	reciprocal thickness of the double layer (3.35)
κ_{sp}	specific conductivity of the solution (5.3)
μ	dipole moment of water (3.1)
$\vec{\mu}_j$	dipole moment of j (6.5)
μ_i	chemical potential of component i in solution (2.1)
μ_i^0	standard chemical potential of component i in solution (2.35)
μ_i^I	chemical potential of component i in the interface (2.62)
μ_i^{I0}	standard chemical potential of component i in the interface (2.62)
μ_i^L	chemical potential of component i in solution (2.60)

μ_i^{L0}	standard chemical potential of component i in solution (2.60)
μ_i^{S}	chemical potential of component i in the solid phase
μ_i^{S0}	standard chemical potential of component i in the solid phase
$\tilde{\mu}$	electrochemical potentials (2.30, chapter 3)
$^*\mu$	eqs. 2.59 and 2.70
$\bar{\mu}_i^{I}$	eqs. 2.66, 2.67, 2.76, 2.77
v	exchange coefficient for adsorption from binary solution (2.57)
ξ^{+}	eq. 2.32a
ξ^{-}	eq. 2.32b
ξ	eq. 2.69
σ	surface charge (2.25a,b)
σ_{+}	K^{+} component of charge (2.26)
σ_{-}	NO_3^{-} component of charge (2.27)
σ_{A+}	A^{+} component of charge (2.28)
σ_{b}	surface charge at the uncovered surface (2.92)
σ_{c}	surface charge at the completely covered surface (2.94)
σ^*	surface charge in some reference point (2.40)
σ_{R}	surface charge where $\Delta\phi(dip)=0$ (6.23)
σ_{m}	surface charge in the adsorption maximum (6.23)
σ_{i}	surface charge at patch i (3.6)
ϕ^{S}	Galvani potential of the solid phase (2.30, 2.31)
ϕ^{L}	Galvani potential of the liquid phase (2.30, 2.31)
ϕ^{A}	Galvani potential at the adsorption site (2.79)
$\phi^{A'}$	first derivative of ϕ^{A} (field strength) (2.79)
$\phi^{A''}$	second derivative of ϕ^{A} (2.79)
$\Delta\phi_{ads}$	$\equiv \phi^{A}-\phi^{L}$ (6.4)

$\Delta\phi$ $\quad\quad\quad$ $\phi^S - \phi^L$ (p.26)

$\Delta\phi_b$ $\quad\quad$ $\Delta\phi$ at the incovered surface (2.97)

$\Delta\phi_c$ $\quad\quad$ $\Delta\phi$ at the completely covered surface (2.97)

$\Delta\phi^0$ $\quad\quad$ $\equiv \Delta\phi_b$ (6.20)

$\Delta\phi^C$ $\quad\quad$ $\equiv \Delta\phi_c$ (6.20)

ϕ_m $\quad\quad\quad$ Galvani potential at the adsorption maximum (6.13b)

$\Delta\phi$ (Stern) Stern layer potential (3.2)

$\Delta\phi$ (dip) $\quad$ dipolar potential (3.1)

$\Delta\phi$ (mol) $\quad$ potential difference in the Stern layer due to the

$\quad\quad\quad\quad\quad$ polarizability (3.3)

$\Delta\phi$ (diff) $\quad$ diffuse layer potential (3.34)

$\Delta\phi$ (ads) $\quad$ $\equiv \phi^A - \phi^L$ (3.23)

$\Delta\phi$ (solid) $\equiv \phi^S - \phi^A$ (3.27)

$\Delta\phi_i(\ldots)$ $\Delta\phi(\ldots)$ at patch i (3.8, 3.9)

$\Delta\phi_N(dip)$ $\quad$ (3.12)

$\Delta\phi_i^R(dip)$ $\quad$ (3.12)

χ $\quad\quad\quad\quad$ χ-potential (general)

χ_1^0 $\quad\quad\quad$ dipolar potential at the uncovered surface at $\sigma=0$ (6.21)

χ_2^0 $\quad\quad\quad$ dipolar potential at the completely covered surface (6.22)

ABBREVIATIONS

TAA	tetraalkylammonium
TMeA	tetramethylammonium
TEtA	tetraethylammonium
TPrA	tetrapropylammonium
TBuA	tetrabutylammonium
TAmA	tetraamylammonium
PhTA	phenyltrimethylammonium
Chol	choline
HeMe	hexamethonium
ADC	Analog-digital convertor
c.i.p.	common intersection point
DEC	Digital Equipment Corporation
FFG	Frumkin, Fowler-Guggenheim
ICT	International Critical Tables
iOp	inner Helmholtz plane
oHp	outer Helmholtz plane
p.d.	potential determining
p.z.c.	point of zero charge

174

SAMENVATTING

Het onderzoek, dat in dit proefschrift is beschreven handelt over verschijnselen op het gebied van de *grensvlakchemie*. Grensvlakken spelen een belangrijke rol op verschillende praktische terreinen zoals in biologische systemen, bij emulsies en in de bodem. In dit onderzoek wordt het grensvlak tussen een vaste stof en een vloeistof, zoals tussen kleideeltjes en grondwater, bestudeerd.

Vast-vloeistof grensvlakken hebben twee belangrijke eigenschappen:

(i) Op de vaste wand bevindt zich meestal een electrische lading, die echter gecompenseerd wordt door een tegengestelde lading in de vloeistof vlak bij de wand; samen vormen zij de z.g. electrische dubbellaag.

(ii) Aan het grensvlak kunnen zich allerlei stoffen ophopen (adsorberen).

Adsorptie aan geladen grensvlakken wordt ook wel *electrosorptie* genoemd. Electrosorptie bepaalt in belangrijke mate het gedrag van b.v. kleideeltjes in de bodem.

Het *doel* van dit onderzoek was nu om theoretisch en experimenteel te bestuderen hoe de adsorptie en de lading op het oppervlak elkaar beïnvloeden. Vanwege deze fundamentele doelstelling is er geen ingewikkeld grensvlak uit de praktijk gekozen, zoals b.v. klei, maar het grensvlak van zilverjodide met water. In een volgende onderzoeksfase kunnen theorieën, ontwikkeld aan dit systeem, worden uitgetest en/of toegepast op meer praktische systemen.

Het zilverjodide-water grensvlak is eigenlijk ideaal voor fundamenteel onderzoek. Zilverjodide is een geel poeder, dat in water kan worden gedispergeerd (verdeeld). Het oppervlak van gedispergeerd AgI kan elektrisch worden opgeladen door toevoeging van zilvernitraat (positieve lading op het oppervlak) of kaliumjodide (negatieve lading op het oppervlak). Het electrische spanningsverschil tussen het vaste zilverjodide en de vloeistof (oppervlakte potentiaal) kan met een speciale voltmeter worden gemeten. Bij vorige onderzoekingen aan dit grensvlak werden ongeladen stoffen geadsorbeerd. Bij dit onderzoek wilden we juist de adsorptie van *geladen* stoffen onderzoeken. De keuze is gevallen op *tetraalkylammonium* ionen. Dit zijn positief geladen, bolvormige deeltjes be-

staande uit 4 alkylstaarten (koolstof en waterstof) verbonden met
een positief geladen stikstofatoom. De grootte van deze positieve
bolletjes kan worden gevarieerd door de lengte van de alkylstaart
groter of kleiner te kiezen.

De Nederlandse titel van dit proefschrift luidt dan ook:

Electrosorptie van tetraalkylammonium ionen op zilverjodide

Bij dit onderzoek zullen we zowel de lading op het oppervlak
meten als het aantal tetraalkylammonium ionen dat op het oppervlak
adsorbeert. Uit deze metingen kunnen verscheidene conclusies worden
getrokken over de wijze waarop de lading van het oppervlak de ad-
sorptie beïnvloedt.

Tetraalkylammonium ionen blijken zich sterk aan het zilver
jodide te hechten. Dit werd ook verwacht. De vier alkylstaarten
van deze ionen zitten namelijk minder graag in water (ze zijn
hydrofoob). Door zich nu aan het AgI oppervlak te hechten hebben
de alkylstaarten zo min mogelijk contact met water en dit bevordert
adsorptie: *hydrofobe binding*. Bovendien verwachten we, dat de bin-
ding sterker wordt naarmate we een langere alkylstaart kiezen. Dit
wordt dan ook duidelijk door de experimenten bevestigd. In de tweede
plaats verwachten we dat de positief geladen tetraalkylammonium
bollen op een positief geladen oppervlak minder gemakkelijk zullen
adsorberen. Ook dit is experimenteel bewezen. Daarentegen zouden we
ook verwachten, dat naarmate het oppervlak steeds meer negatief
wordt deze positieve deeltjes steeds sterker door het grensvlak
worden aangetrokken en dus in grotere aantallen zullen adsorberen.
Het laatste blijkt echter niet het geval. Als de lading van het
oppervlak groter wordt dan een bepaalde waarde neemt de neiging
tot adsorptie weer *af*. Dit is natuurlijk strijdig met de wet van
Coulomb, die zegt dat positieve en negatieve deeltjes elkaar altijd
aantrekken!

De reden voor het falen van de wet van Coulomb bij de adsorp-
tie van tetraalkylammoniun ionen is nogal ingewikkeld. We moeten
ons voorstellen, dat de positieve tetraalkylammonium ionen als zout
zijn opgelost in water, hetgeen ongeladen is. Het watermolecuul is
echter een dipool, d.w.z. er bevindt zich een positieve en negatie-
ve lading binnen het molecuul op korte afstand van elkaar. Als nu

176

een tetraalkylammonium ion adsorbeert, worden watermoleculen aan het grensvlak verdrongen. Echter, naarmate het oppervlak sterker negatief is worden de watermoleculen met hun positieve kant sterker door het oppervlak aangetrokken. Op een gegeven moment is het voor watermoleculen gunstiger om te adsorberen, dan voor tetraalkylammonium ionen. Het feit dat de electrische bijdrage van dipolen tot de neiging voor adsorptie kan concurreren met het effect van geladen deeltjes is een verschijnsel dat men zich meestal niet realiseert.

Tijdens dit onderzoek is het gelukt een theorie te ontwikkelen, die het mogelijk maakt te berekenen bij welke lading op de wand, de adsorptie van water het wint van die van tetraalkylammonium ionen.

Het is duidelijk, dat waterdipolen in contact met het zilverjodide een belangrijke bijdrage leveren tot de eigenschappen van de grenslaag. Er is dan ook een theorie ontwikkeld, die de oriëntatie van de waterdipolen in het grensvlak beschrijft, aannemende dat de ladingen op het oppervlak gedurende voldoende lange tijd op een vaste plaats zitten en relatief ver van elkaar zijn verwijderd. Deze theorie maakt het mogelijk het verband tussen de lading op het zilverjodide en de oppervlaktepotentiaal beter te beschrijven.

Voor de eigenschappen van het zilverjodide-oplossing grensvlak in aanwezigheid van adsorberende organische stoffen bestaat er een theoretische relatie, de z.g. wet van Gibbs, die het mogelijk maakt de adsorptie van de organische stof te berekenen als wij het verband tussen de lading op het oppervlak, de oppervlakte potentiaal en de hoeveelheid organische stof in de oplossing kennen. Reeds bij vorige onderzoekingen is op deze wijze de adsorptie berekend. Het is echter nooit direct aangetoond dat deze berekende adsorptie ook de werkelijke adsorptie is. In het beschreven onderzoek was het echter mogelijk de adsorptie ook direct te meten. Het is gebleken dat de berekende adsorptie binnen de fouten die bij de proeven ontstaan, overeenkomt met de direct gemeten adsorptie. Dit resultaat onderstreept nog eens, dat het zilverjodide systeem erg geschikt is voor fundamenteel onderzoek.

De meting van de lading op het zilverjodide neemt een belangrijke plaats in binnen dit onderzoek. Uit vorige onderzoekingen bleek echter dat deze meting bijzonder tijdrovend was. Tijdens dit

onderzoek is een automatische apparatuur ontwikkeld, die het moge-
lijk maakt dat de metingen dag en nacht worden voortgezet zonder
tussenkomst van de experimentator. De computer, die hiervoor wordt
gebruikt geeft niet alleen de opdracht tot het toevoegen van vloei-
stof, het aan- en uitzetten van een roerder of het meten van een
spanning, doch voert ook de nodige berekeningen uit.

Er is een aantal problemen waarvoor geen bevredigende oplos-
sing is gevonden. We zijn nog steeds niet helemaal zeker hoe ver de
geadsorbeerde tetraalkylammonium bollen nu van elkaar verwijderd
zijn. Verder is er geen sluitende verklaring voor de verschillen
in adsorptie op het zilverjodide oppervlak en het kwik oppervlak.
Toch heeft dit onderzoek de oplossing van deze problemen wel dich-
terbij gebracht.

Er kan worden geconcludeerd dat de electrosorptie van tetra-
alkylammonium ionen op zilverjodide nieuw inzicht heeft verschaft
in enkele algemene en specifieke oppervlakte eigenschappen. Aanmer-
kelijke vooruitgang is geboekt in het experimentele bewijs van de
wet van Gibbs, de beschrijving van het adsorptie maximum en het
gedrag van waterdipolen aan het grensvlak.

CURRICULUM VITAE

Op 23 oktober 1945 ben ik geboren te Werkendam. Ter voorbereiding
op mijn wetenschappelijke opleiding heb ik 3 jaar onderwijs gevolgd
aan de Chr. Ulo te Sleeuwijk en 3 jaar aan de Chr. HBS te Gorinchem.
Het einddiploma HBS-B werd in juni 1964 behaald. Voordat ik mijn
militaire dienstplicht heb vervuld, ben ik 4 maanden werkzaam ge-
weest op het Analytisch Chemisch Laboratorium van de Fabriek voor
Chemische produkten "Vondelingenplaat" te Rotterdam.
In september 1966 ben ik begonnen met de scheikundestudie aan de
Rijksuniversiteit te Utrecht. Het kandidaatsexamen, richting S3,
werd op 10 november 1969 afgelegd. Tijdens de doctoraalstudie heb
ik me gespecialiseerd in de molecuulspectroscopie (prof.drs. M.P.
Groenewege), de electro- en colloidchemie (prof.dr. J.Th.G. Overbeek)
en de theoretische natuurkunde. Het doctoraalexamen scheikunde werd
afgelegd, met lof, op 26 juni 1972. Sinds oktober 1972 ben ik werk-
zaam op het laboratorium voor Fysische en Kolloidchemie van de
Landbouwhogeschool, tot september 1976 aangesteld door de organisa-
tie voor Zuiver Wetenschappelijk Onderzoek (ZWO), daarna als weten-
schappelijk medewerker in dienst van de Landbouwhogeschool.